

ABSTRACT

Several population-based studies have identified elevated intraocular pressure (IOP) as a major causative risk factor associated with primary open angle glaucoma (POAG), the most common form of glaucoma that affects millions of people worldwide. Moreover, multi-ethnic clinical trials in several different countries over the last few decades have provided overwhelming evidence showing correlation between lowering of IOP and reduced progression of vision loss. As a result, IOP reducing therapeutic interventions are the gold standard in glaucoma therapy. Although the role of IOP is evident in pathology of POAG, very few studies have delved into the complex physiological mechanisms that regulate IOP homeostasis. From continuous telemetry recordings in nonhuman primates, we now know that IOP is a dynamic variable that fluctuates throughout the day. However, despite the fluctuations, the mean IOP is still maintained within a narrow physiological range. The level of IOP elevation at any given time depends on the resistance to aqueous humor outflow encountered in the conventional outflow pathway consisting of the trabecular meshwork (TM), Schlemm's canal (SC), and the distal episcleral vessels. Recent studies have suggested that the cells of the outflow pathway have intrinsic ability to detect biomechanical stimuli in their environment (like shear stress) and convert these stimuli into biochemical signals to elicit specific cellular responses. Although mechanotransduction at the TM is deemed critical for IOP homeostasis, we are yet to conclusively identify the exact signaling pathway involved. In this study, we identify the role of transient receptor potential vanilloid IV channels (TRPV4) in sensing mechanical stress on the TM. We show that shear stress activates TRPV4 channels in human primary TM cells, which leads to endothelial nitric oxide synthase (eNOS)-dependent nitric oxide (NO) production. NO, itself has been identified as a key regulator of IOP. Exogenous NO

delivery to the eye has been shown to reduce IOP in humans. However, the underlying mechanism that regulates endogenous levels of NO still remains unknown. To this end, we demonstrate that TRPV4 channels regulate eNOS-dependent NO production in primary human TM cells and ex vivo cultured human TM tissues. We show that TRPV4 activation by mechanical shear leads to activation of eNOS signaling and NO production. Furthermore, pharmacological activation of TRPV4 channels via a selective agonist GSK1016790A (GSK101) leads to eNOS phosphorylation and NO production. In animal models, we demonstrate a role of TRPV4 channels in regulating physiological IOP. Treatment of C57BL/6J mouse eyes with TRPV4 agonist GSK101 leads to reduction in baseline night-time IOP and nominal improvement in outflow facility. We also show that conditional knockout of TRPV4 channels in Ad5-Cre injected TRPV4^{f/f} mice leads to increase in IOP. We use the NOS3^{-/-} (eNOS) to further show that TRPV4 mediated lowering of IOP is eNOS dependent. Dysregulation of the TM cells leads to increase in resistance and IOP elevation. Furthermore, glaucomatous human TM cells show impaired activity of TRPV4 channels and disrupted TRPV4-eNOS signaling. Flow/shear stress activation of TRPV4 channels and subsequent NO release were also impaired in glaucomatous primary human TM cells. Together, our studies demonstrate a central role for TRPV4-eNOS signaling in lowering the resting IOP. Our results also provide evidence that impaired TRPV4 channel activity in TM cells contributes to TM dysfunction and elevated IOP in glaucoma.

**The role of mechanosensory TRPV4 channels and nitric oxide signaling in intraocular
pressure homeostasis, and its impairment in glaucoma.**

DISSERTATION

Presented to the Graduate Council of the Graduate School of Biomedical Sciences University of
North Texas Health Science Center at Fort Worth

In Partial Fulfillment of the Requirements for the Degree of
DOCTOR OF PHILOSOPHY

By

Pinkal D. Patel, M.S.

Fort Worth,

Texas

July 2020

ACKNOWLEDGEMENTS

This work would not have been possible without support and guidance from my mentors, colleagues, collaborators, family members, and friends. I am especially indebted to my major advisor and mentor Dr. Gulab Zode, who has consistently guided and supported me throughout my graduate school career. I am extremely grateful to him for taking me under his wing and challenging me to do better every day. By giving me freedom in the lab in designing experiments, he nurtured my curiosity and allowed me to learn from my mistakes. I also thank him for the constant encouragement and support throughout these years. As my teacher and mentor, he has taught me more than I could ever give him credit for here.

I also take this opportunity to acknowledge and thank my committee members Drs. Abe Clark, Iok-Hou Pang, Raghu Krishnamoorthy, and Caroline Rickards. Their constructive feedback at my committee meetings has played an important role in the development of this dissertation project and my growth as a researcher. By challenging me with insightful questions, they taught me valuable critical thinking skills. I am beyond grateful for their continued interest in my research.

I also wish to express my sincere gratitude to Drs. Abe Clark, Iok-Hou Pang, Tom Yorio, and Gulab Zode for the feedback, extended discussions, and their valuable insights regarding glaucomatous pathology in the anterior chamber, which helped steer my project and allowed me to ask questions beyond the scope of the proposal. I am also very thankful for the gift of human donor tissues generously shared by Dr. Abe Clark and Lab.

The project has also greatly benefited from the technical expertise, comments, and suggestions made by Dr. J. Cameron Millar. I would like to thank Dr. Millar for his help in outflow facility measurements, as well as his discussions regarding real-time measurements of nitric oxide.

I also acknowledge the contributions from our collaborators Drs. Yen-Lin Chen and Swapnil Sonkusare from the University of Virginia Medical School. I would like to thank them for hosting me, teaching me, and helping me conduct critical functional assays for determining TRPV4 function.

I also acknowledge the funding support to Dr. Gulab Zode from National Institutes of Health, the Department of Pharmacology and Neuroscience at UNTHSC, and BrightFocus Foundation. I also thank the Lions Eye Institute and Transplant Services (Tampa, FL) for their generous gift of human donor corneoscleral tissues.

I am grateful to all of those with whom I have had the pleasure to work during this and other related projects. Each of the members of my lab has provided me extensive personal and professional guidance and taught me a great deal about both scientific research and life in general. I would especially like to thank Dr. Ramesh Kasetti and Dr. Prabhavathi Maddineni for their significant role in my training and development as a researcher. I have learned a great deal about research from these two distinguished scientists. I also acknowledge and thank Sherri Feris and Sandra Maansoon for their contribution to this project.

Graduate school has been a roller-coaster ride, with exhaustive failures as well as memorable successes. Throughout the journey, I'm thankful for my graduate student peers and the entire North Texas Eye Research Institute family for keeping me inspired.

My family has been my greatest cheerleader throughout the pursuit of this project. I would like to thank my parents Dilip and Gita; whose love and guidance are with me in whatever I pursue. I would also like to thank Mike and Vanita for their encouragement and support in the last 4 years. Most importantly, I wish to thank my loving and supportive wife, Puja, a source of unending inspiration.

TABLE OF CONTENTS

ACKNOWLEDGEMENTS	V
TABLE OF CONTENTS	VIII
LIST OF FIGURES	IX
LIST OF TABLES	X
CHAPTER I.....	1
Introduction.....	1
REFERENCES	18
CHAPTER II	1
Impaired TRPV4-eNOS signaling in trabecular meshwork contributes to elevation of intraocular pressure in glaucoma	39
ABSTRACT	40
INTRODUCTION	42
METHODS AND MATERIALS	45
RESULTS	54
DISCUSSION.....	74
REFERENCES	80
CHAPTER III.....	95
Direct, real-time electrochemical measurement of nitric oxide in ex vivo cultured human corneoscleral segments.	95
ABSTRACT	96
INTRODUCTION	98
METHODS AND MATERIALS	101
RESULTS	104
DISCUSSION.....	113
REFERENCES	117

LIST OF FIGURES

CHAPTER I.....	1
Figure 1. Schematic of the study design.....	16
CHAPTER II	1
Figure 1. Expression of functional TRPV4 channels in the human TM.	60
Figure 2. TRPV4 Ca ²⁺ sparklets represent Ca ²⁺ influx through TRPV4 channels on TM cell membranes.....	61
Figure 3. Flow/shear stress increases TRPV4 channel activity in TM cells.	62
Figure 4. TRPV4 channels regulate outflow facility and IOP homeostasis.	63
Figure 5. Elevation of IOP in Ad5-Cre transduced TRPV4 ^{f/f} mice.....	64
Figure 6. TRPV4 channels are functionally coupled to eNOS in the human TM cells and tissues.....	65
Figure 7. TRPV4 activation leads to NO production in primary TM cells and ex vivo cultured human TM tissues.....	66
Figure 8. TRPV4-mediated lowering of IOP is eNOS dependent.....	67
Figure 9. Pharmacological activation of TRPV4 channels is impaired in glaucomatous TM cells.....	68
Figure 10. Sensitivity to shear stress is diminished in glaucoma.	69
Figure 11. Shear stress-mediated TRPV4-eNOS signaling is diminished in glaucomatous TM cells.....	70
Figure 12. TRPV4-eNOS coupling is impaired in glaucomatous TM cells.	71
Figure 13. There is no significant change in TRPV4 expression between normal and glaucomatous TM cells.	72
Figure 14. Expression of eNOS is not significantly different in normal and glaucomatous TM.	73
CHAPTER III.....	95
Figure 1. Experimental setup for the study.....	106
Figure 2. Linear regression analysis of the relationship between amount of NO added and the electric current obtained from the NO electrode (ISO-NOPF200).....	107
Figure 3. Detection of NO in human corneoscleral segments after treatment with DETA- NONOate/AM (exogenous NO donor).....	108

Figure 4. A. Increase in DAF-FM fluorescence intensity in quadrants of human corneoscleral segments after treatment with DETA-NONOate/AM (exogenous NO donor) compared to vehicle treated controls..... 109

Figure 5. Dose dependent increase in NO levels in human corneoscleral segments after treatment with Latanoprostene bunod compared to Latanoprost vehicle control..... 110

Figure 6. A. Increase in DAF-FM fluorescence intensity in quadrants of human corneoscleral segments after treatment with Latanoprostene bunod compared to controls treated with vehicle Latanoprost..... 111

LIST OF TABLES

CHAPTER I..... 1

 Table 1 Complications associated with surgical interventions..... 9

CHAPTER III..... 95

 Table 1. Troubleshooting solutions for real-time electrochemical measurement of NO in human corneoscleral segments 112

CHAPTER I

INTRODUCTION

Primary Open Angle Glaucoma (POAG)

Glaucoma is a group of multifactorial neurodegenerative diseases characterized by progressive optic neuropathy that leads to loss of retinal ganglion cells and their axons. It is the leading cause of irreversible vision loss with more than 76 million people affected worldwide (1), and this number is estimated to increase to 111.6 million by the year 2040 (2). Due to the progressive nature of the disease and peripheral vision loss in the beginning stages, glaucoma is mostly asymptomatic until it becomes severe and vision problems arise. As a result, many people affected by this disease remain undiagnosed, and therefore are unaware of their condition. The neurodegeneration associated with this condition also means that there is no existing cure for glaucoma. Current treatments are limited interventions that slows the progression of the disease. Primary open angle glaucoma (POAG) is the most common form of glaucoma, accounting for approximately 70% of all cases (1). Intraocular pressure (IOP) is a major risk factor associated with the development and progression of the disease (3, 4), and it is the only modifiable risk factor in POAG. Therefore, majority of medical and surgical interventions are targeted towards reducing IOP (5).

Intraocular pressure: an important associated risk factor for POAG.

Although cross-sectional associations derived from population-based studies help in identifying the risk for developing a disease, these studies do not necessarily explain the causality. That being

said, there are several risk factors identified in the literature with clear associations with POAG. The three main demographic risk factors associated with POAG are race, age, and family history. Population-based studies have demonstrated that POAG is more prevalent in African American and Hispanic populations than whites living in the same geographical area (6). The prevalence of POAG also increases significantly with age. A multiethnic population-based study in Baltimore has shown a 10-fold increase in POAG prevalence with age (6). A family history of POAG is also associated with an increased risk of developing the disease (7). A study directly examining the first-degree relatives of patients with and without POAG observed that siblings of POAG patients were 9-times more likely to have glaucoma than siblings of controls (8). Given the substantial risk of POAG in family members of existing patients, the genetic basis of familial transmission of glaucoma is largely unknown. Two genes, myocilin (9) and optineurin (10), have been identified for causing autosomal dominant POAG. However, these disease-causing mutations are found only in a small percentage of POAG patients (11). It is now increasingly clear that POAG is a complex multifactorial disease, with pathology resulting from interaction of several different genes that are yet to be identified (12). Interestingly, there has been no consistent association of POAG with gender. Although there are studies that found POAG to be more prevalent among men (13-17), there are other studies that show its prevalence is higher in females (18, 19), and still there are some that show no change in prevalence between males and females (6, 20, 21). The literature on animal models is also inconclusive on the role of gender in susceptibility to POAG. However, this much is clear that more in-depth studies on animals and humans are warranted to unravel the role, if any, played by gender in POAG prevalence. Apart from demographic risk factors, several population-based studies have shown weak associations with systemic diseases. These are called systemic risk factors. Diabetes, hypertension, smoking, alcohol use, and excessive caffeine

consumption have been weakly associated with POAG, and therefore the evidence is inconclusive as it stands (5, 22).

Among the ocular risk factors, intraocular pressure (IOP) is the strongest known causal risk factors associated with both development and progression of POAG. At present, IOP is the only risk factor for which modulation has proven clinically efficacious. Numerous population-based studies across multiple ethnicities have shown strong correlation between chronic elevation in IOP and increased incidence (23, 24) and prevalence (14, 25, 26) of glaucoma. Chronic elevation of IOP leads to pathological damage to the retina and the optic nerve head, resulting in neuronal death and vision loss. The relative risk of glaucomatous optic nerve damage increases 13-fold for an IOP elevation from 15 mmHg to 22-29 mmHg, and 40-fold for an IOP >30 mmHg. This chronic elevation of IOP which is higher than the expected 'normal' baseline levels is called ocular hypertension. In patients with asymmetric IOP elevation in both eyes, visual field loss is more severe in the eye with the higher IOP (27, 28). This finding highlights the importance of IOP in pathology of POAG. Furthermore, IOP being the only modifiable risk factor for progression of the disease, majority of medical and surgical interventions are targeted towards reducing IOP (5). In fact, IOP reducing interventions have been proven clinically efficacious in cases of normal-tension glaucoma, wherein the patients do not have the characteristic elevation of IOP above the presumed 'normal' level yet have visual field loss. The Collaborative Normal-Tension Glaucoma Study (CNTGS) reported less visual field loss in patients with normal-tension glaucoma who have successfully undergone therapy for reducing IOP by 30% to an average of 11 mmHg (29).

Aqueous humor dynamics

Aqueous humor (AH) is the fluid of the anterior chamber that plays an important role in nourishing the eye and maintaining proper IOP. It provides nutrients and removes metabolites from the

various tissues of the eye, including the avascular cornea and lens. After secretion from the ciliary body, the AH flows along the iris into the anterior chamber where it is drained by the iridocorneal angle tissues. This outflow of AH from the eye occurs via two major pathways: 1) the conventional outflow pathway and 2) unconventional outflow pathway. The conventional outflow pathway involves the sieve-like trabecular meshwork (TM) tissue, Schlemm's canal, collecting channels, and the episcleral-conjunctival venous system. The conventional outflow system accounts for ~80% of the AH outflow in human eyes, whereas the unconventional system which involves uveoscleral and uveo-vortex systems account for only ~20 % of total AH outflow (30-32). Intraocular pressure (IOP) is a function of the rate at which aqueous humor (AH) is secreted (inflow) and the rate at which it is drained (outflow) from the eye. When the rate of inflow equals outflow, a steady state exists, and IOP remains constant. The rate of inflow depends on the rate of AH production, whereas outflow depends on the resistance to AH drainage. Therefore, dysregulation in drainage of AH may lead to ocular hypertension. This being said, elevated IOP observed in most forms of glaucoma is associated with increased resistance to AH outflow, while the rate of AH formation does not differ much from that of nonglaucomatous controls.

Outflow resistance in normal and disease conditions

In order to understand 'how' increase in AH outflow resistance regulates IOP, we must know 'what' contributes to the resistance. As discussed above, the conventional pathway (also known as the trabecular pathway) is responsible for majority of outflow in the human eye (30-32). The TM, a molecular sieve-like tissue, is subdivided into three regions that are functionally and morphologically unique. At the proximal end facing the AH, we have the uveal meshwork region that contains lattice-like beams of trabeculae (containing secreted extracellular matrix; ECM) lined with TM cells (33). The arrangement of trabecular beams in this region create irregular openings

(~25-75 μm wide) through which the AH passes into the adjacent region. The corneoscleral meshwork region consists of TM cells lining the ECM-derived trabecular sheets, the structure of which resembles a sponge with elliptical openings (~5-50 μm wide) (33). The flow of AH through these two regions is largely unrestricted, the same cannot be said for the final region of the TM called the juxtacanalicular region (JCT). The JCT is located at the distal end of the TM adjacent to the SC. The cells in this region are embedded into a bed of connective tissue, which generates significant resistance to the flow of AH (34). Adjacent to the JCT lies the inner wall of SC, containing a single layer of endothelial cells. After traversing through the regions of the TM and crossing the inner wall of SC, aqueous humor enters the SC lumen (190-370 μm diameter) which is lined with endothelial cells (35). The distal tissues of the conventional outflow pathway, collecting channels and episcleral veins, that drain the SC also contribute to outflow resistance. Grant demonstrated that removal of TM from nonglaucomatous enucleated human eyes eliminated only 75% of outflow resistance (36). Although the exact site for outflow resistance has not been unambiguously determined, the JCT region of the TM and the inner wall of SC are two sites considered responsible for majority of AH outflow resistance in a normal eye. Furthermore, the exact mechanisms responsible for pathological or age-related increase in resistance are yet to be determined. A previous study has demonstrated that TM tissues from POAG donor eyes are significantly stiffer and less elastic compared to the TM tissues from age-matched control eyes (37-39). Furthermore, previous reports have shown age-related changes in the TM, including decreased cellularity and increased ECM deposition, which leads to age-dependent decrease in AH outflow (40, 41). In POAG, it is known that increase in outflow resistance leads to decrease in facility (egress of AH out of the eye, which is reciprocal to the outflow resistance). As of now, the

most efficacious treatment option for controlling IOP in POAG is to reduce outflow resistance via pharmaceutical or surgical interventions.

Current therapeutic interventions for lowering IOP in POAG

Glaucomatous neurodegeneration occurs first in the peripheral retina resulting in a characteristic loss of peripheral vision. This peripheral vision loss, which marks the onset of the disease, often goes unnoticed until patients undergo clinical evaluation and testing for glaucoma. This is why glaucoma is often referred as a ‘silent thief of vision’, and therefore clinicians often recommend having clinical evaluation twice a year. A single type of clinical test cannot conclusively diagnose the disease or provide sufficient information about its progression and severity. Therefore, clinical evaluation of glaucoma requires a thorough review of patient’s medical and ocular history as well as a comprehensive ocular examination involving a battery of clinical tests. These tests usually include tonometry for determining IOP; pachymetry for evaluating central corneal thickness (an ocular risk factor); gonioscopy for estimating the iridocorneal angle size; visual acuity; optic nerve examination for assessing cup-to-disc ratio (degree of cupping); slit-lamp examination for assessing conjunctival hyperemia (a common side-effect of glaucoma therapy), scleral health, and episcleral vessel dilation; automated perimetry for assessing field of vision; and optical coherence tomography for measuring thinning of retinal nerve fiber layer. Depending on the severity and progression of the disease, clinicians develop a treatment plan suitable for individual patients to help them reach the target IOP. Treatment with topical eyedrops of anti-glaucoma agents is the first line of defense against the disease. The effectiveness of topical anti-glaucoma medications is primarily measured by its ability to lower IOP. However, the impact of other factors like ocular blood supply, local physiological parameters (intracranial pressure and perfusion pressure), neuroprotection of the optic nerve are important variables to consider for assessing and improving

the efficacy of these medications. Prostaglandin analogs (PGAs), a class of drugs (involving latanoprost, bimatoprost, travoprost, and tafluprost) considered the gold standard in glaucoma therapy. Derived from arachidonic acid, prostaglandins play a role in a variety of biological functions. In the eye, prostaglandins are known to large IOP reduction by increasing the uveoscleral outflow (42, 43). This increase in uveoscleral outflow is mediated by modulation of matrix metalloproteinases (44). Prostaglandin analogs latanoprost (0.005%), travoprost (0.004%), and bimatoprost (0.03%) all bind to FP receptors; can reduce IOP during daytime and at night; and only require instillation once daily. Given the benefits, in a small subset of patients PGAs are known to cause side-effects which includes conjunctival hyperemia, pigmentation, burning/stinging sensation, blurred vision, itching, foreign body sensation, and eye pain (45). Beta-blockers are another class of IOP lowering medications available in the anti-glaucoma armamentarium. Stimulation of beta-adrenergic receptors in ciliary body leads to cAMP activation, and protein kinase A mediated production and secretion of aqueous humor by the ciliary body. Beta-blockers like timolol antagonize these adrenergic receptors as a result decreasing aqueous humor production and reducing IOP (46). Apart from ocular side effects like conjunctival hyperemia and dry eye symptoms, beta blockers are known to cause systemic side effects affecting cardiovascular and respiratory systems. Carbonic anhydrase inhibitors (CAIs) is another class of drug known for reducing IOP by decreasing aqueous humor production. Carbonic anhydrase generates HCO_3^- ions, which is essential for active secretion of AH. CAIs inhibit the carbonic anhydrase isoenzyme II thereby decreasing secretion of AH and reducing IOP (47, 48). CAIs can be administered systemically via oral pills or locally via topical eye drops. Oral CAIs produce a greater IOP lowering response but at risk of systemic side effects. These classes of drugs primarily lower IOP by reducing aqueous humor production or increasing uveoscleral outflow but do not

target the underlying pathology at the conventional outflow pathway, which is responsible for majority of resistance to outflow. Parasympathomimetic agents like pilocarpine are known to induce contraction of ciliary muscles, which stretches the TM while opening the intertrabecular spaces and reducing resistance to outflow (49). IOP lowering effect is only modest with the risk of side effects that involve decreased uveoscleral outflow, blurred vision, and retinal detachment. Recently, Rho-kinase inhibitors have shown promise in targeting the conventional outflow pathway. Rho-kinase (ROCK) proteins are serine/threonine kinases with multiple downstream substrates like LIM kinase and MLC kinase, phosphorylation of which leads to actin stabilization and contraction of actin fibers. ROCK inhibitors are a class of compounds targeting the Rho-kinase protein, and in the process reducing IOP by relaxing the TM and increasing conventional outflow facility. Netarsudil (Y-27632; Aerie Pharmaceuticals) a ROCK inhibitor is now approved for IOP reducing therapy in glaucoma patients. The second messenger nitric oxide (NO) has also shown promise in relaxing the TM and reducing IOP by inhibiting contraction of actin fibers in TM cells (50-54). Exogenous NO delivery to the eye via topical eyes drops has been proven to reduce IOP in animal models. Recently, a chimeric formulation containing PGA latanoprost and NO donor butanediol mononitrate (Latanoprostene bunod; Bosch + Lomb) has been approved for IOP lowering therapy in glaucoma patients (55-60).

To maximize the therapeutic outcome, majority of glaucoma patients with mild to moderately elevated IOP are started on combination of these drugs. Due to undesirable side effects, noncompliance and nonadherence to therapy involving glaucoma eye drops is a challenge in the treatment of the disease. Furthermore, IOP lowering effect of these medications is not absolute and may not be long term. For patients with uncontrolled high IOPs, surgical interventions are recommended. These interventions involve, among many, placement of a shunt in the outflow

pathway to dissipate pressure or strip the entire TM (trabeculectomy) along the limbal circumference to reduce the resistance. Although effective for a short period of time, surgical interventions are invasive and need careful consideration due higher rates of failure (61). Table 1 lists the complications often encountered during or after surgery.

Table 1 Complications associated with surgical interventions (61, 62).

Trabeculectomy	Aqueous shunt implantation
Conjunctival buttonhole	Flat anterior chamber
Scleral flap tear	Hypotony
Intraoperative bleeding	Choroidal effusion
Flat anterior chamber	Corneal decompensation
Low filtration	Tube blockage/fibrosis
Bleb leaks and fibrosis	Tube erosion and exposure

Evidence for IOP homeostasis

IOP is maintained under strict homeostatic control, which keeps the pressure within an acceptable physiological range throughout the life of most individuals (63). Continuous measurements of IOP via telemetry in unrestrained, awake nonhuman primates have shown that IOP is dynamic and fluctuates as much as 5 mmHg hour-to-hour (64). Despite the fluctuations, the mean IOP remains close to the physiological normal. The IOP homeostatic effect was first demonstrated in perfusion organ cultures of human anterior segments. Stabilized anterior segments perfused at a physiologically relevant flowrate (2.5 $\mu\text{L}/\text{min}$) were subjected to a 2X increase in flow rate (5 $\mu\text{L}/\text{min}$), which doubled the measured pressure. However, despite the sustained 2X flow rate

applied, the pressure slowly declined (over several days) back to physiological levels. The outflow system here sensed the elevated pressure and adjusted the outflow resistance to bring the pressure back to pre-elevated levels (63, 65). Since this pivotal finding, there has been several reports showing that anterior segments in perfusion organ culture can sense pressure elevation and respond by adjusting outflow resistance. The TM is instrumental in maintaining this homeostatic control over IOP by sensing mechanical perturbations in its environment and constantly adjusting the resistance to AH outflow. When IOP or flow changes are large enough, TM cells sense this as mechanical distortion on cell surface via mechanosensory receptors. It has been shown that mechanical stretching or increased perfusion pressures trigger numerous expression changes that leads to ECM remodeling and reduction of outflow resistance (65). How these mechanical forces are perceived on the TM cells, and the cellular mechanism responsible for IOP homeostasis is yet to be identified.

TRPV4 channels: mechanosensory receptors on the TM

One possible such mechanism for TM cells to sense IOP deviation would be to recognize mechanical distortion on the cell surface via specific mechanoreceptors (65). TM cells are in constant contact with the aqueous humor, and therefore are accustomed to the dynamic fluid flow induced forces like shear stress, stretching, and distortion. It is only intuitive to assume that these cells may have mechanosensory systems at play that help in perceiving the local environmental forces and responding accordingly to mitigate the effects of such forces.

One such receptor known to be expressed on TM cells is the transient receptor protein vanilloid IV (TRPV4) channel. TRPV4 ion channels are Ca^{2+} -permeable nonselective cation channels that are widely expressed in a variety of human tissues. Other than the TM, TRPV4 channels are expressed in several different ocular tissues including ciliary epithelium, corneal endothelium, and

retinal neurons. It is now known that TRPV4 plays a fundamental role in normal physiological processes, and its impairment results in various diseases. By virtue of them being Ca^{2+} influx channels, TRPV4 channels are positioned to regulate a wide array of functions related to maintaining cellular homeostasis. One revealing example of the physiological importance of TRPV4 channels is found in the vascular endothelium, wherein this channel contributes to intracellular Ca^{2+} homeostasis and regulation of cell volume while responding to the mechanical forces on the vasculature. Several reports have demonstrated that TRPV4 channels are sensitive to flow induced shear stress (66). Ca^{2+} influx mediated by activation of endothelial TRPV4 channels is essential for regulating arterial tone, maintaining shear stress-induced arterial vasodilation, as well as regulating membrane permeability. Interestingly, excessive activation of TRPV4 channel leads to circulatory collapse due to leakage of microvascular permeability barrier. Therefore, failure of normal TRPV4 channel expression and function can lead to disease pathology.

The TRPV4 gene is expressed on the long arm of chromosome 12 at position 24.1 (12q24.1). Among the TRPV family of proteins (TRPV1-6), TRPV1 is the best characterized ion channel with major advances made in determination of its structure (67). It is generally accepted that the findings made in TRPV1 channel structure are relevant in context of TRPV4 channels because there is high confidence that many of the structural features are similar. The putative TRPV4 protein is composed of 871 amino acid residues (68). It is normally assembled as a homotetramer, although existence of heterotetramers have been reported as well (69-71). Each TRPV4 monomer has six transmembrane alpha-helices (S1-S6) with a pore loop found between S5-S6 for cation entry. The carboxy and amino termini are located on the cytoplasmic side. The amino terminal of TRPV4 possess six ankyrin repeat domains (ARD). These are 33 residue sequence motifs, which serve as anchoring points for protein-protein interactions and are necessary for the channels to

function. The carboxyl terminus of the TRPV4, located adjacent to the pore loop domain, contains the TRP domain, which essential for tetramerization of TRPV4 channel subunits into functional channels. Furthermore, the carboxyl terminus is also responsible for protein folding, maturation, and trafficking to cell of TRPV4 channels to cell membranes. Finally, the pore region of TRPV4 comprises of a pore loop and two transmembrane domains (S5-S6) on either side. The S6 segments consisting of the pore are helical in structure with two constriction, one large and one small, which open upon different types of stimuli (67, 70, 72). Although TRPV4 is a multimodal channel that opens in response to several types of stimuli, it is not yet clear how the mechanical stress brings about the gating of TRPV4 channels when the channel is activated by flow or shear.

Shear stress evoked by flow, which may inevitably also involve stretch, is known to activate TRPV4 channels in vascular endothelium (66). As an important vasodilatory stimulus, flow increases Ca^{2+} concentration in endothelial cells. This Ca^{2+} response varies with different flow conditions. It has been shown that TRPV4 agonist GSK1016790A increases Ca^{2+} influx, which induces arterial dilation. In cells loaded with Ca^{2+} indicator and depleted of intracellular Ca^{2+} stores, high-speed confocal imaging revealed that TRPV4 activation resulted in Ca^{2+} influx events that were highly localized and transient. These events were named TRPV4 sparklets. The magnitudes of these events were quantal (per single channel), and up to four quantal levels were detected in an optical recording of a single site, indicating simultaneous Ca^{2+} influx through four closely positioned channels. Furthermore, opening of one channel transiently increases intracellular Ca^{2+} , which due the inherent cooperativity between these channels potentiates the activity of nearby TRPV4 channels. Strikingly, direct activation of fewer than three TRPV4 channels per endothelial cell was sufficient to induce maximal vasodilation (66, 73-75). These vasodilatory effects of TRPV4 are evidently mediated by downstream nitric oxide (NO) signaling.

Nitric oxide: a regulator of IOP

The discovery of NOs critical role in vasodilation marked a major advancement in the history of physiology. Thereafter, researchers began to explore the messenger molecule's functions beyond the vessel wall, and they soon recognized that NO was a remarkably versatile messenger playing a complex role in physiological activities of multiple human body systems. NO is a highly lipophilic and volatile gaseous second messenger molecule that is uniquely capable of diffusing readily through multiple cellular membranes. Its short half-life (<6 s) ensures temporal and spatial control of signaling. Endogenous NO is generated from the NOS-mediated reaction that converts L-arginine to L-citrulline. The NOS enzyme has three different isoforms: endothelial NOS (eNOS or NOS3), neuronal NOS (nNOS or NOS1), and inducible NOS (iNOS or NOS2), all encoded by different genes located on different chromosomes. Among the three NOS enzymes, eNOS and nNOS are constitutively expressed in cells of endothelial and neuronal origin respectively, and their activity is Ca^{2+} dependent. Unlike eNOS and nNOS, iNOS is not expressed under physiological conditions, instead its expression is induced in response to inflammatory cytokines or bacterial endotoxins. eNOS is a complex enzyme that requires a number of cofactors but is activated by the Ca^{2+} -dependent binding of calmodulin (45). Once released from the endothelium, NO stimulates soluble guanylate cyclase (sGC), resulting in a rise in cyclic-guanosine monophosphate (cGMP), activation of cGMP-dependent kinase (PKG) and various downstream cellular signaling mechanisms (59, 76-78).

NO has been implicated in numerous physiological processes of the eye, including IOP homeostasis and ocular blood flow (59, 79, 80). Recent studies indicate that NO lowers IOP by modulating TM contractile tone, cell volume and outflow resistance (77, 78, 81-85). Among the outflow pathway tissues, the human TM constitutively expresses eNOS (86). Interestingly,

downregulation of eNOS and upregulation of iNOS was observed in human POAG TM tissues (86). However, signaling mechanisms that regulate NOS activity in the TM remain unknown. In vascular tissues, it has been shown that endothelial TRPV4 channels promote eNOS activity and NO production, resulting in endothelium-dependent vasodilatory effects (66, 87-89). Shear stress has been shown to increase endogenous NO production in the outflow pathway tissues (90, 91), which leads to reduced cell volume and stiffness in outflow pathway cells (90). In the eye, eNOS and NO have an essential role in pressure homeostasis. eNOS is considered a pressure-dependent regulator of IOP (92). Treatment with exogenous NO donors has been reported to reduce IOP and increase outflow facility multiple animal models including mice (81), rabbit (76), non-human primates (84), and human *ex vivo* models (85). Recently, a chimeric prostaglandin analog with NO donating moiety has been approved by the FDA after successful clinical trials in human POAG patients (58, 93-97). The scope of these compounds is limited by the short half-life of NO and tendency of these NO donor compounds to prematurely release NO while *en route* to the TM. Therefore, targeted delivery of exogenous NO has been very challenging. Given its importance in pressure homeostasis, we are yet to unravel the intrinsic upstream mechanisms regulating eNOS activity within the eye. It is crucial to understand how endogenous NO is regulated in the TM to develop novel treatments specific to the conventional outflow pathway.

Significance

In POAG, morphological and biochemical changes at the TM results in increased resistance to AH outflow and chronic elevation of IOP. However, the exact cause of TM dysfunction and IOP elevation is yet to be elucidated. Therefore, it is critical to understand how TM regulates AH outflow facility and IOP homeostasis under physiological conditions in order to develop more specific treatments.

TM cells are in constant contact with the AH, and therefore are exposed to the dynamic fluid forces like shear stress, stretching, and distortion. Transient receptor potential vanilloid 4 (TRPV4) channels are Ca^{2+} -permeable cation channels that can be activated by flow-induced shear stress (98-101). Upon activation, TRPV4 channels allow localized Ca^{2+} influx (TRPV4 sparklets), which influences a variety of cellular homeostatic processes (75, 102). Previous studies have shown that TRPV4 channels are expressed in TM cells and tissues (103, 104). Moreover, selective TRPV4 channel activator GSK1016790A (GSK101) lowered IOP in rats and mice (103). Furthermore, baseline IOP was higher in global TRPV4^{-/-} mice compared to wildtype (WT) littermates (103). Another study by Ryskamp et al. demonstrated that inhibiting TRPV4 channels reduces elevated IOP in a microbead occlusion model of glaucoma (104) (105). The microbead occlusion model physically blocks TM outflow pathway, hence is not suitable for studying TM outflow. Unlike previously published reports, we sought to understand the role of TRPV4 channels in regulating the outflow facility and IOP under physiological conditions.

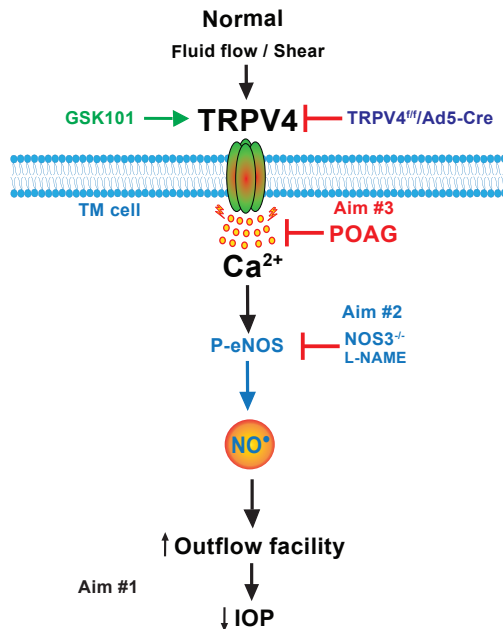
The specific objective of this study is to determine whether activation of the mechanosensory TRPV4 channels improve outflow facility and reduce IOP via eNOS-dependent NO signaling, and whether and whether TRPV4-NO signaling is impaired in glaucoma (Figure 1). Homeostatic systems use sensors to detect the change in the environment, and this input is used to bring the system back within the physiologically acceptable bounds. In the eye, IOP is maintained under strict homeostatic control (63). However, the exact mechanisms used to detect the changes in IOP and maintain homeostatic control are not completely understood. Mechanosensory TRPV4 channels have been previously implicated in regulation of IOP but evidence presented in the literature is inconclusive and contradictory. In this study, we demonstrate that TRPV4 activation via a specific agonist leads to rapid decrease in IOP and increase in outflow facility. It has been

shown in several different tissues that TRPV4 activation leads to eNOS-mediated NO production (87-89). NO is an important regulator of TM tone, and treatment with NO donors is known to reduce IOP (81, 83, 84). We propose that TRPV4 is an intrinsic regulator of endogenous NO in the TM. **We hypothesize that mechanosensory TRPV4 channels regulate IOP and outflow facility via activation of eNOS-dependent NO signaling in TM cells.**

In POAG, morphological and biochemical changes at the TM results in increased resistance to AH outflow and chronic elevation of IOP. However, the exact cause of TM dysfunction and IOP elevation is yet to be elucidated. **We further hypothesize that the TRPV4-eNOS signaling is impaired in context to POAG.**

The following are the three specific aims (Figure 1) investigated in this study:

Figure 1. Schematic of the study design.



- 1) **To determine whether mechanosensory TRPV4 channels regulate IOP and outflow facility.**

To address this aim, we first demonstrated that TRPV4 channels are expressed on the TM, and that these channels are functional at basal levels. Next we showed that TRPV4 channels in primary TM cells can be activated by shear stress, which leads to intracellular influx of Ca^{2+} that is transient and localized. In animal model of C57Bl/6J mice, we showed that topical instillation GSK101 eyedrops leads to rapid decrease in IOP that lasts for at least 24 hours. We also show that TRPV4 agonist GSK101 treatment results in a noticeable increase in outflow that is not statistically significant.

2) To determine whether TRPV4 mediated lowering of IOP is dependent on eNOS signaling.

To address this aim, we first show that shear stress leads to increase in NO production in primary TM cells, and that blocking TRPV4 channels diminish NO production. We next show in pharmacological activation of TRPV4 channels leads to increase in eNOS phosphorylation in primary TM cells and in ex vivo cultured human corneoscleral segments (Chapter III).

3) To determine whether TRPV4-eNOS signaling is impaired in glaucoma.

To address this aim, we first show that mechanical and pharmacological activation of TRPV4 channels does not lead to increase in TRPV4 sparklet activity in glaucomatous primary human TM cells. TRPV4-mediated NO production is also impaired in glaucomatous primary TM cells compared to normal TM cells. Lastly, we show that despite the functional difference between normal and glaucoma TM cells, there is no significant differences in expression of eNOS and TRPV4 protein levels.

REFERENCES

1. Quigley HA, Broman AT. The number of people with glaucoma worldwide in 2010 and 2020. *Br J Ophthalmol*. 2006;90(3):262-7. Epub 2006/02/21. doi: 10.1136/bjo.2005.081224. PubMed PMID: 16488940; PMCID: PMC1856963.
2. Tham YC, Li X, Wong TY, Quigley HA, Aung T, Cheng CY. Global prevalence of glaucoma and projections of glaucoma burden through 2040: a systematic review and meta-analysis. *Ophthalmology*. 2014;121(11):2081-90. Epub 2014/07/01. doi: 10.1016/j.ophtha.2014.05.013. PubMed PMID: 24974815.
3. Omoti AE, Edema OT. A review of the risk factors in primary open angle glaucoma. *Niger J Clin Pract*. 2007;10(1):79-82. Epub 2007/08/03. PubMed PMID: 17668721.
4. Rosenthal J, Leske MC. Open-angle glaucoma risk factors applied to clinical area. *J Am Optom Assoc*. 1980;51(11):1017-24. Epub 1980/11/01. PubMed PMID: 7440868.
5. Weinreb RN, Leung CK, Crowston JG, Medeiros FA, Friedman DS, Wiggs JL, Martin KR. Primary open-angle glaucoma. *Nat Rev Dis Primers*. 2016;2:16067. Epub 2016/09/23. doi: 10.1038/nrdp.2016.67. PubMed PMID: 27654570.

6. Tielsch JM, Sommer A, Katz J, Royall RM, Quigley HA, Javitt J. Racial variations in the prevalence of primary open-angle glaucoma. The Baltimore Eye Survey. *JAMA*. 1991;266(3):369-74. Epub 1991/07/17. PubMed PMID: 2056646.
7. Tielsch JM, Katz J, Sommer A, Quigley HA, Javitt JC. Family history and risk of primary open angle glaucoma. The Baltimore Eye Survey. *Arch Ophthalmol*. 1994;112(1):69-73. Epub 1994/01/01. doi: 10.1001/archopht.1994.01090130079022. PubMed PMID: 8285897.
8. Wolfs RC, Klaver CC, Ramrattan RS, van Duijn CM, Hofman A, de Jong PT. Genetic risk of primary open-angle glaucoma. Population-based familial aggregation study. *Arch Ophthalmol*. 1998;116(12):1640-5. Epub 1998/12/31. doi: 10.1001/archopht.116.12.1640. PubMed PMID: 9869795.
9. Stone EM, Fingert JH, Alward WL, Nguyen TD, Polansky JR, Sunden SL, Nishimura D, Clark AF, Nystuen A, Nichols BE, Mackey DA, Ritch R, Kalenak JW, Craven ER, Sheffield VC. Identification of a gene that causes primary open angle glaucoma. *Science*. 1997;275(5300):668-70. Epub 1997/01/31. doi: 10.1126/science.275.5300.668. PubMed PMID: 9005853.
10. Rezaie T, Child A, Hitchings R, Brice G, Miller L, Coca-Prados M, Heon E, Krupin T, Ritch R, Kreutzer D, Crick RP, Sarfarazi M. Adult-onset primary open-angle glaucoma caused by mutations in optineurin. *Science*. 2002;295(5557):1077-9. Epub 2002/02/09. doi: 10.1126/science.1066901. PubMed PMID: 11834836.

11. Fingert JH, Heon E, Liebmann JM, Yamamoto T, Craig JE, Rait J, Kawase K, Hoh ST, Buys YM, Dickinson J, Hockey RR, Williams-Lyn D, Trope G, Kitazawa Y, Ritch R, Mackey DA, Alward WL, Sheffield VC, Stone EM. Analysis of myocilin mutations in 1703 glaucoma patients from five different populations. *Hum Mol Genet.* 1999;8(5):899-905. Epub 1999/04/10. doi: 10.1093/hmg/8.5.899. PubMed PMID: 10196380.

12. Libby RT, Gould DB, Anderson MG, John SW. Complex genetics of glaucoma susceptibility. *Annu Rev Genomics Hum Genet.* 2005;6:15-44. Epub 2005/08/30. doi: 10.1146/annurev.genom.6.080604.162209. PubMed PMID: 16124852.

13. Foster PJ, Oen FT, Machin D, Ng TP, Devereux JG, Johnson GJ, Khaw PT, Seah SK. The prevalence of glaucoma in Chinese residents of Singapore: a cross-sectional population survey of the Tanjong Pagar district. *Arch Ophthalmol.* 2000;118(8):1105-11. Epub 2000/08/02. doi: 10.1001/archopht.118.8.1105. PubMed PMID: 10922206.

14. Ramakrishnan R, Nirmalan PK, Krishnadas R, Thulasiraj RD, Tielsch JM, Katz J, Friedman DS, Robin AL. Glaucoma in a rural population of southern India: the Aravind comprehensive eye survey. *Ophthalmology.* 2003;110(8):1484-90. Epub 2003/08/15. doi: 10.1016/S0161-6420(03)00564-5. PubMed PMID: 12917161.

15. Leske MC, Connell AM, Schachat AP, Hyman L. The Barbados Eye Study. Prevalence of open angle glaucoma. *Arch Ophthalmol.* 1994;112(6):821-9. Epub 1994/06/01. doi: 10.1001/archopht.1994.01090180121046. PubMed PMID: 8002842.

16. Dielemans I, Vingerling JR, Wolfs RC, Hofman A, Grobbee DE, de Jong PT. The prevalence of primary open-angle glaucoma in a population-based study in The Netherlands. The Rotterdam Study. *Ophthalmology*. 1994;101(11):1851-5. Epub 1994/11/01. doi: 10.1016/s0161-6420(94)31090-6. PubMed PMID: 7800368.
17. Leibowitz HM, Krueger DE, Maunder LR, Milton RC, Kini MM, Kahn HA, Nickerson RJ, Pool J, Colton TL, Ganley JP, Loewenstein JJ, Dawber TR. The Framingham Eye Study monograph: An ophthalmological and epidemiological study of cataract, glaucoma, diabetic retinopathy, macular degeneration, and visual acuity in a general population of 2631 adults, 1973-1975. *Surv Ophthalmol*. 1980;24(Suppl):335-610. Epub 1980/05/01. PubMed PMID: 7444756.
18. Mitchell P, Smith W, Attebo K, Healey PR. Prevalence of open-angle glaucoma in Australia. The Blue Mountains Eye Study. *Ophthalmology*. 1996;103(10):1661-9. Epub 1996/10/01. doi: 10.1016/s0161-6420(96)30449-1. PubMed PMID: 8874440.
19. Dandona L, Dandona R, Srinivas M, Mandal P, John RK, McCarty CA, Rao GN. Open-angle glaucoma in an urban population in southern India: the Andhra Pradesh eye disease study. *Ophthalmology*. 2000;107(9):1702-9. Epub 2000/08/31. doi: 10.1016/s0161-6420(00)00275-x. PubMed PMID: 10964833.
20. Coffey M, Reidy A, Wormald R, Xian WX, Wright L, Courtney P. Prevalence of glaucoma in the west of Ireland. *Br J Ophthalmol*. 1993;77(1):17-21. Epub 1993/01/01. doi: 10.1136/bjo.77.1.17. PubMed PMID: 8435391; PMCID: PMC504415.

21. Liang YB, Friedman DS, Zhou Q, Yang X, Sun LP, Guo LX, Tao QS, Chang DS, Wang NL, Handan Eye Study G. Prevalence of primary open angle glaucoma in a rural adult Chinese population: the Handan eye study. *Invest Ophthalmol Vis Sci.* 2011;52(11):8250-7. Epub 2011/09/08. doi: 10.1167/iovs.11-7472. PubMed PMID: 21896871.
22. Quigley HA. Glaucoma. *Lancet.* 2011;377(9774):1367-77. Epub 2011/04/02. doi: 10.1016/S0140-6736(10)61423-7. PubMed PMID: 21453963.
23. Kass MA, Heuer DK, Higginbotham EJ, Johnson CA, Keltner JL, Miller JP, Parrish RK, 2nd, Wilson MR, Gordon MO. The Ocular Hypertension Treatment Study: a randomized trial determines that topical ocular hypotensive medication delays or prevents the onset of primary open-angle glaucoma. *Arch Ophthalmol.* 2002;120(6):701-13; discussion 829-30. Epub 2002/06/07. doi: 10.1001/archopht.120.6.701. PubMed PMID: 12049574.
24. Leske MC, Heijl A, Hussein M, Bengtsson B, Hyman L, Komaroff E, Early Manifest Glaucoma Trial G. Factors for glaucoma progression and the effect of treatment: the early manifest glaucoma trial. *Arch Ophthalmol.* 2003;121(1):48-56. Epub 2003/01/14. doi: 10.1001/archopht.121.1.48. PubMed PMID: 12523884.
25. Buhrmann RR, Quigley HA, Barron Y, West SK, Oliva MS, Mmbaga BB. Prevalence of glaucoma in a rural East African population. *Invest Ophthalmol Vis Sci.* 2000;41(1):40-8. Epub 2000/01/14. PubMed PMID: 10634599.

26. Sommer A, Tielsch JM, Katz J, Quigley HA, Gottsch JD, Javitt J, Singh K. Relationship between intraocular pressure and primary open angle glaucoma among white and black Americans. The Baltimore Eye Survey. *Arch Ophthalmol.* 1991;109(8):1090-5. Epub 1991/08/01. doi: 10.1001/archopht.1991.01080080050026. PubMed PMID: 1867550.

27. Cartwright MJ, Anderson DR. Correlation of asymmetric damage with asymmetric intraocular pressure in normal-tension glaucoma (low-tension glaucoma). *Arch Ophthalmol.* 1988;106(7):898-900. Epub 1988/07/01. doi: 10.1001/archopht.1988.01060140044020. PubMed PMID: 3390051.

28. Crichton A, Drance SM, Douglas GR, Schulzer M. Unequal intraocular pressure and its relation to asymmetric visual field defects in low-tension glaucoma. *Ophthalmology.* 1989;96(9):1312-4. Epub 1989/09/01. doi: 10.1016/s0161-6420(89)32721-7. PubMed PMID: 2779999.

29. Comparison of glaucomatous progression between untreated patients with normal-tension glaucoma and patients with therapeutically reduced intraocular pressures. Collaborative Normal-Tension Glaucoma Study Group. *Am J Ophthalmol.* 1998;126(4):487-97. Epub 1998/10/21. doi: 10.1016/s0002-9394(98)00223-2. PubMed PMID: 9780093.

30. Jocson VL, Sears ML. Experimental aqueous perfusion in enucleated human eyes. Results after obstruction of Schlemm's canal. *Arch Ophthalmol.* 1971;86(1):65-71. Epub 1971/07/01. doi: 10.1001/archopht.1971.01000010067013. PubMed PMID: 5561383.

31. Bill A, Phillips CI. Uveoscleral drainage of aqueous humour in human eyes. *Exp Eye Res.* 1971;12(3):275-81. Epub 1971/11/01. doi: 10.1016/0014-4835(71)90149-7. PubMed PMID: 5130270.
32. Pederson JE, Gaasterland DE, MacLellan HM. Uveoscleral aqueous outflow in the rhesus monkey: importance of uveal reabsorption. *Invest Ophthalmol Vis Sci.* 1977;16(11):1008-7. Epub 1977/11/01. PubMed PMID: 410750.
33. Flocks M. The anatomy of the trabecular meshwork as seen in tangential section. *AMA Arch Ophthalmol.* 1956;56(5):708-18. Epub 1956/11/01. doi: 10.1001/archopht.1956.00930040716010. PubMed PMID: 13361636.
34. Fine BS. Observations on the Drainage Angle in Man and Rhesus Monkey: A Concept of the Pathogenesis of Chronic Simple Glaucoma. A Light and Electron Microscopic Study. *Invest Ophthalmol.* 1964;3:609-46. Epub 1964/12/01. PubMed PMID: 14238875.
35. Rohen JW, Rentsch FJ. [Morphology of Schlemm's canal and related vessels in the human eye]. *Albrecht Von Graefes Arch Klin Exp Ophthalmol.* 1968;176(4):309-29. Epub 1968/01/01. doi: 10.1007/BF00421587. PubMed PMID: 5305008.
36. Grant WM. Experimental aqueous perfusion in enucleated human eyes. *Arch Ophthalmol.* 1963;69:783-801. Epub 1963/06/01. doi: 10.1001/archopht.1963.00960040789022. PubMed PMID: 13949877.

37. Weinreb RN, Toris CB, Gabelt BT, Lindsey JD, Kaufman PL. Effects of prostaglandins on the aqueous humor outflow pathways. *Surv Ophthalmol.* 2002;47 Suppl 1:S53-64. Epub 2002/09/03. doi: 10.1016/s0039-6257(02)00306-5. PubMed PMID: 12204701.
38. Wang K, Johnstone MA, Xin C, Song S, Padilla S, Vranka JA, Acott TS, Zhou K, Schwaner SA, Wang RK, Sulchek T, Ethier CR. Estimating Human Trabecular Meshwork Stiffness by Numerical Modeling and Advanced OCT Imaging. *Invest Ophthalmol Vis Sci.* 2017;58(11):4809-17. Epub 2017/10/04. doi: 10.1167/iovs.17-22175. PubMed PMID: 28973327; PMCID: PMC5624775.
39. Wang K, Read AT, Sulchek T, Ethier CR. Trabecular meshwork stiffness in glaucoma. *Exp Eye Res.* 2017;158:3-12. Epub 2016/07/28. doi: 10.1016/j.exer.2016.07.011. PubMed PMID: 27448987; PMCID: PMC6501821.
40. Lutjen-Drecoll E, Shimizu T, Rohrbach M, Rohen JW. Quantitative analysis of 'plaque material' in the inner- and outer wall of Schlemm's canal in normal- and glaucomatous eyes. *Exp Eye Res.* 1986;42(5):443-55. Epub 1986/05/01. doi: 10.1016/0014-4835(86)90004-7. PubMed PMID: 3720863.
41. Rohen JW, Lutjen-Drecoll E, Flugel C, Meyer M, Grierson I. Ultrastructure of the trabecular meshwork in untreated cases of primary open-angle glaucoma (POAG). *Exp Eye Res.* 1993;56(6):683-92. Epub 1993/06/01. doi: 10.1006/exer.1993.1085. PubMed PMID: 8595810.

42. Woodward DF, Krauss AH, Chen J, Lai RK, Spada CS, Burk RM, Andrews SW, Shi L, Liang Y, Kedzie KM, Chen R, Gil DW, Kharlamb A, Archeampong A, Ling J, Madhu C, Ni J, Rix P, Usansky J, Usansky H, Weber A, Welty D, Yang W, Tang-Liu DD, Garst ME, Brar B, Wheeler LA, Kaplan LJ. The pharmacology of bimatoprost (Lumigan). *Surv Ophthalmol.* 2001;45 Suppl 4:S337-45. Epub 2001/07/04. doi: 10.1016/s0039-6257(01)00224-7. PubMed PMID: 11434936.
43. Toris CB, Camras CB, Yablonski ME, Brubaker RF. Effects of exogenous prostaglandins on aqueous humor dynamics and blood-aqueous barrier function. *Surv Ophthalmol.* 1997;41 Suppl 2:S69-75. Epub 1997/02/01. doi: 10.1016/s0039-6257(97)80010-0. PubMed PMID: 9154279.
44. Bill A. Uveoscleral drainage of aqueous humor: physiology and pharmacology. *Prog Clin Biol Res.* 1989;312:417-27. Epub 1989/01/01. PubMed PMID: 2678147.
45. Camras CB, Alm A, Watson P, Stjernschantz J. Latanoprost, a prostaglandin analog, for glaucoma therapy. Efficacy and safety after 1 year of treatment in 198 patients. Latanoprost Study Groups. *Ophthalmology.* 1996;103(11):1916-24. Epub 1996/11/01. doi: 10.1016/s0161-6420(96)30407-7. PubMed PMID: 8942890.
46. Coakes RL, Brubaker RF. The mechanism of timolol in lowering intraocular pressure. In the normal eye. *Arch Ophthalmol.* 1978;96(11):2045-8. Epub 1978/11/01. doi: 10.1001/archopht.1978.03910060433007. PubMed PMID: 363105.

47. Lutjen-Drecoll E, Lonnerholm G, Eichhorn M. Carbonic anhydrase distribution in the human and monkey eye by light and electron microscopy. *Graefes Arch Clin Exp Ophthalmol.* 1983;220(6):285-91. Epub 1983/01/01. doi: 10.1007/BF00231357. PubMed PMID: 6414890.
48. Dailey RA, Brubaker RF, Bourne WM. The effects of timolol maleate and acetazolamide on the rate of aqueous formation in normal human subjects. *Am J Ophthalmol.* 1982;93(2):232-7. Epub 1982/02/01. doi: 10.1016/0002-9394(82)90419-6. PubMed PMID: 7039328.
49. Gaasterland D, Kupfer C, Ross K. Studies of aqueous humor dynamics in man. IV. Effects of pilocarpine upon measurements in young normal volunteers. *Invest Ophthalmol.* 1975;14(11):848-53. Epub 1975/11/01. PubMed PMID: 1184317.
50. Chen S, Waxman S, Wang C, Atta S, Loewen R, Loewen NA. Dose-dependent effects of netarsudil, a Rho-kinase inhibitor, on the distal outflow tract. *Graefes Arch Clin Exp Ophthalmol.* 2020;258(6):1211-6. Epub 2020/05/07. doi: 10.1007/s00417-020-04691-y. PubMed PMID: 32372330; PMCID: PMC7237522.
51. Aref AA, Geyman LS, Zakieh AR, Alotaibi HM. Netarsudil and latanoprost ophthalmic solution for the reduction of intraocular pressure in open-angle glaucoma or ocular hypertension. *Expert Rev Clin Pharmacol.* 2019;12(12):1073-9. Epub 2019/12/18. doi: 10.1080/17512433.2019.1701435. PubMed PMID: 31842637.

52. Berrino E, Supuran CT. Rho-kinase inhibitors in the management of glaucoma. *Expert Opin Ther Pat.* 2019;29(10):817-27. Epub 2019/10/02. doi: 10.1080/13543776.2019.1670812. PubMed PMID: 31573364.
53. Ren R, Li G, Le TD, Kopczynski C, Stamer WD, Gong H. Netarsudil Increases Outflow Facility in Human Eyes Through Multiple Mechanisms. *Invest Ophthalmol Vis Sci.* 2016;57(14):6197-209. Epub 2016/11/15. doi: 10.1167/iovs.16-20189. PubMed PMID: 27842161; PMCID: PMC5114035.
54. Sturdivant JM, Royalty SM, Lin CW, Moore LA, Yingling JD, Laethem CL, Sherman B, Heintzelman GR, Kopczynski CC, deLong MA. Discovery of the ROCK inhibitor netarsudil for the treatment of open-angle glaucoma. *Bioorg Med Chem Lett.* 2016;26(10):2475-80. Epub 2016/04/14. doi: 10.1016/j.bmcl.2016.03.104. PubMed PMID: 27072905.
55. Fingeret M, Gaddie IB, Bloomenstein M. Latanoprostene bunod ophthalmic solution 0.024%: a new treatment option for open-angle glaucoma and ocular hypertension. *Clin Exp Optom.* 2019. Epub 2019/01/08. doi: 10.1111/cxo.12853. PubMed PMID: 30614563.
56. Addis VM, Miller-Ellis E. Latanoprostene bunod ophthalmic solution 0.024% in the treatment of open-angle glaucoma: design, development, and place in therapy. *Clin Ophthalmol.* 2018;12:2649-57. Epub 2018/12/28. doi: 10.2147/OPHTH.S156038. PubMed PMID: 30587912; PMCID: PMC6304237.
57. Latanoprostene Bunod. *Drugs and Lactation Database (LactMed).* Bethesda (MD)2006.

58. Weinreb RN, Liebmann JM, Martin KR, Kaufman PL, Vittitow JL. Latanoprostene Bunod 0.024% in Subjects With Open-angle Glaucoma or Ocular Hypertension: Pooled Phase 3 Study Findings. *J Glaucoma*. 2018;27(1):7-15. Epub 2017/12/02. doi: 10.1097/IJG.0000000000000831. PubMed PMID: 29194198.
59. Aliancy J, Stamer WD, Wirostko B. A Review of Nitric Oxide for the Treatment of Glaucomatous Disease. *Ophthalmol Ther*. 2017;6(2):221-32. Epub 2017/06/07. doi: 10.1007/s40123-017-0094-6. PubMed PMID: 28584936; PMCID: PMC5693832.
60. Kaufman PL. Latanoprostene bunod ophthalmic solution 0.024% for IOP lowering in glaucoma and ocular hypertension. *Expert Opin Pharmacother*. 2017;18(4):433-44. Epub 2017/02/25. doi: 10.1080/14656566.2017.1293654. PubMed PMID: 28234563.
61. Rulli E, Biagioli E, Riva I, Gambirasio G, De Simone I, Floriani I, Quaranta L. Efficacy and safety of trabeculectomy vs nonpenetrating surgical procedures: a systematic review and meta-analysis. *JAMA Ophthalmol*. 2013;131(12):1573-82. Epub 2013/10/26. doi: 10.1001/jamaophthalmol.2013.5059. PubMed PMID: 24158640.
62. Gedde SJ, Herndon LW, Brandt JD, Budenz DL, Feuer WJ, Schiffman JC, Tube Versus Trabeculectomy Study G. Postoperative complications in the Tube Versus Trabeculectomy (TVT) study during five years of follow-up. *Am J Ophthalmol*. 2012;153(5):804-14 e1. Epub 2012/01/17. doi: 10.1016/j.ajo.2011.10.024. PubMed PMID: 22244522; PMCID: PMC3653167.

63. Acott TS, Kelley MJ, Keller KE, Vranka JA, Abu-Hassan DW, Li X, Aga M, Bradley JM. Intraocular pressure homeostasis: maintaining balance in a high-pressure environment. *J Ocul Pharmacol Ther.* 2014;30(2-3):94-101. Epub 2014/01/10. doi: 10.1089/jop.2013.0185. PubMed PMID: 24401029; PMCID: PMC3991985.
64. Downs JC, Burgoyne CF, Seigfreid WP, Reynaud JF, Strouthidis NG, Sallee V. 24-hour IOP telemetry in the nonhuman primate: implant system performance and initial characterization of IOP at multiple timescales. *Invest Ophthalmol Vis Sci.* 2011;52(10):7365-75. Epub 2011/07/28. doi: 10.1167/iovs.11-7955. PubMed PMID: 21791586; PMCID: PMC3183973.
65. Bradley JM, Kelley MJ, Zhu X, Anderssohn AM, Alexander JP, Acott TS. Effects of mechanical stretching on trabecular matrix metalloproteinases. *Invest Ophthalmol Vis Sci.* 2001;42(7):1505-13. Epub 2001/05/31. PubMed PMID: 11381054.
66. Hill-Eubanks DC, Gonzales AL, Sonkusare SK, Nelson MT. Vascular TRP channels: performing under pressure and going with the flow. *Physiology (Bethesda).* 2014;29(5):343-60. Epub 2014/09/03. doi: 10.1152/physiol.00009.2014. PubMed PMID: 25180264; PMCID: PMC4214829.
67. Liao M, Cao E, Julius D, Cheng Y. Structure of the TRPV1 ion channel determined by electron cryo-microscopy. *Nature.* 2013;504(7478):107-12. Epub 2013/12/07. doi: 10.1038/nature12822. PubMed PMID: 24305160; PMCID: PMC4078027.

68. Strotmann R, Harteneck C, Nunnenmacher K, Schultz G, Plant TD. OTRPC4, a nonselective cation channel that confers sensitivity to extracellular osmolarity. *Nat Cell Biol.* 2000;2(10):695-702. Epub 2000/10/12. doi: 10.1038/35036318. PubMed PMID: 11025659.
69. Stewart AP, Smith GD, Sandford RN, Edwardson JM. Atomic force microscopy reveals the alternating subunit arrangement of the TRPP2-TRPV4 heterotetramer. *Biophys J.* 2010;99(3):790-7. Epub 2010/08/05. doi: 10.1016/j.bpj.2010.05.012. PubMed PMID: 20682256; PMCID: PMC2913176.
70. Shigematsu H, Sokabe T, Danev R, Tominaga M, Nagayama K. A 3.5-nm structure of rat TRPV4 cation channel revealed by Zernike phase-contrast cryoelectron microscopy. *J Biol Chem.* 2010;285(15):11210-8. Epub 2010/01/02. doi: 10.1074/jbc.M109.090712. PubMed PMID: 20044482; PMCID: PMC2856998.
71. Hellwig N, Albrecht N, Harteneck C, Schultz G, Schaefer M. Homo- and heteromeric assembly of TRPV channel subunits. *J Cell Sci.* 2005;118(Pt 5):917-28. Epub 2005/02/17. doi: 10.1242/jcs.01675. PubMed PMID: 15713749.
72. Jin X, Touhey J, Gaudet R. Structure of the N-terminal ankyrin repeat domain of the TRPV2 ion channel. *J Biol Chem.* 2006;281(35):25006-10. Epub 2006/07/01. doi: 10.1074/jbc.C600153200. PubMed PMID: 16809337.

73. Chen YL, Sonkusare SK. Endothelial TRPV4 channels and vasodilator reactivity. *Curr Top Membr.* 2020;85:89-117. Epub 2020/05/14. doi: 10.1016/bs.ctm.2020.01.007. PubMed PMID: 32402646.
74. Sonkusare SK, Dalsgaard T, Bonev AD, Hill-Eubanks DC, Kotlikoff MI, Scott JD, Santana LF, Nelson MT. AKAP150-dependent cooperative TRPV4 channel gating is central to endothelium-dependent vasodilation and is disrupted in hypertension. *Sci Signal.* 2014;7(333):ra66. Epub 2014/07/10. doi: 10.1126/scisignal.2005052. PubMed PMID: 25005230; PMCID: PMC4403000.
75. Sonkusare SK, Bonev AD, Ledoux J, Liedtke W, Kotlikoff MI, Heppner TJ, Hill-Eubanks DC, Nelson MT. Elementary Ca²⁺ signals through endothelial TRPV4 channels regulate vascular function. *Science.* 2012;336(6081):597-601. Epub 2012/05/05. doi: 10.1126/science.1216283. PubMed PMID: 22556255; PMCID: PMC3715993.
76. Kotikoski H, Alajuuma P, Moilanen E, Salmenpera P, Oksala O, Laippala P, Vapaatalo H. Comparison of nitric oxide donors in lowering intraocular pressure in rabbits: role of cyclic GMP. *J Ocul Pharmacol Ther.* 2002;18(1):11-23. Epub 2002/02/23. doi: 10.1089/108076802317233171. PubMed PMID: 11858611.
77. Dismuke WM, Sharif NA, Ellis DZ. Human trabecular meshwork cell volume decrease by NO-independent soluble guanylate cyclase activators YC-1 and BAY-58-2667 involves the BKCa ion channel. *Invest Ophthalmol Vis Sci.* 2009;50(7):3353-9. Epub 2009/02/24. doi: 10.1167/iovs.08-3127. PubMed PMID: 19234350.

78. Dismuke WM, Liang J, Overby DR, Stamer WD. Concentration-related effects of nitric oxide and endothelin-1 on human trabecular meshwork cell contractility. *Exp Eye Res.* 2014;120:28-35. Epub 2014/01/01. doi: 10.1016/j.exer.2013.12.012. PubMed PMID: 24374036; PMCID: PMC3943640.
79. Toda N, Nakanishi-Toda M. Nitric oxide: ocular blood flow, glaucoma, and diabetic retinopathy. *Prog Retin Eye Res.* 2007;26(3):205-38. Epub 2007/03/06. doi: 10.1016/j.preteyeres.2007.01.004. PubMed PMID: 17337232.
80. Wareham LK, Buys ES, Sappington RM. The nitric oxide-guanylate cyclase pathway and glaucoma. *Nitric Oxide.* 2018;77:75-87. Epub 2018/05/04. doi: 10.1016/j.niox.2018.04.010. PubMed PMID: 29723581; PMCID: PMC6424573.
81. Chang JY, Stamer WD, Bertrand J, Read AT, Marando CM, Ethier CR, Overby DR. Role of nitric oxide in murine conventional outflow physiology. *Am J Physiol Cell Physiol.* 2015;309(4):C205-14. doi: 10.1152/ajpcell.00347.2014. PubMed PMID: 26040898; PMCID: PMC4537932.
82. Dismuke WM, Mbadugha CC, Ellis DZ. NO-induced regulation of human trabecular meshwork cell volume and aqueous humor outflow facility involve the BKCa ion channel. *Am J Physiol Cell Physiol.* 2008;294(6):C1378-86. Epub 2008/04/04. doi: 10.1152/ajpcell.00363.2007. PubMed PMID: 18385281.

83. Ellis DZ, Sharif NA, Dismuke WM. Endogenous regulation of human Schlemm's canal cell volume by nitric oxide signaling. *Invest Ophthalmol Vis Sci.* 2010;51(11):5817-24. Epub 2010/05/21. doi: 10.1167/iovs.09-5072. PubMed PMID: 20484594.
84. Heyne GW, Kiland JA, Kaufman PL, Gabelt BT. Effect of nitric oxide on anterior segment physiology in monkeys. *Invest Ophthalmol Vis Sci.* 2013;54(7):5103-10. Epub 2013/06/27. doi: 10.1167/iovs.12-11491. PubMed PMID: 23800771; PMCID: PMC3729238.
85. Schneemann A, Dijkstra BG, van den Berg TJ, Kamphuis W, Hoyng PF. Nitric oxide/guanylate cyclase pathways and flow in anterior segment perfusion. *Graefes Arch Clin Exp Ophthalmol.* 2002;240(11):936-41. Epub 2002/12/18. doi: 10.1007/s00417-002-0559-7. PubMed PMID: 12486517.
86. Fernandez-Durango R, Fernandez-Martinez A, Garcia-Feijoo J, Castillo A, de la Casa JM, Garcia-Bueno B, Perez-Nievas BG, Fernandez-Cruz A, Leza JC. Expression of nitrotyrosine and oxidative consequences in the trabecular meshwork of patients with primary open-angle glaucoma. *Invest Ophthalmol Vis Sci.* 2008;49(6):2506-11. Epub 2008/02/26. doi: 10.1167/iovs.07-1363. PubMed PMID: 18296660.
87. Marziano C, Hong K, Cope EL, Kotlikoff MI, Isakson BE, Sonkusare SK. Nitric Oxide-Dependent Feedback Loop Regulates Transient Receptor Potential Vanilloid 4 (TRPV4) Channel Cooperativity and Endothelial Function in Small Pulmonary Arteries. *J Am Heart Assoc.* 2017;6(12). Epub 2017/12/25. doi: 10.1161/JAHA.117.007157. PubMed PMID: 29275372; PMCID: PMC5779028.

88. Cabral PD, Garvin JL. TRPV4 activation mediates flow-induced nitric oxide production in the rat thick ascending limb. *Am J Physiol Renal Physiol*. 2014;307(6):F666-72. doi: 10.1152/ajprenal.00619.2013. PubMed PMID: 24966090; PMCID: PMC4166729.
89. Sukumaran SV, Singh TU, Parida S, Narasimha Reddy Ch E, Thangamalai R, Kandasamy K, Singh V, Mishra SK. TRPV4 channel activation leads to endothelium-dependent relaxation mediated by nitric oxide and endothelium-derived hyperpolarizing factor in rat pulmonary artery. *Pharmacol Res*. 2013;78:18-27. Epub 2013/10/01. doi: 10.1016/j.phrs.2013.09.005. PubMed PMID: 24075884.
90. Ashpole NE, Overby DR, Ethier CR, Stamer WD. Shear stress-triggered nitric oxide release from Schlemm's canal cells. *Invest Ophthalmol Vis Sci*. 2014;55(12):8067-76. Epub 2014/11/15. doi: 10.1167/iovs.14-14722. PubMed PMID: 25395486; PMCID: PMC4266075.
91. McDonnell F, Perkumas KM, Ashpole NE, Kalnitsky J, Sherwood JM, Overby DR, Stamer WD. Shear Stress in Schlemm's Canal as a Sensor of Intraocular Pressure. *Sci Rep*. 2020;10(1):5804. Epub 2020/04/04. doi: 10.1038/s41598-020-62730-4. PubMed PMID: 32242066; PMCID: PMC7118084.
92. Stamer WD, Lei Y, Boussommier-Calleja A, Overby DR, Ethier CR. eNOS, a pressure-dependent regulator of intraocular pressure. *Invest Ophthalmol Vis Sci*. 2011;52(13):9438-44. doi: 10.1167/iovs.11-7839. PubMed PMID: 22039240; PMCID: PMC3293415.

93. Weinreb RN, Scassellati Sforzolini B, Vittitow J, Liebmann J. Latanoprostene Bunod 0.024% versus Timolol Maleate 0.5% in Subjects with Open-Angle Glaucoma or Ocular Hypertension: The APOLLO Study. *Ophthalmology*. 2016;123(5):965-73. Epub 2016/02/15. doi: 10.1016/j.ophtha.2016.01.019. PubMed PMID: 26875002.
94. Medeiros FA, Martin KR, Peace J, Scassellati Sforzolini B, Vittitow JL, Weinreb RN. Comparison of Latanoprostene Bunod 0.024% and Timolol Maleate 0.5% in Open-Angle Glaucoma or Ocular Hypertension: The LUNAR Study. *Am J Ophthalmol*. 2016;168:250-9. Epub 2016/05/24. doi: 10.1016/j.ajo.2016.05.012. PubMed PMID: 27210275.
95. Liu JHK, Slight JR, Vittitow JL, Scassellati Sforzolini B, Weinreb RN. Efficacy of Latanoprostene Bunod 0.024% Compared With Timolol 0.5% in Lowering Intraocular Pressure Over 24 Hours. *Am J Ophthalmol*. 2016;169:249-57. Epub 2016/07/28. doi: 10.1016/j.ajo.2016.04.019. PubMed PMID: 27457257.
96. Weinreb RN, Ong T, Scassellati Sforzolini B, Vittitow JL, Singh K, Kaufman PL, Group V. A randomised, controlled comparison of latanoprostene bunod and latanoprost 0.005% in the treatment of ocular hypertension and open angle glaucoma: the VOYAGER study. *Br J Ophthalmol*. 2015;99(6):738-45. Epub 2014/12/10. doi: 10.1136/bjophthalmol-2014-305908. PubMed PMID: 25488946; PMCID: PMC4453588.
97. Araie M, Sforzolini BS, Vittitow J, Weinreb RN. Evaluation of the Effect of Latanoprostene Bunod Ophthalmic Solution, 0.024% in Lowering Intraocular Pressure over 24 h

- in Healthy Japanese Subjects. *Adv Ther.* 2015;32(11):1128-39. Epub 2015/11/14. doi: 10.1007/s12325-015-0260-y. PubMed PMID: 26563323; PMCID: PMC4662725.
98. Darby WG, Potocnik S, Ramachandran R, Hollenberg MD, Woodman OL, McIntyre P. Shear stress sensitizes TRPV4 in endothelium-dependent vasodilatation. *Pharmacol Res.* 2018;133:152-9. Epub 2018/05/23. doi: 10.1016/j.phrs.2018.05.009. PubMed PMID: 29787869.
99. Mendoza SA, Fang J, Gutterman DD, Wilcox DA, Bubolz AH, Li R, Suzuki M, Zhang DX. TRPV4-mediated endothelial Ca²⁺ influx and vasodilation in response to shear stress. *Am J Physiol Heart Circ Physiol.* 2010;298(2):H466-76. Epub 2009/12/08. doi: 10.1152/ajpheart.00854.2009. PubMed PMID: 19966050; PMCID: PMC2822567.
100. Kohler R, Hoyer J. Role of TRPV4 in the Mechanotransduction of Shear Stress in Endothelial Cells. In: Liedtke WB, Heller S, editors. *TRP Ion Channel Function in Sensory Transduction and Cellular Signaling Cascades.* Boca Raton (FL)2007.
101. Hartmannsgruber V, Heyken WT, Kacik M, Kaistha A, Grgic I, Harteneck C, Liedtke W, Hoyer J, Kohler R. Arterial response to shear stress critically depends on endothelial TRPV4 expression. *PLoS One.* 2007;2(9):e827. Epub 2007/09/06. doi: 10.1371/journal.pone.0000827. PubMed PMID: 17786199; PMCID: PMC1959246.
102. White JP, Cibelli M, Urban L, Nilius B, McGeown JG, Nagy I. TRPV4: Molecular Conductor of a Diverse Orchestra. *Physiol Rev.* 2016;96(3):911-73. Epub 2016/06/03. doi: 10.1152/physrev.00016.2015. PubMed PMID: 27252279.

103. Luo N, Conwell MD, Chen X, Kettenhofen CI, Westlake CJ, Cantor LB, Wells CD, Weinreb RN, Corson TW, Spandau DF, Joos KM, Iomini C, Obukhov AG, Sun Y. Primary cilia signaling mediates intraocular pressure sensation. *Proc Natl Acad Sci U S A*. 2014;111(35):12871-6. doi: 10.1073/pnas.1323292111. PubMed PMID: 25143588; PMCID: PMC4156748.
104. Ryskamp DA, Frye AM, Phuong TT, Yarishkin O, Jo AO, Xu Y, Lakk M, Iuso A, Redmon SN, Ambati B, Hageman G, Prestwich GD, Torrejon KY, Krizaj D. TRPV4 regulates calcium homeostasis, cytoskeletal remodeling, conventional outflow and intraocular pressure in the mammalian eye. *Sci Rep*. 2016;6:30583. Epub 2016/08/12. doi: 10.1038/srep30583. PubMed PMID: 27510430; PMCID: PMC4980693.
105. Sappington RM, Carlson BJ, Crish SD, Calkins DJ. The microbead occlusion model: a paradigm for induced ocular hypertension in rats and mice. *Invest Ophthalmol Vis Sci*. 2010;51(1):207-16. Epub 2009/10/24. doi: 10.1167/iovs.09-3947. PubMed PMID: 19850836; PMCID: PMC2869054.

CHAPTER II

IMPAIRED TRPV4-ENOS SIGNALING IN TRABECULAR MESHWORK CONTRIBUTES TO ELEVATION OF INTRAOCULAR PRESSURE IN GLAUCOMA

Pinkal D. Patel¹, Ramesh Kasetti¹, Prabhavathi Maddineni¹, William Mayhew¹, J. Cameron
Millar¹, Yen-Lin Chen², Swapnil K. Sonkusare^{2*} and Gulab Zode^{1*}

¹Department of Pharmacology and Neuroscience, North Texas Eye Research Institute, University
of North Texas Health Science Center at Fort Worth, TX 76107, USA

²Molecular Physiology and Biological Physics, University of Virginia - School of Medicine,
Charlottesville, VA 22908, USA

ABSTRACT

Primary Open Angle Glaucoma (POAG) is the most common form of glaucoma that causes irreversible loss of vision. Sustained elevation of intraocular pressure (IOP) is a major risk factor associated with POAG. The trabecular meshwork (TM), a sieve-like tissue, has an intrinsic ability to sense the aqueous humor (AH) flow and maintain IOP homeostasis. Age-related pathological changes at the TM are known to increase aqueous humor (AH) outflow resistance and cause sustained IOP elevation, thereby contributing to glaucomatous pathophysiology. However, the exact flow-sensing mechanisms in TM that maintain IOP homeostasis are not yet completely understood. Using patch clamp analysis and high-speed calcium imaging, we unraveled the physiological role of transient receptor potential vanilloid 4 (TRPV4) channels in flow-sensing and maintaining IOP homeostasis at the TM. We demonstrate that functional TRPV4 channels expressed on the TM cells can be activated pharmacologically or mechanically via shear stress. We further show that pharmacological activation of TRPV4 channels in mouse eyes leads to lowering of IOP and improvement in outflow facility, and TM-specific loss of TRPV4 channels elevates IOP in conditional floxed TRPV4^{f/f} mice. We then examined the downstream signaling mechanism responsible for TRPV4-mediated lowering of IOP. Interestingly, we observed that TRPV4 channels in TM activate endothelial nitric oxide synthase (eNOS) to promote outflow facility and maintain IOP homeostasis. Activation of TRPV4 channels in the human TM cells and ex vivo cultured human TM tissue leads to initiation of eNOS signaling and production of

endogenous nitric oxide (NO). Using NOS3^{-/-} mice, we demonstrate that functional coupling of TRPV4-eNOS signaling is important in TRPV4-mediated lowering of IOP. To our knowledge, this is the first report demonstrating impairment of TRPV4 channel activity in glaucomatous TM cells. Furthermore, we show that TRPV4-eNOS_{TM} signaling is impaired in glaucoma. Together, our studies indicate that impaired TRPV4-eNOS signaling contributes to IOP elevation in glaucoma.

INTRODUCTION

Glaucoma is a heterogenic group of multifactorial neurodegenerative diseases characterized by progressive optic neuropathy. It is the leading cause of irreversible vision loss with more than 70 million people affected worldwide (1), and the prevalence is estimated to increase to 111.6 million by the year 2040 (2). Primary open angle glaucoma (POAG) is the most common form of glaucoma, accounting for approximately 70% of all cases (1). POAG is characterized by progressive loss of retinal ganglion cell (RGC) axons that can lead to an irreversible loss of vision (1, 3). Elevated intraocular pressure (IOP) is a major, and the only treatable risk factor associated with POAG (4). The trabecular meshwork (TM), a molecular sieve-like structure, maintains homeostatic control over IOP by constantly adjusting the resistance to aqueous humor (AH) outflow. In POAG, there is increased resistance to AH outflow, elevating IOP (5). This increase in AH outflow resistance is associated with dysfunction of the TM (6-8). The flow-sensing signaling mechanisms in TM and why these mechanisms fail to maintain IOP homeostasis in glaucoma are poorly understood.

The TM has an intrinsic ability to sense the AH flow and regulate outflow facility to maintain IOP homeostasis (6). Using *ex vivo* perfusion cultured human eyes, Bradley et al. demonstrated that TM outflow system detects elevated flow and adjusts the outflow resistance to restore pressure back to normal (9). However, these flow sensing mechanisms in TM cells are poorly understood. TM cells are in constant contact with the AH, and therefore are exposed to the dynamic fluid forces like shear stress, stretching, and distortion. Transient receptor potential vanilloid 4 (TRPV4) channels are Ca^{2+} -permeable cation channels that can be activated by flow-induced shear stress (10-13). Upon activation, TRPV4 channels allow localized Ca^{2+} influx (termed as TRPV4

sparklets), which influences a variety of cellular homeostatic processes (14, 15). Previous studies have shown that TRPV4 channels are expressed in TM cells and tissues (16, 17), and treatment with a selective TRPV4 channel activator GSK1016790A (GSK101) lowered IOP in rats and mice (16). Furthermore, baseline IOP was higher in global TRPV4^{-/-} mice compared to their wildtype (WT) littermates (16). Another study by Ryskamp et al. demonstrated that inhibiting TRPV4 channels reduces elevated IOP in a microbead occlusion model of glaucoma (17), which is a model used for studying glaucoma-like pathology in the back of the eye (18). These contradictory reports highlight a need to better understand the role of TRPV4 channels in TM function and physiological regulation of IOP. Using patch-clamp recordings and high-speed Ca²⁺ imaging, we show that functional TRPV4 channels are constitutively expressed on the TM cells, and these channels can be activated pharmacologically or mechanically via fluid-flow mediated shear stress. We further show the role of TRPV4 channels in regulating physiological IOP and AH outflow facility. We observed that TRPV4 activation via topical eyedrops reduces IOP and improves outflow facility. We also show that conditional knockout of TRPV4 in the eye leads to increase in IOP. We next proceeded to determining the downstream signaling mechanism responsible for TRPV-mediated lowering of IOP.

Nitric oxide (NO) has been implicated in numerous physiological processes of the eye, including IOP homeostasis and ocular blood flow (19-21). Recent studies indicate that NO lowers IOP by modulating TM contractile tone, cell volume, and outflow resistance (22-28). In the eye, NO is produced by nitric oxide synthase (NOS) family of enzymes, which includes neuronal nNOS, endothelial eNOS, and inducible iNOS. nNOS and eNOS are constitutive and are tightly regulated by Ca²⁺ signaling. On the contrary, iNOS is Ca²⁺-independent, and it is induced in response to immunologic or inflammatory stimuli. Among the outflow pathway tissues, TM is known to

constitutively expresses eNOS (29), which is a known regulator of outflow facility and IOP homeostasis (22, 24, 27, 30, 31). However, signaling mechanisms that regulate eNOS activity in the TM remain unknown. In vascular tissues, it has been reported that TRPV4 channels promote eNOS activity and cause vasodilation (32-35). Shear stress has been shown to increase endogenous NO production in conventional outflow pathway cells (36, 37). We show that pharmacological or shear-stress mediated mechanical activation of TRPV4 channels lead to initiation of eNOS signaling and endogenous NO production in primary human TM cells and ex vivo cultured human TM tissues. Using wildtype (WT) and NOS3^{-/-} mice, we further show that TRPV4-mediated lowering of IOP is eNOS-dependent. Our data reveal a functional coupling between TRPV4 channels and eNOS in the TM, which is important regulating physiological IOP homeostasis.

Glaucoma-associated pathological changes are known to cause TM dysfunction affecting several physiological processes (8). One of the hallmarks of the glaucomatous TM is its inability to maintain IOP homeostasis and regulate AH outflow resistance (6). However, the exact disease mechanism that contributes to glaucomatous pathophysiology is yet to be unraveled. In this study, we identify for the first time a glaucoma-associated functional impairment of TRPV4 channels, which may contribute to TM dysfunction and IOP dysregulation. We compared TRPV4-eNOS signaling in normal and glaucomatous primary human TM cells and report for the first time that TRPV4 activity is compromised in glaucomatous TM cells. Furthermore, we show that TRPV4-mediated activation of eNOS signaling and production of endogenous NO is significantly diminished in glaucomatous TM cells and ex vivo cultured TM tissues.

METHODS AND MATERIALS

Antibodies and reagents

Rabbit TRPV4 antibody (1:250; catalogue number ACC034; Alomone Labs), rabbit phospho-eNOS antibody (1:1000; catalog number PA5-35879; Thermo Fisher Scientific), rabbit Total eNOS antibody (1:100-500; catalog number NB300-500; Novus Biologicals), rabbit alpha-smooth muscle actin antibody (1:100; catalog number ab5694; Abcam), GSK1016790A (catalogue number G0798-10MG; Sigma Aldrich), GSK2193874 (catalogue number 5106; Tocris), NONOate (catalogue number 136587-13-8; Cayman Chemicals), pan-NOS inhibitor L-NAME (N5751-5G; Sigma Aldrich).

Animal models

Male and female C57BL/6J and NOS3^{-/-} mice on C57BL/6J background were obtained from the Jackson Laboratory (Bar Harbor, ME). TRPV4^{ff} mice on a C57BL/6J background were kindly gifted by Wolfgang B. Liedtke (Duke University School of Medicine, NC, USA) (38). All mice were 3-4 months old at the start of experiments. All mouse studies and care were performed in compliance with the Association for Research in Vision and Ophthalmology Statement of the Use of Animals in Ophthalmic and Vision Research and the University of North Texas Health Science Center Institutional Animal Care and Use Committee regulations (Approved protocol: IACUC2018-0032). Mice were housed under controlled temperature (21°C to 26°C) and humidity (40% to 70%), with a 12-hour light/12-hour dark cycle (8:00 PM to 8:00 AM). Food and water were provided ad libitum. The number of animals used in each experiment is indicated in the corresponding figure legends.

Intraocular Pressure (IOP) Measurement

Night-time Intraocular pressure (IOP) measurements in isoflurane anesthetized (2.5% isoflurane and 0.8 L/minute O₂) mice were performed using Tonolab rebound tonometry (Colonial Medical Supply) as previously described (39, 40). Nighttime IOPs were measured under low-intensity red light during night-time in dark-adapted conditions. An average of five individual readings was considered as one reading, and six such readings were recorded for each eye. All IOP measurements were taken in a masked manner.

Aqueous humor outflow facility measurement

Aqueous humor outflow facility (C) was measured in live anesthetized mice using constant-flow infusion method as described previously (41-43). Animals were anesthetized by intraperitoneal injections of 100/10 mg/kg ketamine/xylazine cocktail. A quarter to half of this dose was administered for maintenance of anesthesia as necessary. Both eyes were then administered a drop of proparacaine HCl (0.5%; Akorn Inc.) for topical anesthesia. Anesthetized mice were placed on a heated mat (37 °C) for maintenance of body temperature throughout the procedure. The anterior chambers of both eyes were cannulated (1-2 mm posterior to the limbus) using a 30-gauge needle inserted across the chamber carefully avoiding contact with the iris, lens capsule or epithelium. The cannula is connected to a calibrated BLPR-2 flow-through blood pressure transducer (World Precision Instruments; WPI) for the continuous determination of pressure within the eye. A topical ocular drop of sterile PBS (Amresco®, Solon) was also instilled upon each eye to prevent corneal drying. The opposing end of each transducer was connected to a 3-way valve, which in turn was connected to a 50 µL glass microsyringe (Hamilton Company) filled with sterile PBS (previously filtered through a 0.2 µm HT Tuffryn Membrane Acrodisc syringe filter; PALL Gelman

Laboratory) loaded into an SP101i microdialysis infusion pump (WPI), and (2) an open-ended, variable-height manometer. Signals from the pressure transducers were passed via a TBM4M Bridge Amplifier (WPI) and a Lab-Trax analog-to-digital converter (WPI) to a computer. Data were recorded using Lab-Scribe2 software (WPI). Eyes were initially infused at a constant flow rate of 0.1 $\mu\text{L}/\text{minute}$. Following stabilization of pressure after 10-30 minutes, pressure measurements were recorded over a 15-minute period, then the flow rates were increased sequentially to 0.2, 0.3, 0.4, and 0.5 $\mu\text{L}/\text{minute}$. For each flow rate, three stabilized pressures at 5-minute interval were recorded. Aqueous humor outflow facility (C) in each eye of each animal was calculated as the reciprocal of a slope mean stabilized pressure across the different flow rates.

Intravitreal injection for viral vectors

A 33-gauge needle with a glass microsyringe (10- μL volume; Hamilton Company) was used for intravitreal injection of Adenovirus serotype 5 encoding Cre (Ad5-Cre) and Ad5 encoding scramble sequence (Ad5-Empty). The eye was proptosed, and the needle was inserted through the equatorial sclera into the vitreous chamber at an angle of approximately 45 degrees, carefully avoiding contact with the posterior lens capsule or the retina. Viral vectors in a volume of 2 μL (1×10^7 pfu/eye) were slowly injected into the vitreous and the needle was then left in place for an additional 30 seconds to avoid leakage, before being withdrawn.

Cell culture

Primary human TM cells were isolated as reported previously (44, 45). Primary human TM cells from normal (n=4 cell strains) and glaucoma (n=4 cell strains) donor eyes and transformed GTM3 cells were cultured in Dulbecco's Modified Eagle's Medium (DMEM; Sigma Aldrich; catalogue D6046-500ML) supplemented with 10% FBS, 1% penicillin-streptomycin (Sigma Aldrich), L-glutamine and incubated at 5% CO_2 and 37°C in humidified conditions. Cell lysates were collected

in 1X radioimmunoprecipitation assay (RIPA) buffer (Sigma Aldrich; catalogue R0278) containing protease inhibitor cocktail and phosphatase inhibitor (Roche Life Sciences).

Ex vivo culture of human corneoscleral segments

Transplant ineligible, deidentified human corneoscleral segments were acquired from Lions Eye Institute (Tampa, FL) in conformity to the guidelines outlined in the Declaration of Helsinki. According to approved protocols for the Lions Eye Institute, informed consent was obtained from the next of kin for use of ocular tissues for research purposes. Upon receipt, the corneoscleral segments were washed 3 times with PBS (7.4 pH; Sigma Aldrich; catalogue 806552) and then cultured at 37 °C and 5% CO₂ in phenol red-free Dulbecco's Modified Eagle's Medium (DMEM; Sigma Aldrich; catalogue# D4947-500ML) supplemented with 10% FBS (Sigma Aldrich), L-glutamine (Sigma Aldrich), and 1% Pen-Strep (Sigma Aldrich) as described previously (46). The corneoscleral segments were utilized within 24 hours after receiving.

DAF-FM assay for nitric oxide detection

DAF-FM (4-Amino-5-methylamino- 2',7'-difluorofluorescein diacetate; Sigma Aldrich) assay was performed to detect NO as described previously (47) with minor modifications. Human donor corneoscleral segments were divided into quadrants and cultured in phenol red-free DMEM medium (Sigma Aldrich) supplemented with 0.2% FBS and 1% penicillin-streptomycin (Sigma Aldrich). The control and experimental treatments were performed on the quadrants of the same eye to reduce variability associated with the use of contralateral eye. Quadrants were pre-treated with 10 µM DAF-FM (Sigma Aldrich) dye and incubated at 37 °C for 30 minutes. Following incubation, quadrants were washed 3 times with PBS and incubated for an additional 30 minutes at 37 °C to allow proper incorporation and activation of intracellular dye. The quadrants were then treated either with vehicle (0.001% DMSO), GSK101 (20 nM), L-NAME (100 µM; negative

control), or NONOate (100 μM ; positive control), and further incubated for 30 minutes at 37 °C. After the incubation period, the quadrants were washed 3 times with PBS and prepared for imaging. The TM rim (including the inner wall of Schlemm's canal) was carefully dissected from the unfixed corneoscleral quadrants and placed between coverslips for imaging under the fluorescence microscope (Keyence).

Primary human TM cells were cultured on glass-bottom 24-well plates in phenol red-free DMEM medium (Sigma Aldrich) supplemented with 0.2% FBS and 1% penicillin-streptomycin (Sigma Aldrich). Cells were pre-treated with 10 μM DAF-FM (Sigma Aldrich) dye and incubated at 37 °C for 30 minutes. Following incubation, cells were washed 3 times with PBS and incubated for an additional 30 minutes at 37 °C. The cells were then treated either with vehicle (0.001% DMSO), GSK101 (20 nM), L-NAME (100 μM), or NONOate (100 μM), and further incubated for 30 minutes at 37 °C. After the incubation period, the cells were washed 3 times with PBS and imaged under a fluorescence microscope (Keyence).

DAF-FM fluorescence images were analyzed by quantifying fluorescence intensity per unit area ($\text{IntDen}/\mu\text{m}^2$) using ImageJ (National Institutes of Health; Bethesda; MD) as described previously (48, 49).

Immunostaining

Paraffin-embedded human tissue sections from age-matched normal (n=6) and glaucoma (n=5) donors were deparaffinized in xylene and rehydrated twice each with 100%, 95%, 70%, and 50% ethanol for 5 minutes. For antigen retrieval, the tissue sections were incubated in citrate buffer (pH 6.0) at 100 °C for 15 minutes and then at room temperature for another 30 minutes. Tissue sections were blocked with 10% goat serum made in 1x PBS containing 0.2% Triton-X 100 for 2 hours in a dark and humid chamber. Tissue sections were then washed briefly with PBS and immunolabeled

with primary antibody and incubated overnight at 4 °C. Tissue sections incubated without primary antibody served as a negative control. After the incubation, tissue sections were washed three times with PBS and further incubated for 2 hours at room temperature with the appropriate secondary antibodies (1:500; Alexa goat anti-rabbit 568 or Alexa donkey anti-goat; Thermo Fisher Scientific). Tissue sections were washed with PBS and mounted with mounting medium containing DAPI nuclear stain (Vector Labs, Inc.). Images were captured using a fluorescence microscope (Keyence).

Western blot analysis

Total protein (~30 µg) from cell lysates or corneoscleral segment TM rim lysates was run on denaturing 4–12% gradient polyacrylamide ready-made gels (NuPAGE Bis-Tris gels, Life technologies) and transferred onto PVDF membranes. Blots were blocked with 10% non-fat milk in PBST solution (1X PBS + 0.1% TWEEN20; Sigma Aldrich) for 2 hours and then incubated overnight with specific primary antibodies at 4 °C on a rotating shaker at 100 RPM. The membranes were washed thrice with PBST and incubated with corresponding HRP-conjugated secondary antibody for 2 hours. The proteins were then visualized using SuperSignal West Femto Maximum Sensitivity detection reagent (Life technologies). Densitometric analysis was performed on immunoblots using ImageJ (National Institutes of Health; Bethesda; MD).

Shear stress

Shear stress was applied to normal and glaucomatous primary human TM cells using the Ibidi pump system (Ibidi, Munich, Germany). Primary TM cells (2×10^5 cells/slide) were seeded onto IbiTreat µ-slides T^{0.6} (Ibidi) and placed in an incubator at 37 °C with 5.0% CO₂. Primary TM cells were allowed to settle for 3 days and become confluent before induction of shear. The Ibidi pump system (Ibidi) was set up as per the manufacturer's instructions and proprietary software was used

to control the level of shear applied to cells by controlling total media flow rate. Shear levels were simulated as 0.0, 1.0, and 3.0 dyne/cm² for no-shear, low-shear, and high-shear conditions respectively. DAF-FM assay (Millipore Sigma) was performed to determine the levels of NO produced in response to shear.

Ca²⁺ imaging and analysis.

Primary human TM cells from normal individuals or glaucoma patients were incubated with fluo-4 AM (10 μM) and pluronic acid (0.04%) at 30 °C for 30 min. Ca²⁺ images were acquired at 30 frames per second using Andor Revolution WD (with Borealis) spinning-disk confocal imaging system (Andor Technology, Belfast, UK) comprising of an upright Nikon microscope with a 60X water dipping objective (numerical aperture 1.0) and an electron multiplying charge coupled device camera (50). Fluo-4 was excited using a 488 nm solid-state laser and emitted fluorescence was captured using a 525/36 nm band-pass filter. TM cells were treated with cyclopiazonic acid (CPA; 20 μM), a sarco-endoplasmic reticulum (SR/ER) Ca²⁺-ATPase inhibitor, for 10-min. CPA *per se* does not alter the activity of TRPV4 sparklets (51, 52). TRPV4 sparklet activity was recorded 5 minutes after the administration of TRPV4 activator GSK1016790A (GSK101, 3 nM). Specific TRPV4 channel inhibitor GSK2193874 (GSK219, 100 nM, 10 min) was used to inhibit TM TRPV4 sparklet activity.

The flow rate of the physiological salt solution was adjusted to obtain a shear stress of 1 dyne/cm², as calculated using the equation:

$$Q = \frac{\tau \cdot w \cdot h^2}{6 \cdot \mu} ;$$

where Q is the flow rate, τ is the shear stress, w is the width of the flow chamber, h is the height of the flow chamber, and μ is the viscosity of the solution (0.9 cP).

Ca^{2+} images were analyzed using a custom-designed SparkAn software (developed by Dr. Adrian Bonev, University of Vermont) (32, 51, 52). Fractional fluorescence traces (F/F_0) were obtained by placing a $1.7 \mu\text{m}^2$ region of interest (ROI) at the peak event amplitude and were filtered using a Gaussian filter and a cutoff corner frequency of 4 Hz. TRPV4 Ca^{2+} sparklet activity was analyzed as previously described (52, 53). TRPV4 sparklet activity is calculated as NP_O (where N is number of TRPV4 channels per site and P_O is the open state probability of the channel), which was calculated using the Single Channel Search module of Clampfit, previously reported quantal amplitudes derived from all-points histograms ($0.29 \Delta F/F_0$ for fluo-4-loaded MAs), and the following equation (14).

$$NP_O = \left[\frac{(T_{level1} + 2T_{level2} + 3T_{level3} + 4T_{level4})}{T_{total}} \right]$$

where T represents the dwell time at each quantal level and T_{total} is the total recording duration. TRPV4 sparklet sites per cell was obtained by dividing total sparklet sites in a field by the number of TM cells in that field.

TM cell patch clamp

TRPV4 channel currents were recorded in Trypsinized TM cells. Patch clamp electrodes (pipette resistance $\approx 4\text{--}6 \Omega\text{M}$) were pulled from borosilicate glass (O.D.: 1.5 mm; I.D.: 1.17 mm; Sutter Instruments, Novato, CA, USA) using Narishige PC-100 puller (Narishige International USA, INC., Amityville, NY, USA) and polished using MicroForge MF-830 polisher (Narishige

International USA, INC., Amityville, NY, USA). Whole-cell currents were measured at room temperature using a conventional whole-cell patch configuration. The bathing solution consisted of 10 mM HEPES, 134 mM NaCl, 6 mM KCl, 2 mM CaCl₂, 10 mM glucose, and 1 mM MgCl₂ (adjusted to pH 7.4 with NaOH). The intracellular solution consisted of 20 mM CsCl, 100 mM Cs-aspartate, 1 mM MgCl₂, 4 mM ATP, 0.08 mM CaCl₂, 10 mM BAPTA, 10 mM HEPES, pH 7.2 (adjusted with CsOH). GSK101 (10 nM)-induced outward current was assessed in response to a 200-ms voltage step from -100 mV to +100 mV 5 minutes after the addition of GSK101. The effect of TRPV4 inhibitor GSK219 (100 nM) on the outward currents was recorded 5 minutes after the addition of GSK219. The data were acquired using HEKA EPC 10 amplifier and PatchMaster v2X90 program (Harvard Bioscience, Holliston, MA, USA). The patch clamp recordings were analyzed using FitMaster v2X73.2 (Harvard Bioscience, Holliston, MA, USA) and MATLAB R2018a (MathWorks, Natick, MA, USA).

Statistical Analysis

Statistical Analysis was performed using GraphPad Prism 8 (San Diego, CA). Data are expressed in means \pm SEM. Two-group comparisons were analyzed by Unpaired Student's t-test. Multiple comparisons were analyzed by Two-way ANOVA with Bonferroni *post hoc* test. Significance was designated at *P < 0.05, **P < 0.01, and ***P < 0.001.

RESULTS

Presence of functional TRPV4 channels in human primary TM cells and tissues.

We first examined localization of TRPV4 protein in TM tissue by immunostaining post-mortem human donor eyes. In agreement with a previous report (17), TRPV4 protein was localized to TM tissue and the endothelial lining the SC (Figure 1A). Next, we examined TRPV4 channel activity in human primary TM cells (n=4 donor strains) using high speed Ca^{2+} imaging and patch clamp analysis. Ca^{2+} influx signals through individual TRPV4_{TM} channels (“TRPV4 sparklets”,(14)) were recorded in fluo-4AM-loaded TM cells using spinning disk confocal microscopy (Figure 2A). A 1.6 μm^2 region of interest (ROI) was placed at each sparklet site to generate the fractional fluorescence (F/F_0) traces (Figure 2B). The quantal level, or single channel amplitude, was $\Delta F/F_0$ of 0.29, similar to what we have reported in vascular cells (54). The activity of TRPV4_{TM} sparklets was increased by GSK101 (3 nM), and inhibited by TRPV4 inhibitor GSK2193874 (GSK219, 100 nM, Figure 2C). GSK101 also elicited GSK219-sensitive ionic currents in TM cells (Figures 2D, E). These results firmly establish the presence of functional TRPV4 channels and Ca^{2+} influx through these channels in TM cells.

Fluid flow mediated shear stress activates TRPV4 channels in the TM.

TRPV4 channels are known to be activated by increases in shear stress, although a direct mechanosensation by TRPV4 channels is debatable. Fluid flow-induced shear stress is an essential promoter of TM function and IOP homeostasis. We hypothesized that increased shear stress activates TRPV4_{TM} channels, thereby promoting TM function and lowering IOP. Shear stress was increased by altering the fluid flow in a rectangular flow chamber. Increasing the shear stress from

0 dynes/cm² to 1 dyne/cm² increased the number of TRPV4_{TM} sparklet sites and activity per TRPV4_{TM} sparklet site in human primary TM cells in a reversible manner (Figures 3A-B). Moreover, in the presence of TRPV4 channel inhibitor GSK219, increased shear stress was unable to activate TRPV4_{TM} sparklets (Figures 3C-D). These results provided the first direct evidence that increased fluid flow/shear stress promotes Ca²⁺ influx through TRPV4_{TM} channels.

TRPV4 channels maintain outflow facility and IOP homeostasis in mice.

Previous studies have reported conflicting results regarding the role of TRPV4 in IOP regulation. Luo et al. demonstrated that activation of TRPV4 channels reduce IOP in rats and mice (16). Another study by Ryskamp et al. demonstrated that inhibiting TRPV4 channels reduces elevated IOP in a microbead occlusion model of glaucoma (17) (18). Unlike previously published reports, we sought to understand the role of TRPV4 channels in regulating the outflow facility and IOP under physiological conditions. Following measurements of baseline night-time IOP, 3 months old C57BL/6J mice were treated with 5 μ L eyedrops of 20 μ M GSK101 in one eye and vehicle (0.01% DMSO) in the contralateral control eye. IOP was measured at 0.5, 1, 2, and 24 hours post-treatment. GSK101 treatment significantly reduced the IOP, a decrease in IOP that started at 0.5 hours and lasted until 24 hours post-treatment (Figure 4A). No decrease in IOP was observed in the control eyes. Next we determined whether activation of TRPV4 channels regulate outflow facility. C57BL/6J mice were treated with 5 μ L eyedrops of 20 μ M GSK101 or 0.01% DMSO vehicle 30 minutes prior to measurement of conventional outflow facility using constant flow infusion method (42). A noticeable increase in outflow facility was observed in GSK101 treated eyes compared to vehicle treated controls (Figure 4B). Although we did not find the difference to be statistically significant, it is likely of biological relevance given that TRPV4 activation improved outflow facility above normal baseline levels in WT mice. To determine the importance

of TRPV4 channels in maintaining physiological IOP homeostasis, we induced conditional knockout of TRPV4 from TM tissue (TRPV4^{-/-}_{TM}) by intravitreal injections of adenovirus (Ad) 5 expressing Cre in TRPV4^{f/f} mice. The contralateral eyes were injected with Ad5-Empty. Weekly night-time IOP measurements revealed a significant increase of IOP starting at week 2 post-transduction in Ad5-Cre injected eyes compared to Ad5-Empty injected contralateral control eyes (Figure 5A). We next examined specificity of GSK101-mediated IOP lowering on TRPV4 channels in TM using above TRPV4^{-/-}_{TM} mice. Following week 4 IOP measurements on TRPV4^{f/f} mice, both eyes were treated with topical eyedrops of 20 μ M GSK101 and IOP measurements were performed 30 minutes post treatment. A significant decrease in IOP was observed in Ad5-Empty transduced eyes compared to a slight drop in Ad5-Cre transduced eye (Figure 5A). Absence of IOP lowering effect in Ad5-Cre transduced TRPV4^{f/f} indicates that GSK101 selectively targets TRPV4 channels for regulation of IOP. Together, these data indicate critical role of TRPV4 channels in regulation of IOP.

TRPV4 is functionally coupled to eNOS signaling in the TM.

In vascular tissues, we and others have shown that TRPV4 channels promote eNOS activity and cause vasodilation (32-35). Shear stress has been shown to increase eNOS phosphorylation and endogenous NO production in outflow pathway cells (36). We therefore hypothesize that mechanically activated TRPV4_{TM} channels reduce IOP and improve outflow facility via activation of eNOS_{TM} and NO release. Previous studies suggest an important role for eNOS in human TM and SC cells (19, 22, 30). Here, we further sought to confirm eNOS expression in human TM tissues. Age-matched paraffin-fixed human anterior segment tissues (n=6 donors) were stained with eNOS antibody. In agreement with a previous report (55), we observed robust eNOS labeling in the TM and SC endothelial cells. (Figure 6A). We next sought to examine whether TRPV4

channel activator GSK101 promotes eNOS activity in human TM cells and TM tissues (Figures 6B-E). Human TM cells treated with GSK101 for 30 min also showed increased eNOS phosphorylation (Figure 6B). GTM3 cells were treated with either vehicle or GSK101 for various time periods and cellular lysates were examined by Western blot analysis (Figure 6C). Treatment with GSK101 led to increase in eNOS phosphorylation levels starting at 10 minutes post treatment. Using recently developed ex vivo cultured corneoscleral segment model (46), we further demonstrate that GSK101 treatment induces phosphorylation of eNOS in human TM tissues (Figure 6D-E). Human cultured corneoscleral segments were treated with GSK101 or vehicle for 30 min. Western blot analysis revealed increased levels of p-eNOS after treatment with GSK101. We next examined whether activation of TRPV4 channels leads to an increase in NO production using fluorescent NO indicator, 4-amino-5 methylamino-2',7'-difluorofluorescein diacetate (DAF-FM) staining. Human TM cells (Figure 7A-B) and ex vivo cultured human corneoscleral segment tissues (Figure 7C-D) were pretreated with DAF-FM and then subsequently treated with 20 nM GSK101 with or without L-NAME (pan-NOS inhibitor; negative control) or DETA-NONOate (NO donor; positive control). Treatment with GSK101 significantly increased NO production in TM cells and tissues as evident from increased DAF-FM fluorescence intensity, which was partially blocked by pan-NOS inhibitor. Positive control, DETA-NONOate also significantly increased NO production in primary human TM cells.

TRPV4 lowers IOP by activating eNOS signaling.

eNOS-derived NO is an essential regulator of IOP homeostasis and eNOS activity is known to be reduced in glaucoma (22, 28, 30, 56). We first sought to examine whether global NOS3^{-/-} mice develop elevated IOP. Night-time IOPs were significantly higher in global NOS3^{-/-} mice compared to age-matched WT littermates (Figure 8A). This suggest a role for eNOS in IOP regulation. Next,

we utilized NOS3^{-/-} mice to determine whether TRPV4-mediated lowering of IOP is dependent on eNOS signaling. WT and NOS3^{-/-} mice were treated with 20 μ M GSK101 in one eye and 0.01% DMSO vehicle in the contralateral control eye 30 minutes prior to night-time IOP measurements. GSK101 treatment significantly lowered IOP in WT mice but not in NOS3^{-/-} mice (Figure 8B). This indicates that eNOS is necessary for TRPV4-mediated physiological regulation of IOP.

TRPV4 channel activity is impaired in glaucoma.

Although TM senses the changes in flow and maintains IOP, pathological mechanisms for the failure of TM to maintain IOP homeostasis in glaucoma remain elusive. We hypothesized that impairment of TRPV4_{TM} channels contributes to reduced eNOS activity, elevating IOP in glaucoma. We first examined TRPV4_{TM} sparklet activity in normal and glaucomatous primary human TM cells treated with 3 nM GSK101 (Figure 9). TRPV4 sparklet activity per site and the number of sparklet sites were significantly lower in TM cells from glaucoma patients. While an increase in shear stress from 0 dynes/cm² to 1 dyne/cm² elevated TRPV4_{TM} sparklet activity in normal TM cells (Figure 10), it was unable to increase TRPV4_{TM} activity in glaucomatous TM cells, further supporting impaired TRPV4_{TM} channel regulation in glaucoma. We next examined whether lower TRPV4 activity is a result of lower protein expression levels (Figure 6B-C). Western blot analysis demonstrated slightly increased TRPV4 protein levels in glaucomatous TM cells, indicating that impaired channel regulation, rather than channel expression, contributes to the lowering of TRPV4 channel activity in glaucoma.

TRPV4-mediated shear stress transduction is compromised in glaucoma.

TRPV4 channels are widely known to be activated by flow/shear stress (10, 12, 33). Shear stress has also been shown to increase eNOS phosphorylation and endogenous NO production in outflow pathway cells (36). We next examined whether TRPV4 is essential in shear stress mediated NO

production in normal and glaucomatous primary human TM cells. We subjected normal and glaucomatous primary human TM cells to various magnitudes of shear stress (0, 1, or 3 dyne/cm²) and measured NO production using intracellular NO-binding DAF-FM assay (Figure 11). We observed a slight increase in NO production in normal TM cells treated with 1 dyne/cm² shear stress compared to 0 dyne/cm² treatments, and this increase was even higher in 3 dyne/cm². This effect was inhibited by TRPV4 antagonist GSK219, signifying that TRPV4 plays a crucial role in shear stress mediated NO regulation. Furthermore, we did not observe any noticeable changes in shear stress induced NO levels in glaucomatous TM cells.

Coupled TRPV4-eNOS signaling is disrupted in glaucoma.

We further tested the hypothesis that impaired TRPV4 activity in glaucoma results in reduced eNOS activity and NO production. DAF-FM assay for measurements of intracellular NO levels revealed that GSK101 significantly increased NO production in primary TM cells from normal donor but not in glaucomatous TM cells (Figure 12A-B). This was corroborated by Western blot analysis of p-eNOS (Figure 12C-D), which revealed a 3-fold increase in eNOS phosphorylation in GSK101-treated normal TM cells over vehicle-treated normal TM cells. In glaucomatous TM cells, however, GSK101 was unable to increase eNOS phosphorylation.

Expression of TRPV4 and eNOS in normal and glaucomatous TM

We next examined whether lower TRPV4 activity is a result of lower protein expression levels (Figure 13). Western blot analysis demonstrated slightly increased TRPV4 protein levels in glaucomatous TM cells that was not significant. We next examined expression levels in TM tissues from normal and glaucoma donors (Figure 14). Immunohistochemistry analysis demonstrated only a slight increase in eNOS protein levels in glaucomatous TM cells, which was not significant. This

data indicates that perhaps impaired function, rather than expression, contributes to the lowering of TRPV4 channel activity in glaucoma.

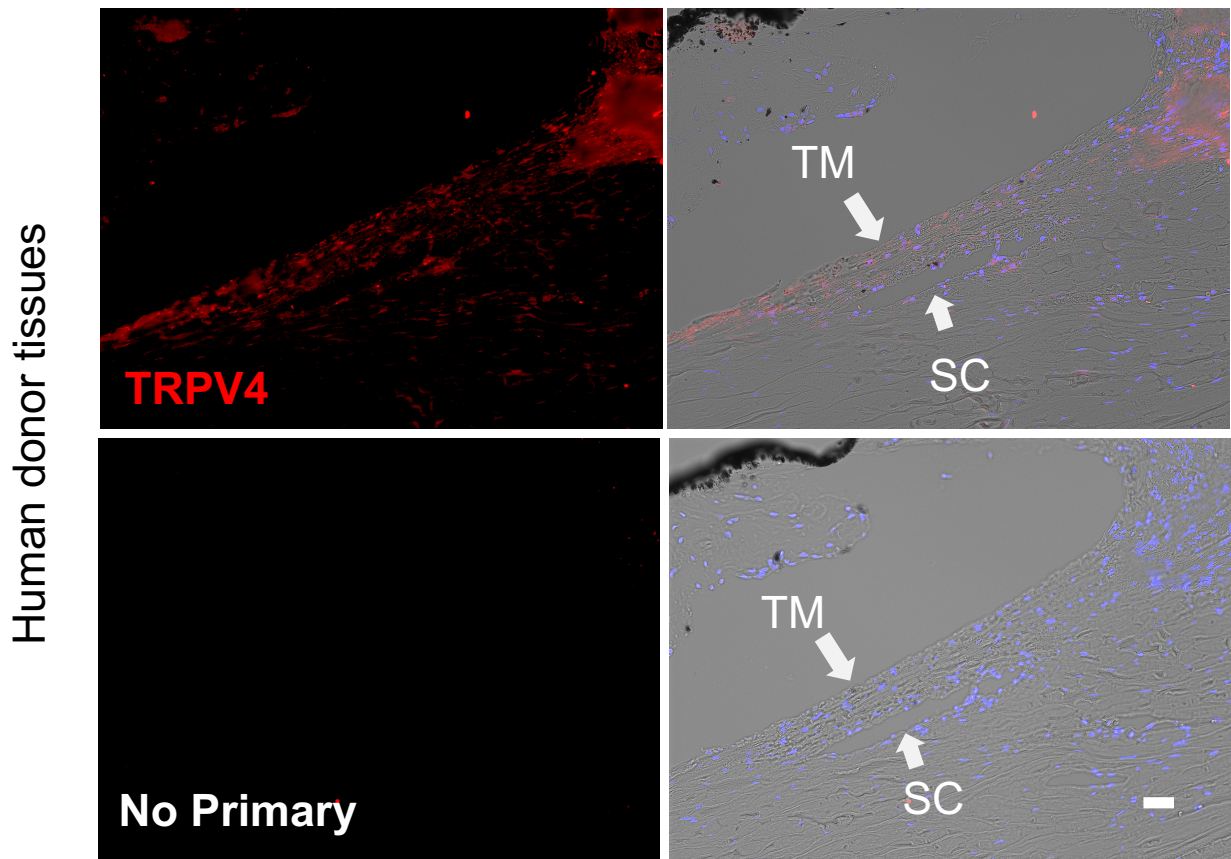


Figure 1. Expression of functional TRPV4 channels in the human TM. Immunohistochemical images showing expression of TRPV4 (red) in the human TM and SC endothelium. No primary antibody control (bottom). n = 5, scale bar = 50 μ m.

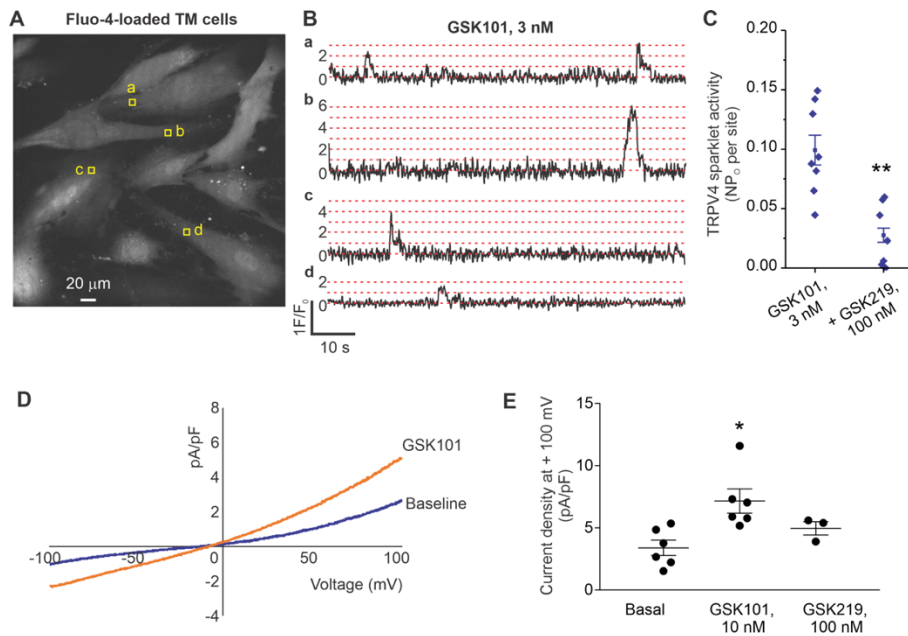


Figure 2. TRPV4 Ca^{2+} sparklets represent Ca^{2+} influx through TRPV4 channels on TM cell membranes. **A.** A greyscale image of a field of view with ~ 10 TM cells; square boxes represent the regions of interest (ROIs) placed at TRPV4 sparklet sites; experiments were performed in the presence of cyclopiazonic acid (SERCAA inhibitor, CPA, $20 \mu\text{M}$) and GSK1016790A (GSK101, TRPV4 activator, 3 nM). **B.** Representative F/F_0 traces generated using the ROIs shown in (A) indicate GSK101-elicited TRPV4 sparklets. Dotted red lines represent quantal level or single channel openings. **C.** Averaged TRPV4 sparklet activity before or after the addition of TRPV4 inhibitor GSK219 (100 nM , $n=7-8$). $**p < 0.01$ vs. GSK101 (3 nM). TRPV4 sparklet activity is expressed as NP_0 per site. N represents the number of TRPV4 channels at a site and P_0 is the open state probability of the channels. **D.** Representative traces for ionic currents through TRPV4 channels in TM cells under baseline condition and in the presence of GSK101 (10 nM), recorded in the whole-cell patch configuration. **E.** Averaged outward currents in TM cells at $+100 \text{ mV}$ under basal conditions, and in the presence of GSK101 (10 nM) or GSK101 + GSK219 (100 nM). $*p < 0.05$ vs. Basal. Data are presented as mean \pm SEM.

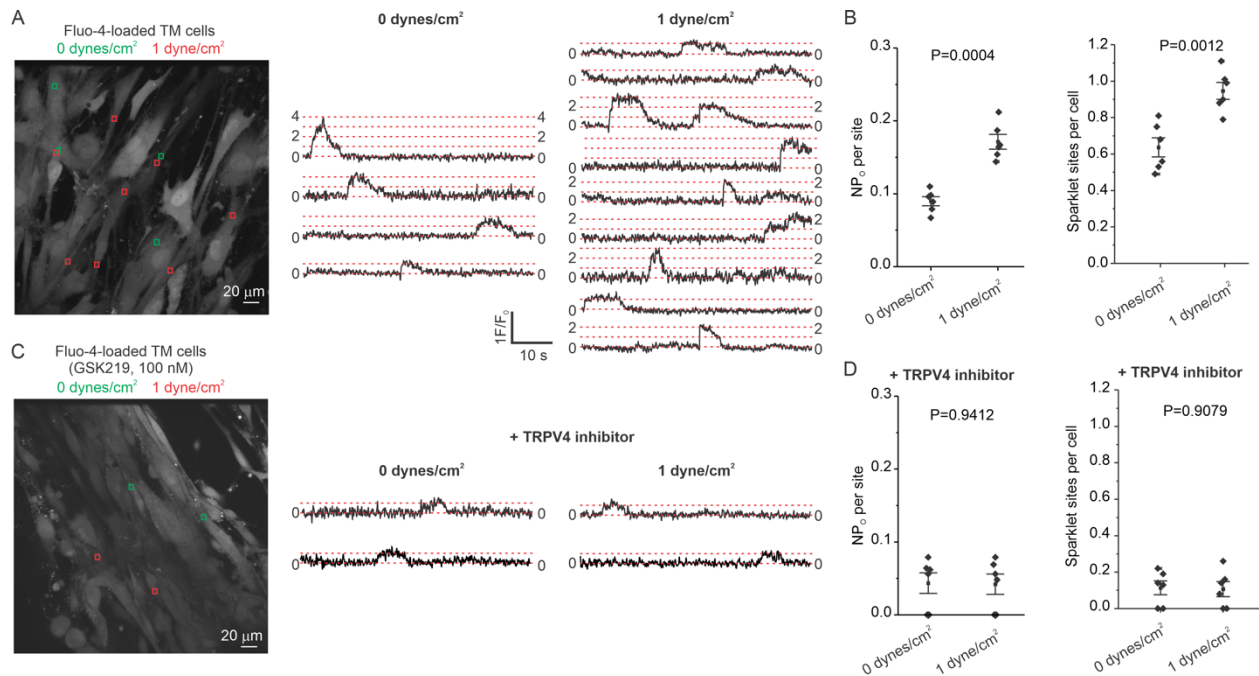


Figure 3. Flow/shear stress increases TRPV4 channel activity in TM cells. **A.** *Left*, a greyscale image of fluo-4-loaded TM cells; the ROIs represent TRPV4 sparklet sites in the absence of flow (green square boxes; 0 dyne/cm²) or the presence of flow/shear stress (red square boxes; 1 dyne/cm²); *right*, F/F₀ traces from the ROIs shown in the greyscale image indicate TRPV4 sparklet activity before (0 dyne/cm²) and after (1 dyne/cm²) flow/shear stress. **B.** Averaged TRPV4 sparklet activity (left) or the number of sparklet sites per cell (right) in the absence (0 dyne/cm², n=6) or presence of flow (1 dyne/cm², n=6). **C.** *Left*, a greyscale image of fluo-4-loaded TM cells in the presence of GSK219 (TRPV4 inhibitor, 100 nM); the ROIs represent TRPV4 sparklet sites in the absence (green square boxes; 0 dyne/cm²) and or presence of flow/shear stress (red square boxes; 1 dyne/cm²); *right*, F/F₀ traces from the ROIs on the grayscale image indicate TRPV4 sparklet activity before (0 dyne/cm²) and after (1 dyne/cm²) flow/shear stress. Experiments were performed in the presence of the TRPV4 channel inhibitor GSK219 (100 nM). **D.** Averaged TRPV4 sparklet

activity (left) or the number of sparklet sites per cell (right) in the absence (0 dyne/cm², n=6) or presence of flow (1 dyne/cm², n=6). Experiments were performed in the presence of the TRPV4 channel inhibitor GSK219. Data are presented as mean ± SEM.

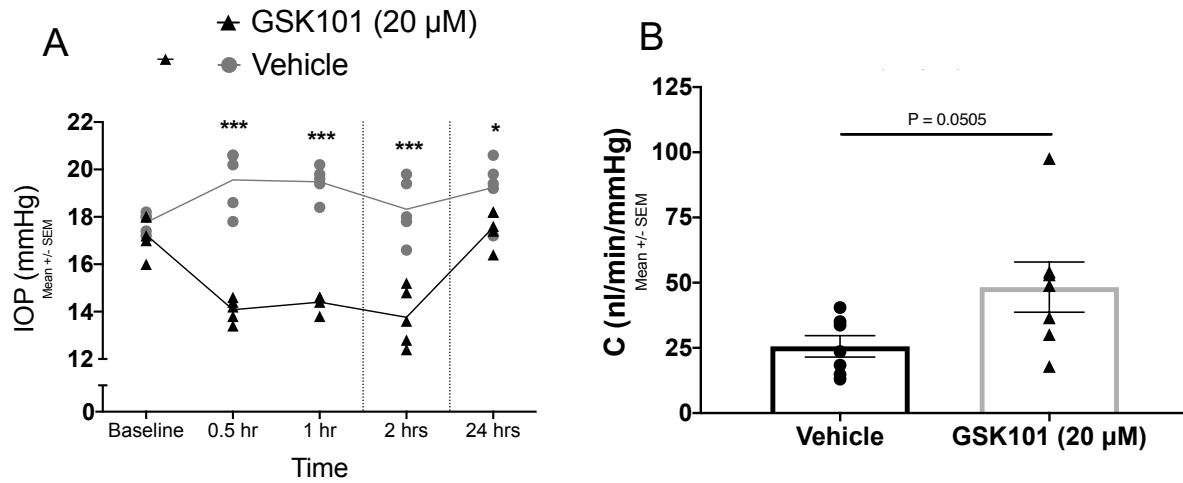


Figure 4. TRPV4 channels regulate outflow facility and IOP homeostasis. **A.** TRPV4-activation lowers IOP in C57BL/6J mice. Following measurement of dark-adapted baseline IOP, animals were topically administered 5 ul eyedrops of 20 μM GSK101 in one eye and 0.01% DMSO vehicle in the contralateral eye. Dark-adapted IOP was measured at 0.5, 1, 2, and 24 hours intervals post treatment. Data are represented as mean ± SEM. $P < 0.001$ vs same time-point in vehicle group, $n = 5$ eyes/group; Two-way analysis of variance, followed by Bonferroni's post-hoc test. **B.** Comparison of conventional outflow facility between GSK101 treated and vehicle treated mouse eyes. Animals were administered 5 ul eyedrops of 20 μM GSK101 in one eye and 0.01% DMSO in contralateral eye 30 minutes prior to measurement of conventional outflow facility using constant flow infusion method. Data are represented as mean ± SEM. $P = 0.0505$ vs vehicle, $n = 7$ eyes/group; Unpaired two-tailed t-test.

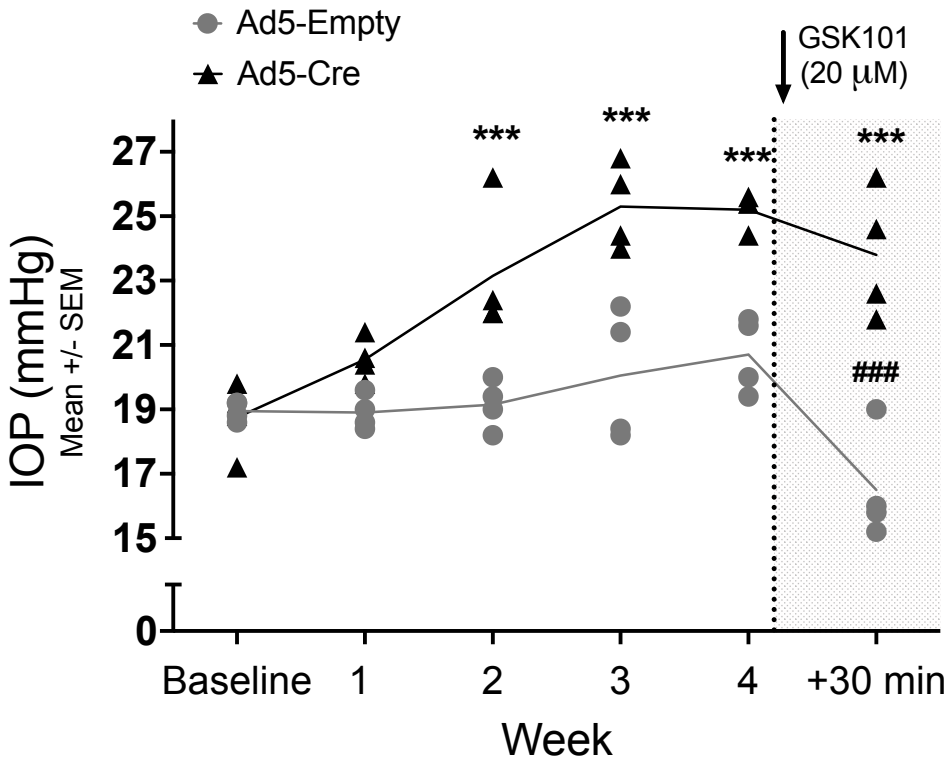


Figure 5. Elevation of IOP in Ad5-Cre transduced TRPV4^{f/f} mice. Following baseline measurement of dark-adapted IOP, animals were injected with Ad5-Cre in one eye and Ad5-Empty in the contralateral control eye. Dark-adapted IOP was measured at 1, 2, 3, and 4th week intervals. Following the 4th week IOP measurement, both eyes were treated with 5 ul GSK101 (20 μM) and dark-adapted IOP was measured 30 min post-treatment. Data are represented as mean ± SEM. ****P* < 0.001 vs same time-point in control group (Ad5-Empty), ###*P* < 0.001 vs previous time point (4 week) in same group. n = 4 eyes/group; Two-way analysis of variance, followed by Bonferroni's post-hoc test.

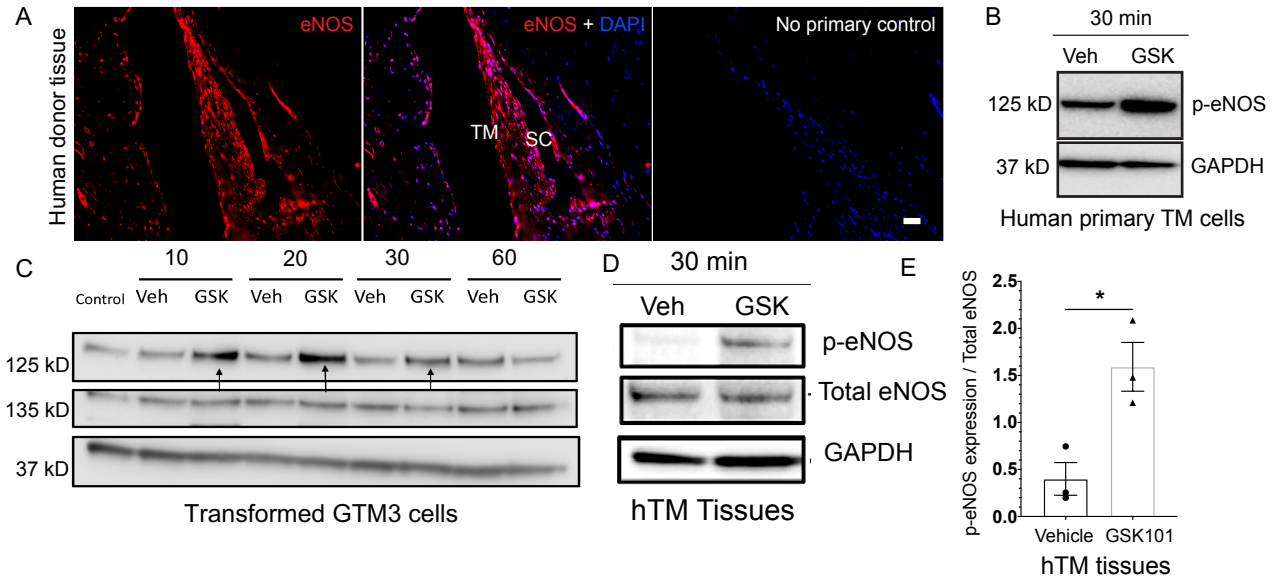


Figure 6. TRPV4 channels are functionally coupled to eNOS in the human TM cells and tissues.

A. Immunohistochemical images showing expression of eNOS (red) in the human TM and SC endothelium (n=6). Nuclei counterstained with DAPI (blue; center image). No primary antibody control (right image). Scale bar = 50 μ m. **B-C.** TRPV4-activation leads to phosphorylation of eNOS in TM cells. Representative Western blot image (B) showing expression of p-eNOS in primary human TM cells (n=3) treated with 20 nM GSK101 or 0.001% DMSO vehicle control. Representative Western blot image (C) showing expression of p-eNOS, total eNOS, and GAPDH in lysates from cultured transformed TM cells (GTM3; n = 3) treated with 20 nM GSK101 or 0.001% DMSO vehicle for 10, 20, 30, and 60 min intervals. **D-E.** TRPV4-mediated phosphorylation of eNOS in human donor TM tissues. Representative Western blot showing expression of p-eNOS, total eNOS, and GAPDH in ex vivo cultured human TM tissues treated with 20 nM GSK101 and 0.01% DMSO vehicle. Densitometric analysis compares ratio of p-eNOS/total eNOS between the groups. $P < 0.05$ vs vehicle, n = 3/group; Unpaired two-tailed t-test.

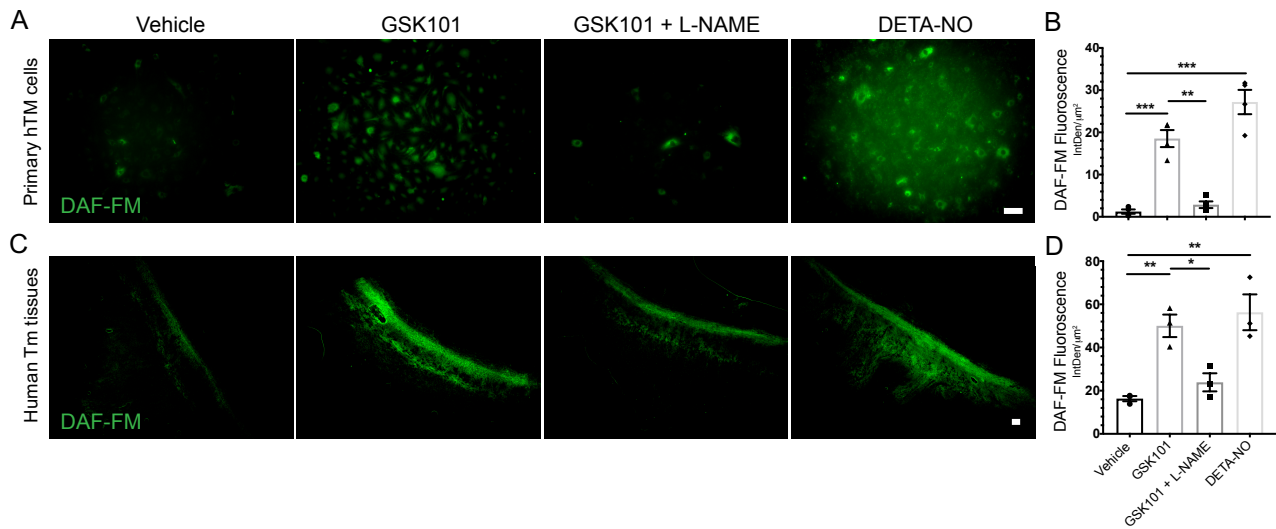


Figure 7. TRPV4 activation leads to NO production in primary TM cells and ex vivo cultured human TM tissues. **A-D** Images and comparisons of DAF-FM intensity (IntDen/ μm^2) in normal human TM cells (A-B) and ex vivo cultured primary human TM tissues (C-D) treated with 0.001% DMSO vehicle, 20 nM GSK101, 20 nM GSK101 + 100 μM L-NAME, or 100 μM DETA/NO. Scale bar = 50 μm (top panel); 100 μm (bottom panel). $P < 0.001$, $n = 3$ cell strains /group; One-way analysis of variance, followed by Bonferroni's post-hoc test.

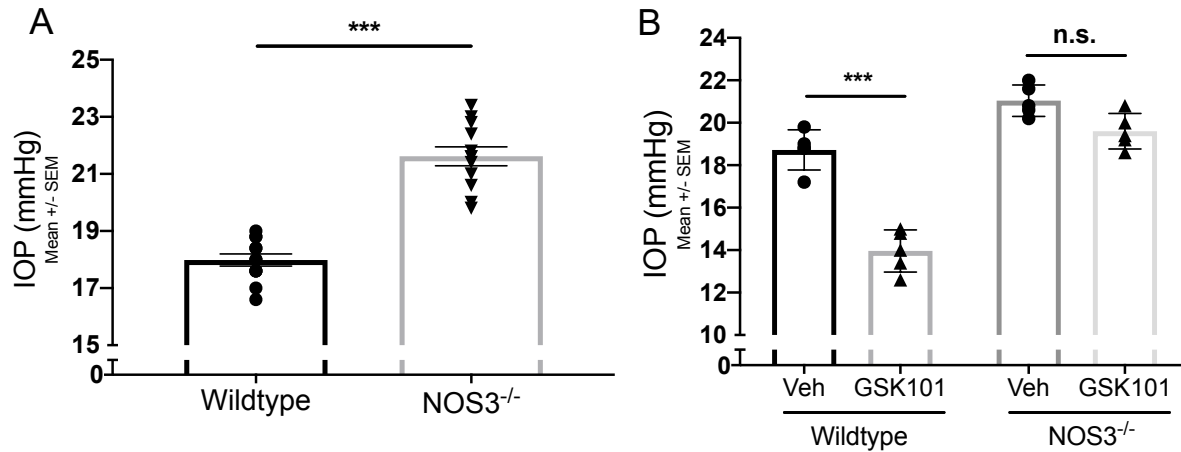


Figure 8. TRPV4-mediated lowering of IOP is eNOS dependent. **A.** Dark-adapted baseline IOP in WT C57BL/6J mice and NOS3^{-/-} mice. Data are represented as mean ± SEM. $P < 0.001$ vs WT, $n = 12$ eyes/group; Unpaired two-tailed t-test. **B.** Effect of TRPV4-activation on IOP in WT and NOS3^{-/-} mice. WT and NOS3^{-/-} animals were administered 5 ul eyedrops of 20 μ M GSK101 in one eye and 0.01% DMSO in contralateral eye 30 min prior to measurement of dark-adapted IOP. Data are represented as mean ± SEM. $P < 0.001$ vs vehicle group, $n = 5$ eyes/group; One-way analysis of variance, followed by Bonferroni's post-hoc test.

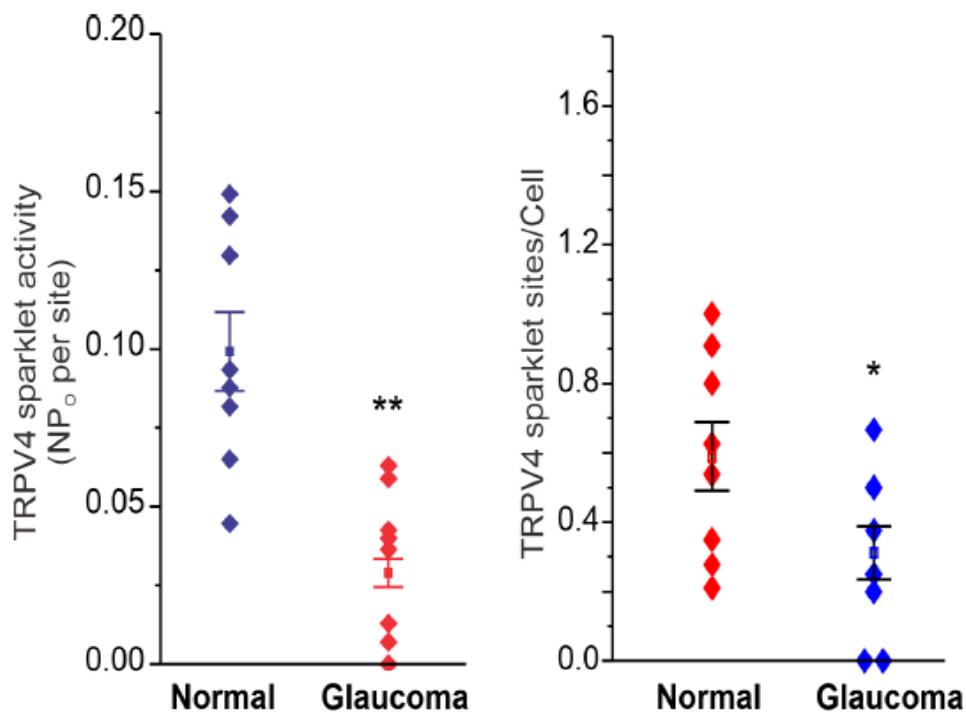


Figure 9. Pharmacological activation of TRPV4 channels is impaired in glaucomatous TM cells. Averaged TRPV4 sparklet activity in normal (n=3) and glaucomatous (n=3) primary human TM cells treated with 3 nM TRPV4 agonist GSK101. TRPV4 sparklet activity is expressed as NP₀ per site and number of sparklet sites per cell. N represents the number of channels at a site and P_O is the open state probability of the channels. Data are presented as mean ± SEM.

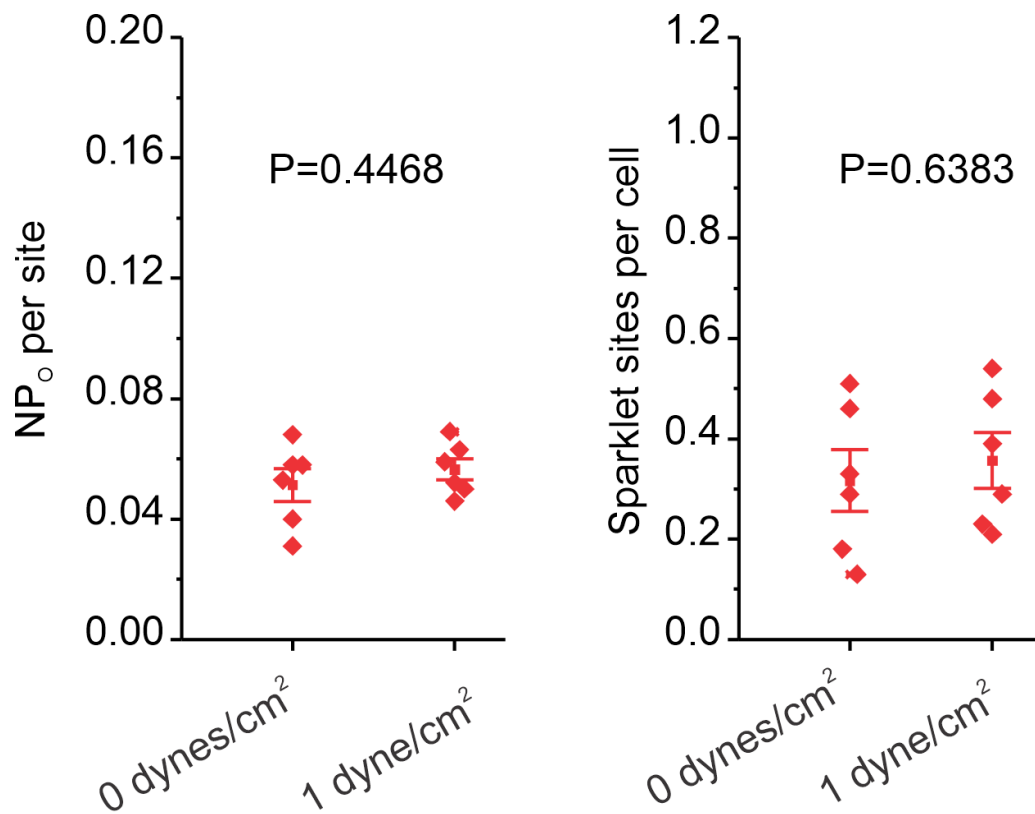


Figure 10. Sensitivity to shear stress is diminished in glaucoma. Averaged TRPV4 sparklet activity in the absence (0 dyne/cm², n=6) or presence (1 dyne/cm², n = 6) of flow/shear stress. The experiments were performed in the presence of GSK101 (3 nM). TRPV4 sparklet activity is expressed as NP_O per site and number of sparklet sites per cell. N represents the number of channels at a site and P_O is the open state probability of the channels. Data are presented as mean ± SEM.

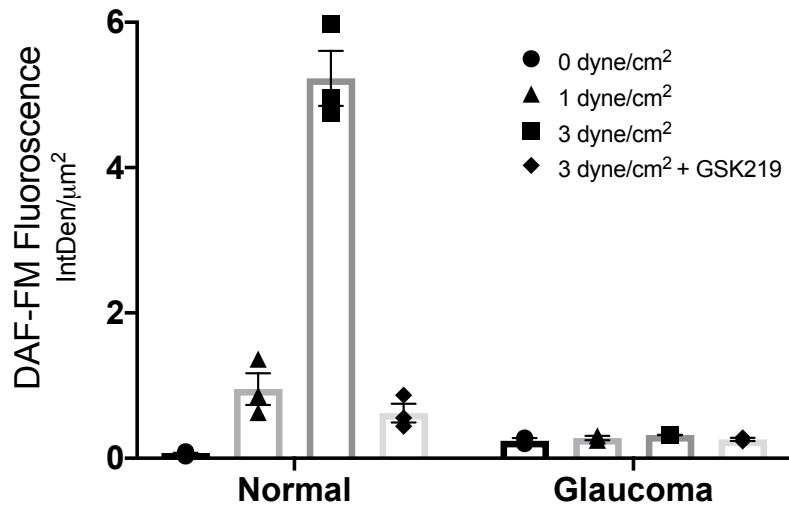
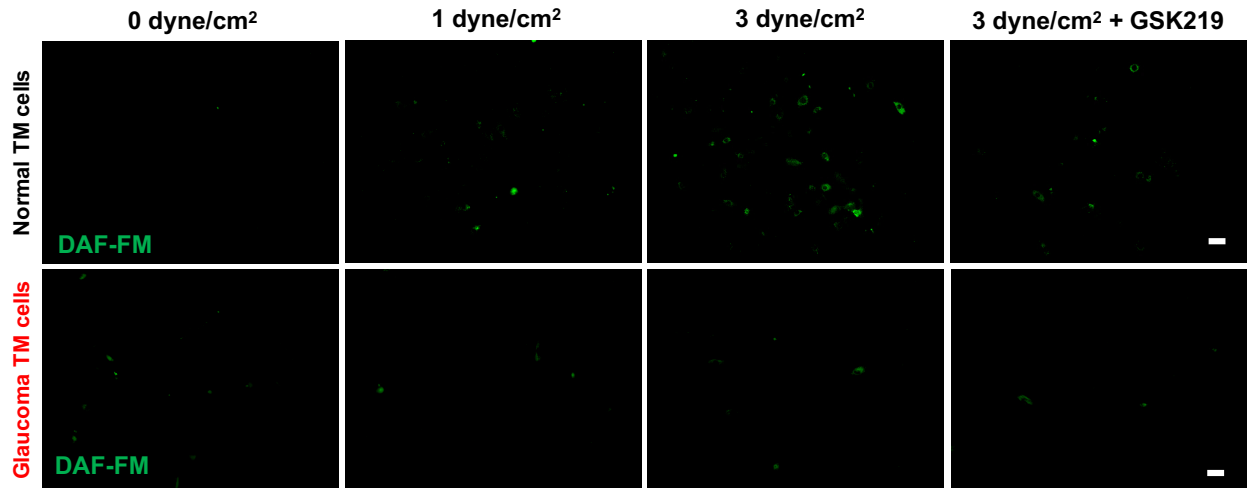


Figure 11. Shear stress-mediated TRPV4-eNOS signaling is diminished in glaucomatous TM cells. **A.** Normal and glaucomatous primary human TM cells were subjected to different shear stress conditions (0, 1, and 3 dyn/cm²), and treated with NO-binding DAF-FM dye to determine shear stress-mediated NO production. TRPV4 antagonist GSK219 (100 nM) was used to determine the role of TRPV4 in shear stress transduction. High shear stress (3 dyn/cm²) led to increased DAF-FM fluorescence intensity, which was reduced by TRPV4 antagonist GSK219. n = 3 normal, 2 glaucoma; scale = 50 μM. **B.** Mean DAF-FM fluorescence intensity/μm² in normal and glaucomatous primary TM cells.

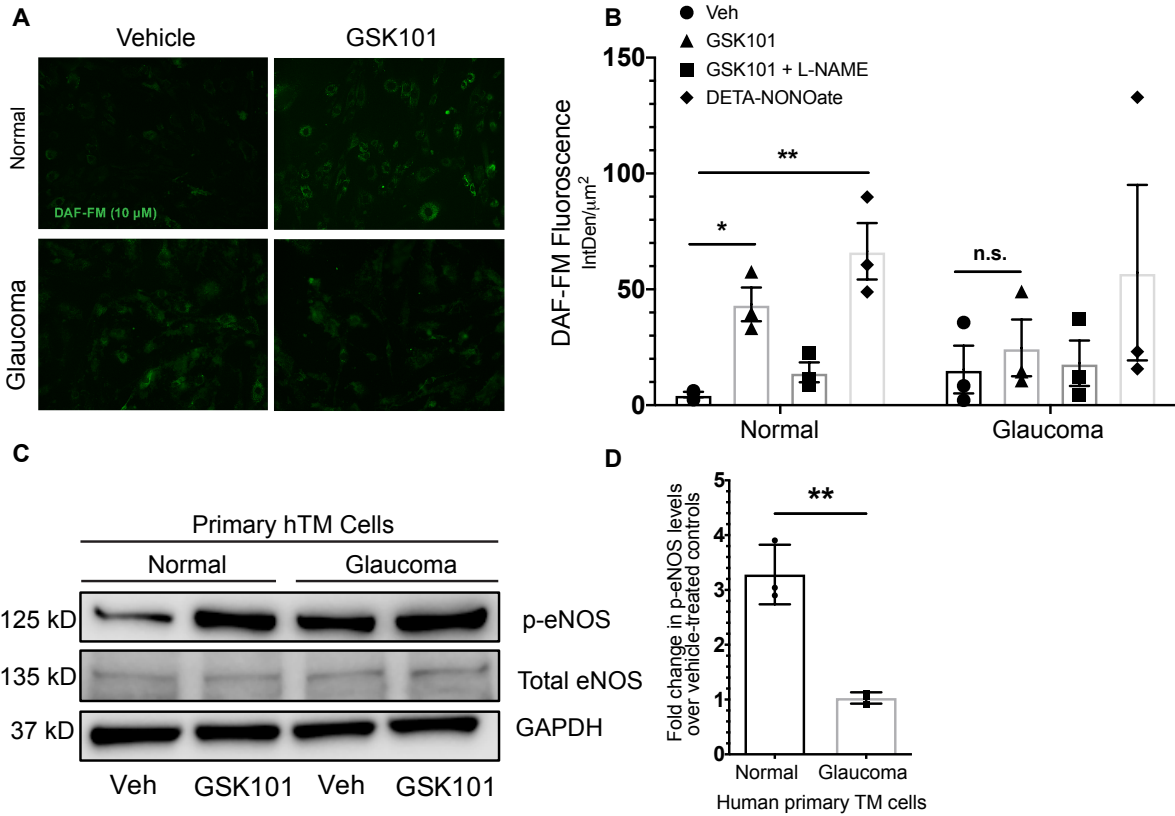


Figure 12. TRPV4-eNOS coupling is impaired in glaucomatous TM cells. **A.** Representative image comparing TRPV4-mediated NO production in normal and glaucomatous primary human TM cells using DAF-FM assay. Normal and glaucomatous primary TM cells were pretreated with NO-binding DAF-FM fluorescent dye (green) and then treated with 0.001% DMSO vehicle, 20 nM GSK101, 20 nM GSK101 + 100 μM L-NAME, or 100 μM DETA/NO. *n* = 3/group, scale = 50 μm. **B.** Quantification of DAF-FM fluorescence intensity/μm² in normal and glaucomatous primary TM cells. *P* < 0.001 vs vehicle treated group, *n* = 3 cell strains/group; One-way analysis of variance, followed by Bonferroni's post-hoc test. **C-D.** Representative immunoblot image comparing p-eNOS, total eNOS and GAPDH levels in normal and glaucomatous TM cells after treatment with 20 nM GSK101 or equivalent vehicle control (0.001% DMSO). Densitometric analysis showing relative fold change in p-eNOS levels in normal and glaucomatous primary

human TM cells over their respective vehicle treated controls. n = 3 cell strains/group; Unpaired two-tailed t-test.

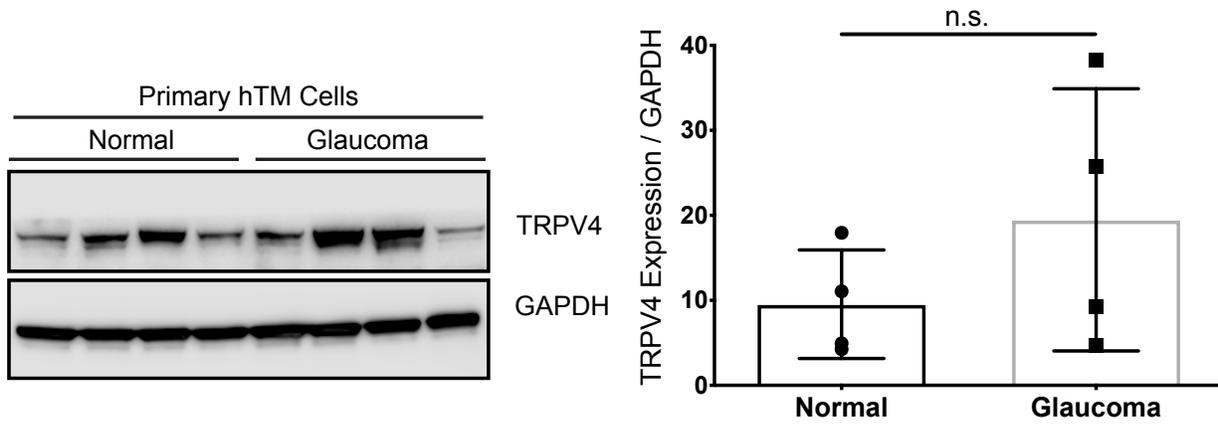


Figure 13. There is no significant change in TRPV4 expression between normal and glaucomatous TM cells. Immunoblot detection of TRPV4 channels in normal and glaucomatous primary human TM cells. Densitometric analysis comparing TRPV4/GAPDH ratio in both groups is shown (C). n = 4/group; Unpaired two-tailed t-test.

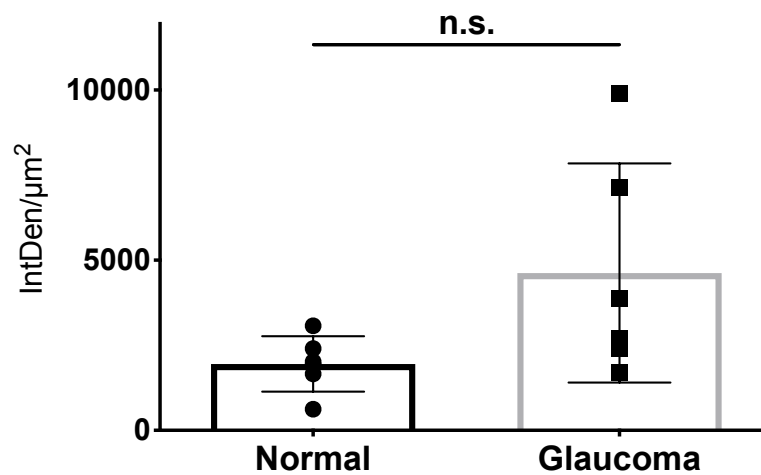
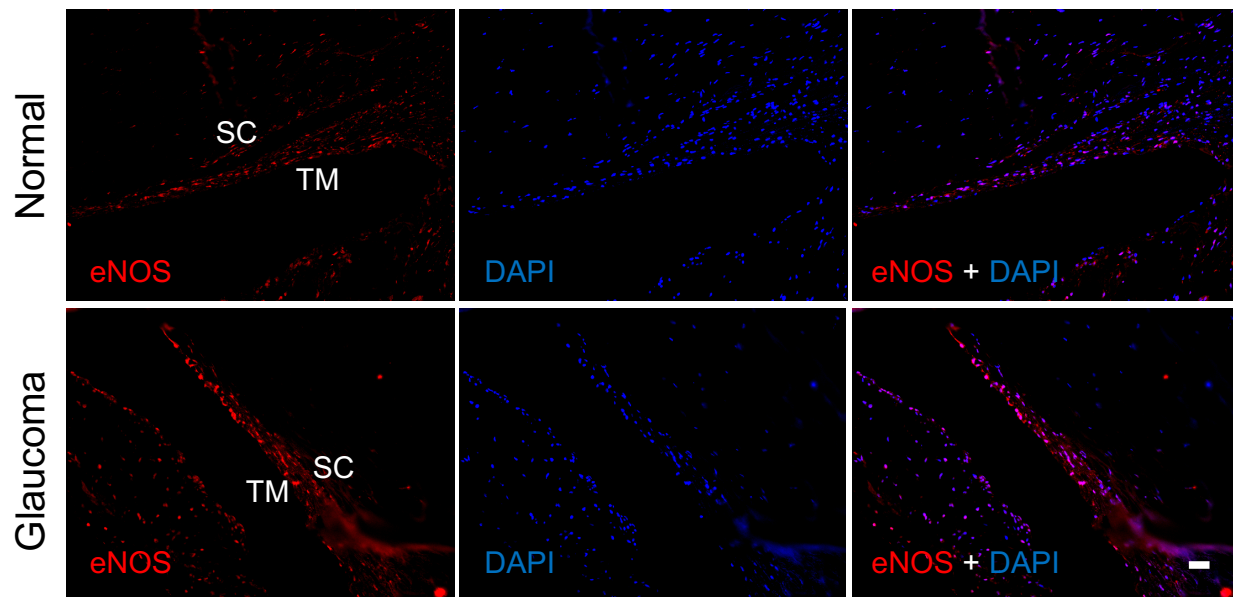


Figure 14. Expression of eNOS is not significantly different in normal and glaucomatous TM. Immunohistochemistry analysis of eNOS expression in normal and glaucomatous human TM from donor tissues. Quantification of fluorescence intensity/ μm^2 in normal (n=6) and glaucomatous (n=6) human TM tissues. Unpaired two-tailed t-test.

DISCUSSION

In this study, we assessed the role of TRPV4_{TM} channels in flow-sensing signaling mechanisms under physiological conditions and its impairment in glaucoma. We show that TRPV4_{TM} channels sense the flow induced shear, promote TM function and maintain IOP homeostasis. Furthermore, we demonstrate for the first time that these channels are functionally impaired in glaucoma, rendering TM cells insensitive to fluid-flow induced shear stress. This glaucoma-associated functional impairment of TRPV4_{TM} channels may contribute to IOP elevation over time, leading to glaucomatous neurodegeneration.

We show that mechanical or pharmacological activation of TRPV4 channels leads to influx of extracellular calcium, detected as TRPV4 sparklets in real-time using high-speed Ca²⁺ imaging. Although global calcium influx for extended period of time is considered toxic for cells, our high-speed confocal imaging reveals that TRPV4 sparklets are highly localized and occur over a very short period of time. Furthermore, TM cells have high tolerance for calcium, an important second messenger necessary for several cellular processes including cytoskeletal remodeling and cell volume regulation. Interestingly, we also observed localization of TRPV4 sparklets in membrane protrusions that connect neighboring TM cells located tens of microns apart. These membrane protrusions closely resembled the previously described structures (57) called tunneling nanotubes (TNTs). TNTs aid in cell-to-cell communication permitting the exchange of membrane and cytoplasmic materials between neighboring TM cells (58, 59). TNTs have also been shown to mediate transmission of intercellular Ca²⁺ signals, which in a manner is analogous to the well-established intercellular transmission of Ca²⁺ waves via gap junctions (59). Although this data

suggests a role for TRPV4 sparklets in cell-to-cell propagation of mechanosensory signals in TM cells, more work is needed to further characterize this type of communication.

Trabecular meshwork cells are in constant contact with the AH, and therefore are exposed to an array of dynamic fluid forces like shear stress, stretching, and distortion. From a biomechanical standpoint, the TM tissue, due to its complex architecture, experiences a variety of mechanical forces depending on the region of interest. For example, the juxtacanalicular region of the TM, a densely packed layer of TM cells embedded in ECM, is likely to experience more strain and distension as a result of hydrostatic pressure. On the other hand, the uveal and corneoscleral meshwork regions of the TM which consists of lattice-like collagenous beams lined with specialized TM cells, allow little resistance to the flow of AH through the intertrabecular space. Therefore, TM cells in these regions are more likely to experience shear generated by AH flow. Previous reports have demonstrated the capability of TM cells to experience fluid-flow induced shear stress (36, 60). However, the exact molecular mechanisms involved in shear-stress sensation at the TM are still unknown. In this study, we show that TRPV4_{TM} channels sense the flow-induced shear, which leads to downstream signaling necessary for maintenance of IOP homeostasis. TRPV4 channels are calcium permeable channels that are known to be activated by flow-induced shear stress (10, 12, 33). We demonstrate that the induction of shear stress on primary human TM cells leads to a significant increase in Ca²⁺ sparklets, a transient and localized spike in Ca²⁺. This effect was reversed by selective TRPV4 channel antagonist GSK219, indicating that TRPV4 channels play an important mechanosensory role in the TM. Pathological changes at the TM are known to accumulate overtime and contribute towards TM dysfunction, as a result affecting several physiological processes including IOP homeostasis (8). We demonstrate that induction of shear-stress in glaucomatous TM cells derived from POAG donors did not result in an increase in

Ca²⁺ sparklets. This indicates that TRPV4-mediated mechanosensing is impaired in glaucomatous primary TM cells.

Given its mechanosensory role in TM cells, we examined whether TRPV4 channels regulate IOP and outflow facility in WT C57BL/6J mouse model. Topical instillation of TRPV4 agonist GSK101 to mouse eyes resulted in a significant decrease in IOP over vehicle treat control eyes starting at 30 minutes post treatment, and this effect lasted until 24 hours. These results are in agreement with a previous study reporting that activation of TRPV4 channels via intraperitoneal delivery of GSK101 lowers IOP in rats and mice (16). On the other hand, a separate study by Ryskamp et al. reported that inhibition of TRPV4 channels by a selective antagonist reduces elevated IOP in microbead-injected ocular hypertensive mice (17). This contradictory effect may be attributed to their use of TRPV4 antagonist in a glaucoma model system that involves injection of micro-beads to the irideocorneal angle, which physically blocks the outflow pathway and elevates IOP. In contrast, we used WT C57BL/6J mouse model to study the effects of TRPV4 agonist GSK101 on baseline IOP, when delivered topically. Compared to previous studies, which did not study TM outflow pathway, our study demonstrates that GSK101 lowers IOP by increasing AH outflow facility as measured using the constant-flow infusion method (41-43). Although the GSK101 mediated improvement in outflow facility was not statistically significant ($P = 0.0505$), we consider it to be biologically relevant given that this increase in outflow facility is above baseline levels in WT C57BL/6J mice. To show the importance of TRPV4 channels in maintenance of physiological IOP homeostasis, we selectively deleted TRPV4 from mouse TM by intravitreally injecting Ad5-Cre in TRPV4^{f/f} mouse eyes. Selective deletion of TRPV4 from the TM using Ad5-Cre vector resulted in a more pronounced elevation in IOP compared to previously reported global knockout mouse model (16). TRPV4 channels that are expressed in

several different ocular tissues including ciliary body, retina, and corneal endothelium. Thus, global knockout of TRPV4 may affect other physiological parameters like AH production and blood pressure, which can lead to confounding effects. Moreover, we observed that GSK101 treatment did not have a significant IOP lowering effect in Ad5-Cre transduced TRPV4^{f/f} mouse eyes when compared to Ad5-Empty transduced control eyes. The diminished IOP-lowering effect of GSK101 in TRPV4^{f/f} mouse eyes indicates that GSK101 is selective against TRPV4 channels. These data implicate TRPV4 in the physiological regulation of IOP and outflow facility.

Nitric oxide is a known modulator of numerous physiological processes of the eye, including IOP homeostasis and ocular blood flow (19-21). In the TM cells, shear stress has been shown to increase NO production (36), which can lead to relaxation of TM (23) by modulating the contractile tone of the TM (24, 27, 30). Furthermore, treatment with exogenous NO donor compounds has been reported to reduce IOP and increase outflow facility in mice (22), rabbit (31), non-human primates (27), and human *ex vivo* models (28). Recently, a chimeric drug containing prostaglandin analog latanoprost and NO donating moiety butanediol mononitrate has been approved for glaucoma therapy by the United States Food and Drug Administration (FDA) after successful clinical trials in human POAG patients (61-66). Despite the apparent therapeutic benefits of exogenous NO, it is important to acknowledge the paradoxical effects of excess NO that may lead to pathological outcomes. At lower concentrations, NO is an important homeostatic mediator that is beneficial for cell survival, whereas at high concentrations excess NO can lead to nitrosative stress and physiological dysregulation (67). Given the importance of NO in glaucoma, very little is known about the upstream mechanisms that regulate endogenous NO production in the eye. The NOS isoform eNOS is considered a major contributor to the NO biosynthesis in the TM, and increased eNOS levels in the mouse TM has been associated with reduction of IOP (30).

In contrast to a previous study (68), we observed robust expression of eNOS in human TM tissues obtained from donor eyes. Expression of eNOS was also observed in human primary TM cells and mouse tissues. We further demonstrate that mechanical or pharmacological activation of TRPV4 channels leads to NO production in primary TM cells and ex vivo cultured donor tissues, and this TRPV4-mediated production of NO is impaired in glaucomatous TM cells. Furthermore, our data indicates that TRPV4 is an intrinsic regulator of eNOS-NO signaling based on the following two observations: 1) Treatment with TRPV4 agonist GSK101 increased p-eNOS levels in primary human TM cells and ex vivo cultured tissues; 2) Similarly, treatment with GSK101 led to an increase in endogenous NO production in TM cells and ex vivo cultured TM tissues. 3) Furthermore, GSK101-mediated lowering of IOP was diminished in NOS3^{-/-} global knockout mouse model. To account for the confounding effects of global NOS3^{-/-} model, we treated mouse eyes with pan-NOS inhibitor L-NAME and observed similar effect. In agreement with a previous report (69), we observed that NOS3^{-/-} mice have higher baseline IOP compared to their WT littermates. Downregulation of eNOS activity and a reduced availability of NO is associated with POAG (21, 56, 70). Our data indicates that TRPV4-eNOS signaling pathway is affected in glaucoma. We observed that TRPV4-mediated eNOS phosphorylation is diminished in glaucomatous primary TM cells when compared to normal TM cells. Furthermore, treatment with GSK101 did not result in an increase in NO production in glaucomatous human TM cells. We further showed that induction of fluid-flow induced shear stress leads to an increase in NO production in normal TM cells but not in glaucomatous TM cells. Shear stress mediated production of endogenous NO was reduced in cell treated with TRPV4 antagonist GSK219, indicating an important role for TRPV4 channels in shear stress mediated NO production. In conclusion, our data substantiates the role of TRPV4 channels in shear stress sensation at the TM, nitric oxide

regulation, and physiological regulation of IOP and outflow facility. Upon mechanical activation, these channels intrinsically regulate endogenous NO production in primary human TM cells. We also demonstrate that TRPV4-mediated lowering of IOP requires activation of downstream eNOS signaling. To our knowledge, this is the first report showing functional impairment of TRPV4-eNOS signaling in glaucomatous primary human TM cells. In POAG, TRPV4-eNOS impairment may perhaps be affecting TM cells ability to detect and mitigate pathophysiological changes in the AH outflow pathway. From a clinical perspective, this study identifies a key physiological pathway responsible for homeostatic regulation of IOP in normal human beings, which is impaired in glaucoma patients. Future studies will target this pathway in order to alleviate disease-associated pathology.

REFERENCES

1. Quigley HA, Broman AT. The number of people with glaucoma worldwide in 2010 and 2020. *Br J Ophthalmol.* 2006;90(3):262-7. Epub 2006/02/21. doi: 10.1136/bjo.2005.081224. PubMed PMID: 16488940; PMCID: PMC1856963.
2. Tham YC, Li X, Wong TY, Quigley HA, Aung T, Cheng CY. Global prevalence of glaucoma and projections of glaucoma burden through 2040: a systematic review and meta-analysis. *Ophthalmology.* 2014;121(11):2081-90. Epub 2014/07/01. doi: 10.1016/j.ophtha.2014.05.013. PubMed PMID: 24974815.
3. Quigley HA. Neuronal death in glaucoma. *Prog Retin Eye Res.* 1999;18(1):39-57. Epub 1999/01/27. doi: S1350-9462(98)00014-7 [pii]. PubMed PMID: 9920498.
4. Rosenthal J, Leske MC. Open-angle glaucoma risk factors applied to clinical area. *J Am Optom Assoc.* 1980;51(11):1017-24. Epub 1980/11/01. PubMed PMID: 7440868.
5. Tamm ER, Braunger BM, Fuchshofer R. Intraocular Pressure and the Mechanisms Involved in Resistance of the Aqueous Humor Flow in the Trabecular Meshwork Outflow Pathways. *Prog Mol Biol Transl Sci.* 2015;134:301-14. Epub 2015/08/28. doi: 10.1016/bs.pmbts.2015.06.007. PubMed PMID: 26310162.

6. Acott TS, Kelley MJ, Keller KE, Vranka JA, Abu-Hassan DW, Li X, Aga M, Bradley JM. Intraocular pressure homeostasis: maintaining balance in a high-pressure environment. *J Ocul Pharmacol Ther.* 2014;30(2-3):94-101. Epub 2014/01/10. doi: 10.1089/jop.2013.0185. PubMed PMID: 24401029; PMCID: PMC3991985.
7. Keller KE, Aga M, Bradley JM, Kelley MJ, Acott TS. Extracellular matrix turnover and outflow resistance. *Exp Eye Res.* 2009;88(4):676-82. Epub 2008/12/18. doi: 10.1016/j.exer.2008.11.023. PubMed PMID: 19087875; PMCID: PMC2700052.
8. Braunger BM, Fuchshofer R, Tamm ER. The aqueous humor outflow pathways in glaucoma: A unifying concept of disease mechanisms and causative treatment. *Eur J Pharm Biopharm.* 2015;95(Pt B):173-81. Epub 2015/05/11. doi: 10.1016/j.ejpb.2015.04.029. PubMed PMID: 25957840.
9. Bradley JM, Kelley MJ, Zhu X, Anderssohn AM, Alexander JP, Acott TS. Effects of mechanical stretching on trabecular matrix metalloproteinases. *Invest Ophthalmol Vis Sci.* 2001;42(7):1505-13. Epub 2001/05/31. PubMed PMID: 11381054.
10. Darby WG, Potocnik S, Ramachandran R, Hollenberg MD, Woodman OL, McIntyre P. Shear stress sensitizes TRPV4 in endothelium-dependent vasodilatation. *Pharmacol Res.* 2018;133:152-9. Epub 2018/05/23. doi: 10.1016/j.phrs.2018.05.009. PubMed PMID: 29787869.
11. Mendoza SA, Fang J, Gutterman DD, Wilcox DA, Bubolz AH, Li R, Suzuki M, Zhang DX. TRPV4-mediated endothelial Ca²⁺ influx and vasodilation in response to shear stress. *Am J*

Physiol Heart Circ Physiol. 2010;298(2):H466-76. Epub 2009/12/08. doi:

10.1152/ajpheart.00854.2009. PubMed PMID: 19966050; PMCID: PMC2822567.

12. Kohler R, Hoyer J. Role of TRPV4 in the Mechanotransduction of Shear Stress in Endothelial Cells. In: Liedtke WB, Heller S, editors. TRP Ion Channel Function in Sensory Transduction and Cellular Signaling Cascades. Boca Raton (FL)2007.

13. Hartmannsgruber V, Heyken WT, Kacik M, Kaistha A, Grgic I, Harteneck C, Liedtke W, Hoyer J, Kohler R. Arterial response to shear stress critically depends on endothelial TRPV4 expression. PLoS One. 2007;2(9):e827. Epub 2007/09/06. doi: 10.1371/journal.pone.0000827. PubMed PMID: 17786199; PMCID: PMC1959246.

14. Sonkusare SK, Bonev AD, Ledoux J, Liedtke W, Kotlikoff MI, Heppner TJ, Hill-Eubanks DC, Nelson MT. Elementary Ca²⁺ signals through endothelial TRPV4 channels regulate vascular function. Science. 2012;336(6081):597-601. Epub 2012/05/05. doi: 10.1126/science.1216283. PubMed PMID: 22556255; PMCID: PMC3715993.

15. White JP, Cibelli M, Urban L, Nilius B, McGeown JG, Nagy I. TRPV4: Molecular Conductor of a Diverse Orchestra. Physiol Rev. 2016;96(3):911-73. Epub 2016/06/03. doi: 10.1152/physrev.00016.2015. PubMed PMID: 27252279.

16. Luo N, Conwell MD, Chen X, Kettenhofen CI, Westlake CJ, Cantor LB, Wells CD, Weinreb RN, Corson TW, Spandau DF, Joos KM, Iomini C, Obukhov AG, Sun Y. Primary cilia signaling mediates intraocular pressure sensation. Proc Natl Acad Sci U S A.

2014;111(35):12871-6. doi: 10.1073/pnas.1323292111. PubMed PMID: 25143588; PMCID: PMC4156748.

17. Ryskamp DA, Frye AM, Phuong TT, Yarishkin O, Jo AO, Xu Y, Lakk M, Iuso A, Redmon SN, Ambati B, Hageman G, Prestwich GD, Torrejon KY, Krizaj D. TRPV4 regulates calcium homeostasis, cytoskeletal remodeling, conventional outflow and intraocular pressure in the mammalian eye. *Sci Rep.* 2016;6:30583. Epub 2016/08/12. doi: 10.1038/srep30583. PubMed PMID: 27510430; PMCID: PMC4980693.

18. Sappington RM, Carlson BJ, Crish SD, Calkins DJ. The microbead occlusion model: a paradigm for induced ocular hypertension in rats and mice. *Invest Ophthalmol Vis Sci.* 2010;51(1):207-16. Epub 2009/10/24. doi: 10.1167/iovs.09-3947. PubMed PMID: 19850836; PMCID: PMC2869054.

19. Aliancy J, Stamer WD, Wirostko B. A Review of Nitric Oxide for the Treatment of Glaucomatous Disease. *Ophthalmol Ther.* 2017;6(2):221-32. Epub 2017/06/07. doi: 10.1007/s40123-017-0094-6. PubMed PMID: 28584936; PMCID: PMC5693832.

20. Toda N, Nakanishi-Toda M. Nitric oxide: ocular blood flow, glaucoma, and diabetic retinopathy. *Prog Retin Eye Res.* 2007;26(3):205-38. Epub 2007/03/06. doi: 10.1016/j.preteyeres.2007.01.004. PubMed PMID: 17337232.

21. Wareham LK, Buys ES, Sappington RM. The nitric oxide-guanylate cyclase pathway and glaucoma. *Nitric Oxide*. 2018;77:75-87. Epub 2018/05/04. doi: 10.1016/j.niox.2018.04.010. PubMed PMID: 29723581; PMCID: PMC6424573.
22. Chang JY, Stamer WD, Bertrand J, Read AT, Marando CM, Ethier CR, Overby DR. Role of nitric oxide in murine conventional outflow physiology. *Am J Physiol Cell Physiol*. 2015;309(4):C205-14. doi: 10.1152/ajpcell.00347.2014. PubMed PMID: 26040898; PMCID: PMC4537932.
23. Dismuke WM, Liang J, Overby DR, Stamer WD. Concentration-related effects of nitric oxide and endothelin-1 on human trabecular meshwork cell contractility. *Exp Eye Res*. 2014;120:28-35. Epub 2014/01/01. doi: 10.1016/j.exer.2013.12.012. PubMed PMID: 24374036; PMCID: PMC3943640.
24. Dismuke WM, Mbadugha CC, Ellis DZ. NO-induced regulation of human trabecular meshwork cell volume and aqueous humor outflow facility involve the BKCa ion channel. *Am J Physiol Cell Physiol*. 2008;294(6):C1378-86. Epub 2008/04/04. doi: 10.1152/ajpcell.00363.2007. PubMed PMID: 18385281.
25. Dismuke WM, Sharif NA, Ellis DZ. Human trabecular meshwork cell volume decrease by NO-independent soluble guanylate cyclase activators YC-1 and BAY-58-2667 involves the BKCa ion channel. *Invest Ophthalmol Vis Sci*. 2009;50(7):3353-9. Epub 2009/02/24. doi: 10.1167/iovs.08-3127. PubMed PMID: 19234350.

26. Ellis DZ, Sharif NA, Dismuke WM. Endogenous regulation of human Schlemm's canal cell volume by nitric oxide signaling. *Invest Ophthalmol Vis Sci.* 2010;51(11):5817-24. Epub 2010/05/21. doi: 10.1167/iovs.09-5072. PubMed PMID: 20484594.
27. Heyne GW, Kiland JA, Kaufman PL, Gabelt BT. Effect of nitric oxide on anterior segment physiology in monkeys. *Invest Ophthalmol Vis Sci.* 2013;54(7):5103-10. Epub 2013/06/27. doi: 10.1167/iovs.12-11491. PubMed PMID: 23800771; PMCID: PMC3729238.
28. Schneemann A, Dijkstra BG, van den Berg TJ, Kamphuis W, Hoyng PF. Nitric oxide/guanylate cyclase pathways and flow in anterior segment perfusion. *Graefes Arch Clin Exp Ophthalmol.* 2002;240(11):936-41. Epub 2002/12/18. doi: 10.1007/s00417-002-0559-7. PubMed PMID: 12486517.
29. Fernandez-Durango R, Fernandez-Martinez A, Garcia-Feijoo J, Castillo A, de la Casa JM, Garcia-Bueno B, Perez-Nievas BG, Fernandez-Cruz A, Leza JC. Expression of nitrotyrosine and oxidative consequences in the trabecular meshwork of patients with primary open-angle glaucoma. *Invest Ophthalmol Vis Sci.* 2008;49(6):2506-11. Epub 2008/02/26. doi: 10.1167/iovs.07-1363. PubMed PMID: 18296660.
30. Stamer WD, Lei Y, Boussommier-Calleja A, Overby DR, Ethier CR. eNOS, a pressure-dependent regulator of intraocular pressure. *Invest Ophthalmol Vis Sci.* 2011;52(13):9438-44. doi: 10.1167/iovs.11-7839. PubMed PMID: 22039240; PMCID: PMC3293415.

31. Kotikoski H, Alajuuma P, Moilanen E, Salmenpera P, Oksala O, Laippala P, Vapaatalo H. Comparison of nitric oxide donors in lowering intraocular pressure in rabbits: role of cyclic GMP. *J Ocul Pharmacol Ther.* 2002;18(1):11-23. Epub 2002/02/23. doi: 10.1089/108076802317233171. PubMed PMID: 11858611.
32. Marziano C, Hong K, Cope EL, Kotlikoff MI, Isakson BE, Sonkusare SK. Nitric Oxide-Dependent Feedback Loop Regulates Transient Receptor Potential Vanilloid 4 (TRPV4) Channel Cooperativity and Endothelial Function in Small Pulmonary Arteries. *J Am Heart Assoc.* 2017;6(12). doi: 10.1161/JAHA.117.007157. PubMed PMID: 29275372; PMCID: PMC5779028.
33. Hill-Eubanks DC, Gonzales AL, Sonkusare SK, Nelson MT. Vascular TRP channels: performing under pressure and going with the flow. *Physiology.* 2014;29(5):343-60. Epub 2014/09/03. doi: 10.1152/physiol.00009.2014. PubMed PMID: 25180264; PMCID: 4214829.
34. Cabral PD, Garvin JL. TRPV4 activation mediates flow-induced nitric oxide production in the rat thick ascending limb. *Am J Physiol Renal Physiol.* 2014;307(6):F666-72. Epub 2014/06/27. doi: 10.1152/ajprenal.00619.2013. PubMed PMID: 24966090; PMCID: PMC4166729.
35. Sukumaran SV, Singh TU, Parida S, Narasimha Reddy Ch E, Thangamalai R, Kandasamy K, Singh V, Mishra SK. TRPV4 channel activation leads to endothelium-dependent relaxation mediated by nitric oxide and endothelium-derived hyperpolarizing factor in rat

pulmonary artery. *Pharmacol Res.* 2013;78:18-27. Epub 2013/10/01. doi:
10.1016/j.phrs.2013.09.005. PubMed PMID: 24075884.

36. Ashpole NE, Overby DR, Ethier CR, Stamer WD. Shear stress-triggered nitric oxide release from Schlemm's canal cells. *Invest Ophthalmol Vis Sci.* 2014;55(12):8067-76. Epub 2014/11/15. doi: 10.1167/iovs.14-14722. PubMed PMID: 25395486; PMCID: PMC4266075.

37. McDonnell F, Perkumas KM, Ashpole NE, Kalnitsky J, Sherwood JM, Overby DR, Stamer WD. Shear Stress in Schlemm's Canal as a Sensor of Intraocular Pressure. *Sci Rep.* 2020;10(1):5804. Epub 2020/04/04. doi: 10.1038/s41598-020-62730-4. PubMed PMID: 32242066; PMCID: PMC7118084.

38. Moore C, Cevikbas F, Pasolli HA, Chen Y, Kong W, Kempkes C, Parekh P, Lee SH, Kontchou NA, Yeh I, Jokerst NM, Fuchs E, Steinhoff M, Liedtke WB. UVB radiation generates sunburn pain and affects skin by activating epidermal TRPV4 ion channels and triggering endothelin-1 signaling. *Proc Natl Acad Sci U S A.* 2013;110(34):E3225-34. Epub 2013/08/10. doi: 10.1073/pnas.1312933110. PubMed PMID: 23929777; PMCID: PMC3752269.

39. Patel GC, Phan TN, Maddineni P, Kasetti RB, Millar JC, Clark AF, Zode GS. Dexamethasone-Induced Ocular Hypertension in Mice: Effects of Myocilin and Route of Administration. *Am J Pathol.* 2017;187(4):713-23. Epub 2017/02/09. doi:
10.1016/j.ajpath.2016.12.003. PubMed PMID: 28167045; PMCID: PMC5397678.

40. Wang WH, Millar JC, Pang IH, Wax MB, Clark AF. Noninvasive measurement of rodent intraocular pressure with a rebound tonometer. *Invest Ophthalmol Vis Sci.* 2005;46(12):4617-21. Epub 2005/11/24. doi: 10.1167/iovs.05-0781. PubMed PMID: 16303957.
41. Millar JC, Phan TN, Pang IH, Clark AF. Strain and Age Effects on Aqueous Humor Dynamics in the Mouse. *Invest Ophthalmol Vis Sci.* 2015;56(10):5764-76. Epub 2015/09/02. doi: 10.1167/iovs.15-16720. PubMed PMID: 26325415.
42. Millar JC, Clark AF, Pang IH. Assessment of aqueous humor dynamics in the mouse by a novel method of constant-flow infusion. *Invest Ophthalmol Vis Sci.* 2011;52(2):685-94. Epub 2010/09/24. doi: 10.1167/iovs.10-6069. PubMed PMID: 20861483.
43. Millar JC, Phan TN, Pang IH. Assessment of Aqueous Humor Dynamics in the Rodent by Constant Flow Infusion. *Methods Mol Biol.* 2018;1695:109-20. Epub 2017/12/01. doi: 10.1007/978-1-4939-7407-8_11. PubMed PMID: 29190023.
44. Keller KE, Bhattacharya SK, Borrás T, Brunner TM, Chansangpetch S, Clark AF, Dismuke WM, Du Y, Elliott MH, Ethier CR, Faralli JA, Freddo TF, Fuchshofer R, Giovingo M, Gong H, Gonzalez P, Huang A, Johnstone MA, Kaufman PL, Kelley MJ, Knepper PA, Kopczyński CC, Kuchtey JG, Kuchtey RW, Kuehn MH, Lieberman RL, Lin SC, Liton P, Liu Y, Lutjen-Drecoll E, Mao W, Masis-Solano M, McDonnell F, McDowell CM, Overby DR, Pattabiraman PP, Raghunathan VK, Rao PV, Rhee DJ, Chowdhury UR, Russell P, Samples JR, Schwartz D, Stubbs EB, Tamm ER, Tan JC, Toris CB, Torrejon KY, Vranka JA, Wirtz MK, Yorio T, Zhang J, Zode GS, Fautsch MP, Peters DM, Acott TS, Stamer WD. Consensus

recommendations for trabecular meshwork cell isolation, characterization and culture. *Exp Eye Res.* 2018;171:164-73. Epub 2018/03/13. doi: 10.1016/j.exer.2018.03.001. PubMed PMID: 29526795; PMCID: PMC6042513.

45. Stamer DW, Roberts BC, Epstein DL, Allingham RR. Isolation of primary open-angle glaucomatous trabecular meshwork cells from whole eye tissue. *Curr Eye Res.* 2000;20(5):347-50. Epub 2000/06/16. PubMed PMID: 10855028.

46. Kasetti RB, Patel PD, Maddineni P, Zode GS. Ex-vivo cultured human corneoscleral segment model to study the effects of glaucoma factors on trabecular meshwork. *PLoS One.* 2020;15(6):e0232111. Epub 2020/06/25. doi: 10.1371/journal.pone.0232111. PubMed PMID: 32579557; PMCID: PMC7314024.

47. Patel PD, Kasetti RB, Sonkusare SK, Zode GS. Technical brief: Direct, real-time electrochemical measurement of nitric oxide in ex vivo cultured human corneoscleral segments. *Mol Vis.* 2020;26:434-44. Epub 2020/06/23. PubMed PMID: 32565671; PMCID: PMC7300198.

48. Peters JC, Bhattacharya S, Clark AF, Zode GS. Increased Endoplasmic Reticulum Stress in Human Glaucomatous Trabecular Meshwork Cells and Tissues. *Invest Ophthalmol Vis Sci.* 2015;56(6):3860-8. doi: 10.1167/iovs.14-16220. PubMed PMID: 26066753; PMCID: 4468426.

49. Medina-Ortiz WE, Belmares R, Neubauer S, Wordinger RJ, Clark AF. Cellular fibronectin expression in human trabecular meshwork and induction by transforming growth

factor-beta2. Invest Ophthalmol Vis Sci. 2013;54(10):6779-88. doi: 10.1167/iovs.13-12298.
PubMed PMID: 24030464; PMCID: PMC3799562.

50. Ottolini M, Hong K, Cope Eric L, Daneva Z, DeLalio Leon J, Sokolowski Jennifer D, Marziano C, Nguyen Nhiem Y, Altschmied J, Haendeler J, Johnstone Scott R, Kalani Mohammad Y, Park Min S, Patel Rakesh P, Liedtke W, Isakson Brant E, Sonkusare Swapnil K. Local Peroxynitrite Impairs Endothelial TRPV4 Channels and Elevates Blood Pressure in Obesity. Circulation. 2020;0(0). Epub Ahead of print. doi: 10.1161/CIRCULATIONAHA.119.043385.

51. Hong K, Cope EL, DeLalio LJ, Marziano C, Isakson BE, Sonkusare SK. TRPV4 (Transient Receptor Potential Vanilloid 4) Channel-Dependent Negative Feedback Mechanism Regulates Gq Protein-Coupled Receptor-Induced Vasoconstriction. Arterioscler Thromb Vasc Biol. 2018;38(3):542-54. Epub 2018/01/06. doi: 10.1161/ATVBAHA.117.310038. PubMed PMID: 29301784; PMCID: PMC5823749.

52. Ottolini M, Hong K, Cope EL, Daneva Z, DeLalio LJ, Sokolowski JD, Marziano C, Nguyen NY, Altschmied J, Haendeler J, Johnstone SR, Kalani MY, Park MS, Patel RP, Liedtke W, Isakson BE, Sonkusare SK. Local Peroxynitrite Impairs Endothelial Transient Receptor Potential Vanilloid 4 Channels and Elevates Blood Pressure in Obesity. Circulation. 2020;141(16):1318-33. Epub 2020/02/06. doi: 10.1161/CIRCULATIONAHA.119.043385. PubMed PMID: 32008372; PMCID: PMC7195859.

53. Sonkusare SK, Dalsgaard T, Bonev AD, Hill-Eubanks DC, Kotlikoff MI, Scott JD, Santana LF, Nelson MT. AKAP150-dependent cooperative TRPV4 channel gating is central to endothelium-dependent vasodilation and is disrupted in hypertension. *Sci Signal*. 2014;7(333):ra66. Epub 2014/07/10. doi: 10.1126/scisignal.2005052. PubMed PMID: 25005230; PMCID: PMC4403000.
54. Sonkusare SK, Bonev AD, Ledoux J, Liedtke W, Kotlikoff MI, Heppner TJ, Hill-Eubanks DC, Nelson MT. Elementary Ca²⁺ signals through endothelial TRPV4 channels regulate vascular function. *Science*. 2012;336:597-601. Epub 2012/05/05. doi: 10.1126/science.1216283. PubMed PMID: 22556255; PMCID: 3715993.
55. Nathanson JA, McKee M. Identification of an extensive system of nitric oxide-producing cells in the ciliary muscle and outflow pathway of the human eye. *Invest Ophthalmol Vis Sci*. 1995;36(9):1765-73. Epub 1995/08/01. PubMed PMID: 7543462.
56. Doganay S, Evereklioglu C, Turkoz Y, Er H. Decreased nitric oxide production in primary open-angle glaucoma. *Eur J Ophthalmol*. 2002;12(1):44-8. Epub 2002/04/09. doi: 10.1177/112067210201200109. PubMed PMID: 11936443.
57. Keller KE, Bradley JM, Sun YY, Yang YF, Acott TS. Tunneling Nanotubes are Novel Cellular Structures That Communicate Signals Between Trabecular Meshwork Cells. *Invest Ophthalmol Vis Sci*. 2017;58(12):5298-307. Epub 2017/10/20. doi: 10.1167/iovs.17-22732. PubMed PMID: 29049733; PMCID: PMC5656416.

58. Keller KE. Tunneling nanotubes and actin cytoskeleton dynamics in glaucoma. *Neural Regen Res.* 2020;15(11):2031-2. Epub 2020/05/13. doi: 10.4103/1673-5374.282254. PubMed PMID: 32394952.
59. Chinnery HR, Keller KE. Tunneling Nanotubes and the Eye: Intercellular Communication and Implications for Ocular Health and Disease. *Biomed Res Int.* 2020;2020:7246785. Epub 2020/05/01. doi: 10.1155/2020/7246785. PubMed PMID: 32352005; PMCID: PMC7171654.
60. Kumar A, Chen X, Conwell M, Luo N, Obukhov A, Sun Y. In vivo live-cell imaging of human trabecular meshwork cells under laminar flow. *Invest Ophthalmol Visual Sci.* 2013;54(15):3574-.
61. Weinreb RN, Liebmann JM, Martin KR, Kaufman PL, Vittitow JL. Latanoprostene Bunod 0.024% in Subjects With Open-angle Glaucoma or Ocular Hypertension: Pooled Phase 3 Study Findings. *J Glaucoma.* 2018;27(1):7-15. Epub 2017/12/02. doi: 10.1097/IJG.0000000000000831. PubMed PMID: 29194198.
62. Weinreb RN, Scassellati Sforzolini B, Vittitow J, Liebmann J. Latanoprostene Bunod 0.024% versus Timolol Maleate 0.5% in Subjects with Open-Angle Glaucoma or Ocular Hypertension: The APOLLO Study. *Ophthalmology.* 2016;123(5):965-73. Epub 2016/02/15. doi: 10.1016/j.ophtha.2016.01.019. PubMed PMID: 26875002.

63. Medeiros FA, Martin KR, Peace J, Scassellati Sforzolini B, Vittitow JL, Weinreb RN. Comparison of Latanoprostene Bunod 0.024% and Timolol Maleate 0.5% in Open-Angle Glaucoma or Ocular Hypertension: The LUNAR Study. *Am J Ophthalmol.* 2016;168:250-9. Epub 2016/05/24. doi: 10.1016/j.ajo.2016.05.012. PubMed PMID: 27210275.
64. Liu JHK, Slight JR, Vittitow JL, Scassellati Sforzolini B, Weinreb RN. Efficacy of Latanoprostene Bunod 0.024% Compared With Timolol 0.5% in Lowering Intraocular Pressure Over 24 Hours. *Am J Ophthalmol.* 2016;169:249-57. Epub 2016/07/28. doi: 10.1016/j.ajo.2016.04.019. PubMed PMID: 27457257.
65. Weinreb RN, Ong T, Scassellati Sforzolini B, Vittitow JL, Singh K, Kaufman PL, Group V. A randomised, controlled comparison of latanoprostene bunod and latanoprost 0.005% in the treatment of ocular hypertension and open angle glaucoma: the VOYAGER study. *Br J Ophthalmol.* 2015;99(6):738-45. Epub 2014/12/10. doi: 10.1136/bjophthalmol-2014-305908. PubMed PMID: 25488946; PMCID: PMC4453588.
66. Araie M, Sforzolini BS, Vittitow J, Weinreb RN. Evaluation of the Effect of Latanoprostene Bunod Ophthalmic Solution, 0.024% in Lowering Intraocular Pressure over 24 h in Healthy Japanese Subjects. *Adv Ther.* 2015;32(11):1128-39. Epub 2015/11/14. doi: 10.1007/s12325-015-0260-y. PubMed PMID: 26563323; PMCID: PMC4662725.
67. Canto A, Olivar T, Romero FJ, Miranda M. Nitrosative Stress in Retinal Pathologies: Review. *Antioxidants (Basel).* 2019;8(11):543. Epub 2019/11/14. doi: 10.3390/antiox8110543. PubMed PMID: 31717957; PMCID: PMC6912788.

68. Patel G, Fury W, Yang H, Gomez-Caraballo M, Bai Y, Yang T, Adler C, Wei Y, Ni M, Schmitt H, Hu Y, Yancopoulos G, Stamer WD, Romano C. Molecular taxonomy of human ocular outflow tissues defined by single-cell transcriptomics. *Proc Natl Acad Sci U S A*. 2020;117(23):12856-67. Epub 2020/05/23. doi: 10.1073/pnas.2001896117. PubMed PMID: 32439707.
69. Lei Y, Zhang X, Song M, Wu J, Sun X. Aqueous Humor Outflow Physiology in NOS3 Knockout Mice. *Invest Ophthalmol Vis Sci*. 2015;56(8):4891-8. Epub 2015/08/01. doi: 10.1167/iovs.15-16564. PubMed PMID: 26225628.
70. Galassi F, Renieri G, Sodi A, Ucci F, Vannozzi L, Masini E. Nitric oxide proxies and ocular perfusion pressure in primary open angle glaucoma. *Br J Ophthalmol*. 2004;88(6):757-60. Epub 2004/05/19. doi: 10.1136/bjo.2003.028357. PubMed PMID: 15148207; PMCID: PMC1772173.

CHAPTER III

DIRECT, REAL-TIME ELECTROCHEMICAL MEASUREMENT OF NITRIC OXIDE IN EX VIVO CULTURED HUMAN CORNEOSCLERAL SEGMENTS.

Pinkal D. Patel¹, Ramesh B. Kasetti¹, Swapnil K. Sonkusare², and Gulab S. Zode¹

¹Department of Pharmacology and Neuroscience, North Texas Eye Research Institute, University
of North Texas Health Science Center at Fort Worth, TX 76107, USA

²Molecular Physiology and Biological Physics, University of Virginia - School of Medicine,
Charlottesville, VA 22901, USA

ABSTRACT

Chronic elevation of intraocular pressure (IOP) is a major risk factor associated with Primary Open Angle Glaucoma (POAG), a common form of progressive optic neuropathy that can lead to debilitating loss of vision. Recent studies have identified the role of nitric oxide (NO) in regulation of IOP, and as a result several therapeutic ventures are currently targeting enhancement of NO signaling in the eye. Although low level of NO is important for the ocular physiology, excess exogenous NO can be detrimental. Therefore, ability to directly measure NO in real-time is essential for determining the role of NO signaling in glaucomatous pathophysiology. Historically, NO activity in human tissues has been determined by indirect methods that measure levels of NO metabolites (nitrate/nitrite) or downstream components of NO signaling pathway (cGMP). In this proof-of-concept work, we assess the feasibility of direct, real-time measurement of NO in *ex vivo* cultured human corneoscleral segments using electrochemistry. NO-selective electrode (ISO-NOPF200) paired to a free-radical analyzer (TBR1025) was placed upon the TM rim for real-time measurement of NO released from cells. Exogenous NO produced within cells was measured after treatment of corneoscleral segments with esterase-dependent NO-donors DETA-NONOate/AM (20 μ M) and Latanoprostene bunod (5-20 μ M). DAF-FM assay (fluorescent NO-binding dye) was used for validation. A linear relationship was observed between the electric currents measured by NO-sensing electrode and the NO standard concentrations, thereby establishing a robust calibration curve. Treatment of *ex vivo* cultured human donor corneoscleral segments with DETA-NONOate/AM and Latanoprostene bunod led to a significant increase in NO production compared to vehicle treated controls, as detected electrochemically. Furthermore, DAF-FM fluorescence intensity was higher in outflow pathway tissues of corneoscleral segments treated with DETA-

NONOate/AM and Latanoprostene bunod compared to vehicle treated controls. In conclusion, these results demonstrate that NO-sensing electrodes can be used to directly measure NO levels in real-time from the tissues of the outflow pathway.

INTRODUCTION

Glaucoma is a complex multifactorial neurodegenerative disease characterized by progressive optic neuropathy. It is the leading cause of irreversible loss of vision with more than 70 million people affected worldwide (1), and this number is estimated to increase to 111.6 million by the year 2040 (2). Primary open angle glaucoma (POAG) is the most common form of glaucoma, accounting for approximately 70% of all cases (1). Elevated intraocular pressure (IOP) is a major risk factor associated with the development and progression of the disease (3, 4), and it is the only modifiable risk factor in POAG. Therefore, majority of medical and surgical interventions are targeted towards reduction of IOP (5).

IOP is tightly regulated by the balance in secretion of the aqueous humor (AH) from the ciliary epithelium and its rate of elimination from the eye by the conventional and unconventional outflow pathways. The conventional outflow pathway consisting of a sieve-like tissue called trabecular meshwork (TM) is responsible for the majority of resistance to AH outflow (5-7). Increase in resistance at the TM leads to chronic IOP elevation and glaucomatous pathology (8-10). Therefore, current drug therapies are targeted at the TM outflow pathway for lowering IOP and reducing resistance to aqueous humor outflow.

Nitric oxide (NO) has been implicated in numerous physiological processes of the eye, including IOP homeostasis and ocular blood flow (11-13). Recent body of evidence strongly implicates NO in regulation of IOP by modulating TM contractile tone and outflow resistance (14-20). It has been shown that exogenous delivery of NO via donor compounds reduces IOP in mice (14), rabbit (21), non-human primates (19), and human ex vivo tissue models (20). Latanoprostene bunod, a

chimeric prostaglandin analog with NO donating moiety has been recently approved by the United States Food and Drug Administration (FDA) as an IOP reducing therapeutic after successful clinical trials in humans (22-27). Although the benefits of exogenous NO delivery in glaucoma are apparent, it is important to acknowledge the paradoxical role of NO that may also contribute to disease pathology. The effect of NO is largely concentration dependent. At lower concentrations, NO can be beneficial to cell survival and can act as an important homeostatic mediator, whereas at high concentrations excess NO can lead to nitrosative stress and physiological dysregulation (28). Exogenous NO donor drugs get activated in cells via nonspecific esterase-dependent NO release mechanisms which can lead to unwanted release of NO in nontargeted tissues. In the eye, nitric oxide synthase (NOS) family of enzymes are primarily responsible for the production of endogenous NO. This endogenous NO produced in very low amounts is responsible for regulation of enzymatic processes and physiological pathways (20, 29, 30).

Given the benefits, we are yet to elucidate the intrinsic regulatory pathways controlling endogenous production of NO in the eye. The spatial and temporal concentrations of NO are of extreme importance for determining the role of NO signaling in pathophysiology of glaucoma. High reactivity, rapid diffusion, and short half-life of NO makes it challenging to accurately measure its level in biological tissues. Although several techniques have been utilized for indirect measurement of NO, electrochemical (amperometric) detection of NO is the only available technique sensitive enough to determine physiologically relevant concentrations of NO in real time (31, 32). To assess the role of NO in glaucomatous pathophysiology and to determine the release profile of NO donor drugs, it is crucial to directly and accurately measure the NO levels in real-time. A previous study used a derivative of Clark-type NO-sensing electrode setup for measuring NO produced in enucleated bovine eyes (33). Due to advancement in electrode technology, these

Clark-type electrodes can now be made in the microscale size and be highly flexible for use in ex vivo or in vivo settings. Here we used a commercially available, microscale (200 μm diameter) version of the Clark-type electrode for detection of NO in human ex vivo cultured corneoscleral tissue.

Although animal and human models share remarkable physiological and anatomical similarities, the results obtained in animal models rarely translate to disease modifying outcomes. We have previously reported the use of ex vivo cultured human corneoscleral segments in modeling glaucomatous pathology (manuscript in review). These human corneoscleral segments with intact TM and outflow pathway tissues are gifted post-mortem for corneal transplant. Corneoscleral segments that are ineligible for transplant are made available for biomedical research at a fraction of the processing cost compared to whole globes. This ex vivo cultured human corneoscleral model allows study of physiological processes and disease pathology in a system that closely mimics the in vivo state.

In this proof of concept study, we utilize the ex vivo cultured human corneoscleral segment model to electrochemically measure the NO generated from donor compounds in real-time at the TM outflow pathway. We further validate these results using a secondary, fluorescence-based DAF-FM assay for NO detection.

METHODS AND MATERIALS

Ex vivo culture of human corneoscleral segments

Transplant ineligible, deidentified human corneoscleral segments were acquired from Lions Eye Institute (Tampa, FL) in conformity to the guidelines outlined in the Declaration of Helsinki. Upon receipt, the corneoscleral segments were washed 3 times with PBS (7.4 pH; SigmaAldrich; St. Louis, MO) and then cultured at 37 °C and 5% CO₂ in DMEM culture medium supplemented with 10% FBS (Sigma Aldrich; St. Louis, MO), L-glutamine (Sigma Aldrich; St. Louis, MO), and 1% Pen-Strep (Sigma Aldrich; St. Louis, MO). The culture medium was exchanged daily with fresh medium.

Electrode calibration and NO-sensing electrode setup

Direct measurements of NO were performed using TBR1024 Free Radical Analyzer and NO sensing electrode (ISO-NOPF200) obtained from World Precision Instruments (WPI; Sarasota, FL). Currents reading were recorded in the LabScribe-3 software (WPI; Sarasota, FL). Electrodes were calibrated prior to experiments according to the manufacturer's instructions by the decomposition of a NO donor S-nitroso-N-acetyl-penicillamine (SNAP; WPI; Sarasota, FL) using CuCl₂. SNAP was prepared by dissolving 5 mg EDTA (Sigma Aldrich; St. Louis, MO) and 5.0 mg of SNAP in 250 mL HPLC grade water. The electrode was immersed in 20 mL of 0.1 M CuCl₂ (Sigma Aldrich; St. Louis, MO) in distilled water until the electrode stabilized (1–2 hrs). A calibration curve was created by sequentially adding bolus volumes of SNAP after each signal reached a plateau. The sampling rate used was 10 samples/s. The change in recorded current was converted to corresponding molarities of NO produced by SNAP addition. The efficiency of the

conversion of SNAP to NO was 0.6. All measurements were performed within a chemical hood in constant airflow and at room temperature in order to avoid any temperature fluctuations and electrical interference. Prior to each measurement the electrode was polarized for 2 hours in PBS. Human corneoscleral segments with intact TM rims were washed 3 times with PBS and placed in a 24 well plate submerged in 1 mL PBS. Measurements were performed in PBS instead of complete media in order to avoid interference from other nitrogen containing compounds. We anticipated that the length/area of TM may influence the amount of NO generated. To normalize this variable, we use the entire corneoscleral segment with an intact TM rim for real-time electrochemical measurement of NO. Furthermore, to reduce the variability between different donors, we use pairs of corneoscleral segments from the same donor for vehicle and drug treatments. The electrode was lowered into the well and clamped in such a way that the tip of the electrode remained in contact with the TM rim throughout the experiment (Figure 1A). A stable baseline was achieved following which the corneoscleral segments were treated with NO-donor drugs or vehicle. Troubleshooting of common problems encountered during application of the technique are listed in Supplementary Table 2. DETA-NONOate/AM (O₂-acetoxymethylated diazeniumdiolate; MilliporeSigma; Burlington, MA) (34) and 0.024% Latanoprostene bunod (Bausch & Lomb, Bridgewater, NJ) are the two NO-donor compounds tested in this study. Latanoprost was used as the vehicle against the NO-donor Latanoprostene bunod. Both ophthalmic solutions (Latanoprostene bunod and Latanoprost) were obtained from a local pharmacy Daniel Drugs (Fort Worth, TX).

Fluorochemical DAF-FM Assay for nitric oxide labeling

Human donor corneoscleral segments were divided into quadrants and cultured in phenol red-free DMEM media (Sigma Aldrich; St. Louis, MO) supplemented with 0.2% FBS and 1% Pen-Strep

(Sigma Aldrich; St. Louis, MO). The vehicle and experimental treatments were performed on the same eye to reduce variability associated with the contralateral eye. Quadrants from each eye were first treated with 10 μ M DAF-FM (Millipore Sigma; Burlington, MA) dye and incubated at 37 °C for 30 min. Quadrants were then washed 3 times with PBS and incubated for an additional 30 min at 37 °C to allow proper incorporation and activation of dye within cells. The quadrants were then treated either with different NO-donor compounds or with appropriate vehicle controls, and further incubated for 30 min at 37 °C. After the incubation period, the quadrants were washed 3 times with PBS and prepared for imaging (Figure 1B). The TM rim (including the inner wall of Schlemm's canal) was carefully dissected from the unfixed corneoscleral quadrants and placed between coverslips for imaging under the microscope (Keyence; Itasca, IL). DAF-FM fluorescence images were analyzed by quantifying fluorescence intensity per unit area ($\text{IntDen}/\mu\text{m}^2$) using ImageJ (National Institute of Health; Bethesda; MD) as described previously (35, 36).

Statistical Analysis

Statistical Analysis was performed using GraphPad Prism 8 (San Diego, CA). Data are expressed in means \pm SEM. Two-group comparisons were analyzed by Unpaired Student's t-test. Multiple comparisons were analyzed by Two-way ANOVA with Bonferroni *post hoc* test. Significance was designated at *P < 0.05, **P < 0.01, and ***P < 0.001.

RESULTS

Electrochemical detection of NO involves the oxidation of NO on the electrode surface and subsequent measurement of the redox current generated. When the NO microelectrode (consisting of a working and reference electrode pair) is immersed in a solution containing NO and a positive potential is applied, NO is oxidized at the working electrode surface producing a redox current. Thus, the amount of NO oxidized is proportional to the current flow at the electrode, which is measured by the free radical analyzer. As recommended by the manufacturer, NO generated by decomposition of SNAP was used to calibrate the NO-sensing electrode (ISONOPF-200). The calibration curve demonstrates a linear relationship between the amount of NO generated from SNAP and the current detected at the electrode (Figure 2).

A previous study has demonstrated electrochemical measurement of NO in enucleated bovine eyes (33). Here we examined whether ex vivo cultured human corneoscleral segments can be used to detect chemically generated NO in the outflow pathway tissues. Our improved understanding of the NO signaling pathway and its involvement in several disease pathologies has aided development of several esterase-dependent NO donor compounds for therapy. We asked whether this NO-sensing electrode setup can be utilized for measuring NO in human tissues. We tested two NO-donor compounds, DETA-NONOate/AM and the clinically tested and FDA approved Latanoprostene bunod. DETA-NONOate/AM is a commercially available intracellular NO donor compound with esterase-dependent NO release mechanism (34). Each pair of human corneoscleral segments were treated with 20 μ M DETA-NONOate/AM or equivalent vehicle. Representative response graph shows an increase in detected current from the segments treated with DETA-NONOate/AM compared to vehicle treated control (Figure 3A). A 'no tissue' control was used to determine

whether extracellular degradation of NO in aqueous solution was contributing to the detected current. We did not observe an increase in NO current after addition of DETA-NONOate/AM in aqueous PBS (Figure 3A). Furthermore, treatment of corneoscleral segments with 20 μ M DETA-NONOate/AM for 30 min resulted in a significant increase in NO production compared to vehicle treated controls (Figure 3B). We further used DAF-FM assay to fluorescently label NO in the outflow pathway tissues in order to validate the results obtained via electrochemistry. Quadrants of human corneoscleral segments were pretreated with DAF-FM and then subsequently treated with 20 μ M DETA-NONOate/AM or vehicle control. A significant increase in DAF-FM fluorescence intensity was observed in quadrants of corneoscleral segments treated with DETA-NONOate/AM compared to vehicle treated control (Figure 4A-B).

Latanoprostene bunod is an aqueous soluble chimeric compound constituting Latanoprost (IOP lowering prostaglandin analog) linked to butanediol mononitrate (NO-donor moiety). The NO released from Latanoprostene bunod is implicated in regulating AH outflow resistance at the conventional outflow pathway and has been recently approved for IOP lowering therapy in human glaucoma patients (22-25, 37). Each pair of ex vivo cultured human corneoscleral segments was treated with increasing concentrations of 5-20 μ M Latanoprostene bunod or equivalent vehicle Latanoprost. The NO-sensing electrode setup was used to measure the subsequent NO production. A dose-dependent increase in NO production was observed in the segments treated with Latanoprostene bunod compared to vehicle Latanoprost (Figure 5). Furthermore, DAF-FM staining intensity was significantly higher in the segments treated with 20 μ M Latanoprostene bunod compared to Latanoprost vehicle (Figure 6A-B).

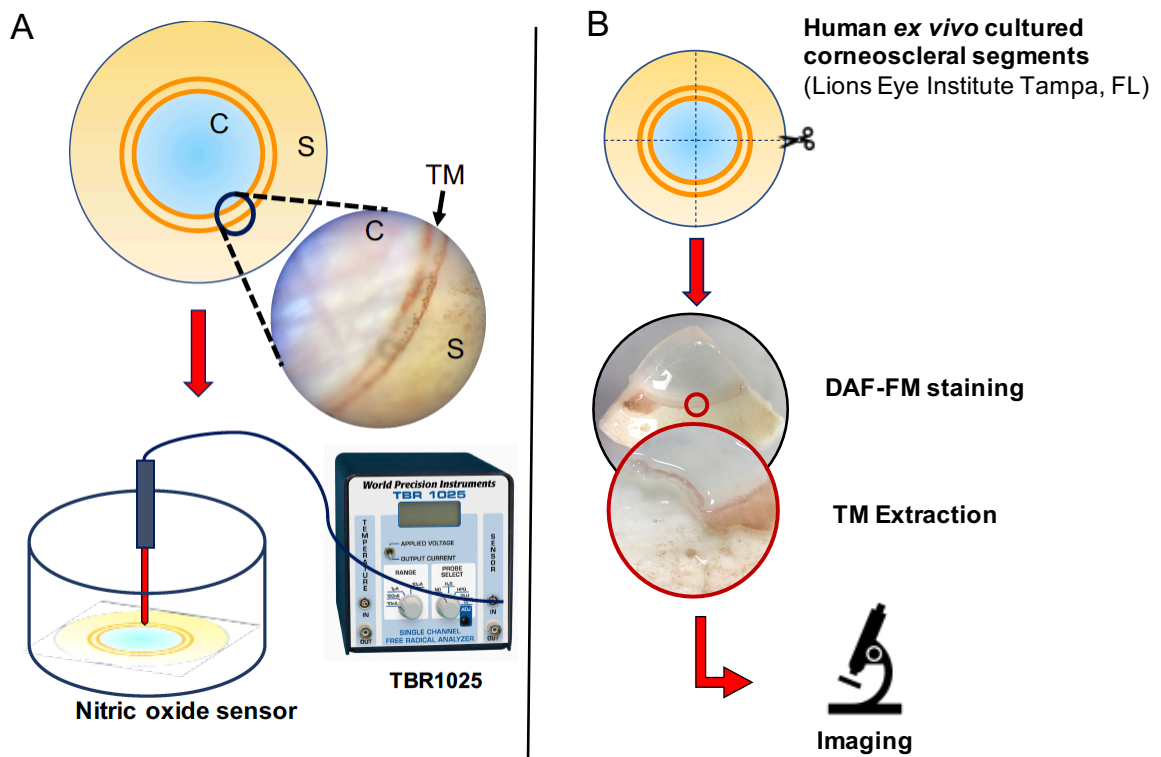


Figure 1. Experimental setup for the study. A. Workflow for electrochemical NO measurement using NO-sensing electrode. Cultured human donor corneoscleral segments were washed 3X with PBS and placed in 24 well plate with 1 mL PBS. Drug treatments were performed after stable baseline was achieved. The output current corresponds to level of NO generated (~ 10 pA/nM) which is detected at the free radical analyzer (TBR1025). The signal is amplified by a 4-channel Lab-Trax amplifier and analyzed using LabScribe3 software (by WPI). B. Workflow for fluorochemical measurement of NO using DAF-FM assay (intracellular NO-binding dye). Quadrants of human donor corneoscleral segment were cultured at 37°C in DMEM media supplemented with 2% FBS and 1% PS and treated with $10\ \mu\text{M}$ Nitric Oxide binding fluorescent DAF-FM dye for 30 min. Cells and tissues were washed with 1X PBS and treated with different drugs or vehicle and incubated at 37°C for additional 30 min. Tissues were then washed 3X with PBS and TM rim was removed and imaged using fluorescence microscopy.

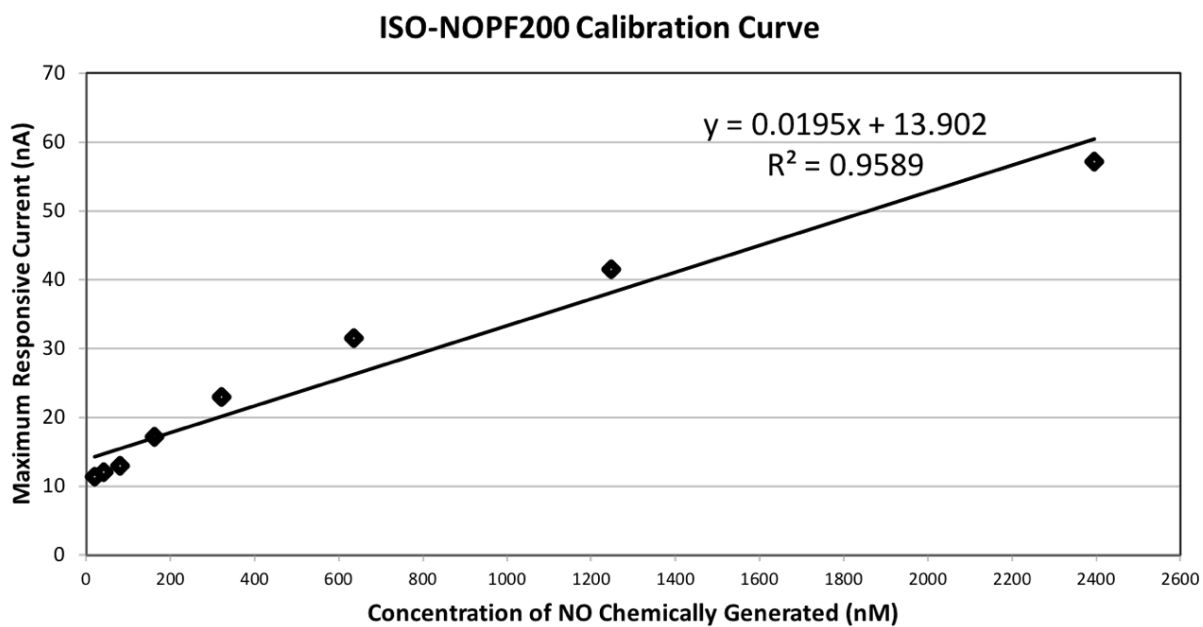


Figure 2. Linear regression analysis of the relationship between amount of NO added and the electric current obtained from the NO electrode (ISO-NOPF200).

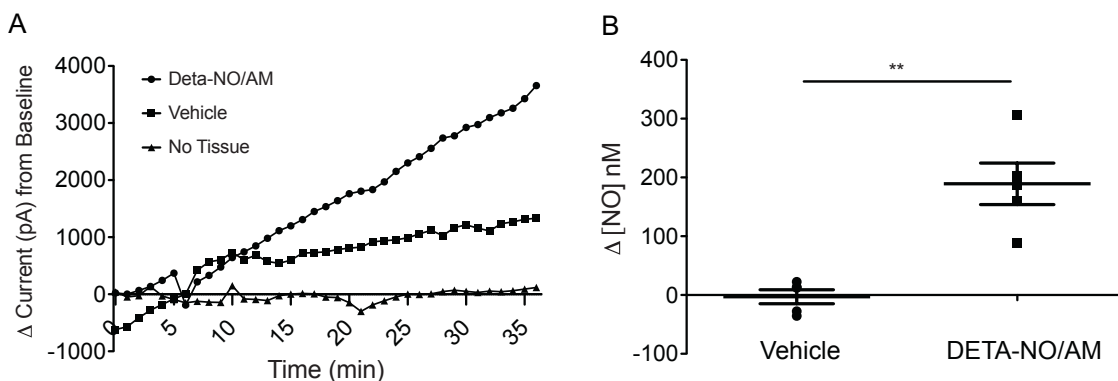


Figure 3. Detection of NO in human corneoscleral segments after treatment with DETA-NONOate/AM (exogenous NO donor). A. Representative response plot showing amperometric current readings obtained after treatment of *ex vivo* cultured human corneoscleral tissues with an exogenous NO donor DETA-NONOate/AM or equivalent vehicle. A visible spike in recorded current was observed as a result of DETA-NONOate/AM treatment on human corneoscleral segments. A ‘no tissue’ control was employed to ensure that the detection of NO signal was tissue dependent and not a result of NO release in aqueous PBS. B. Change in NO concentration from baseline after 30 min of treatment with Deta-NONOate/AM (20 μ M) or equivalent vehicle (0.1% DMSO) at room temperature. Data are expressed as means \pm SEM; n = 5 for each group; ** P < 0.001; Two-tailed unpaired Student’s t test.

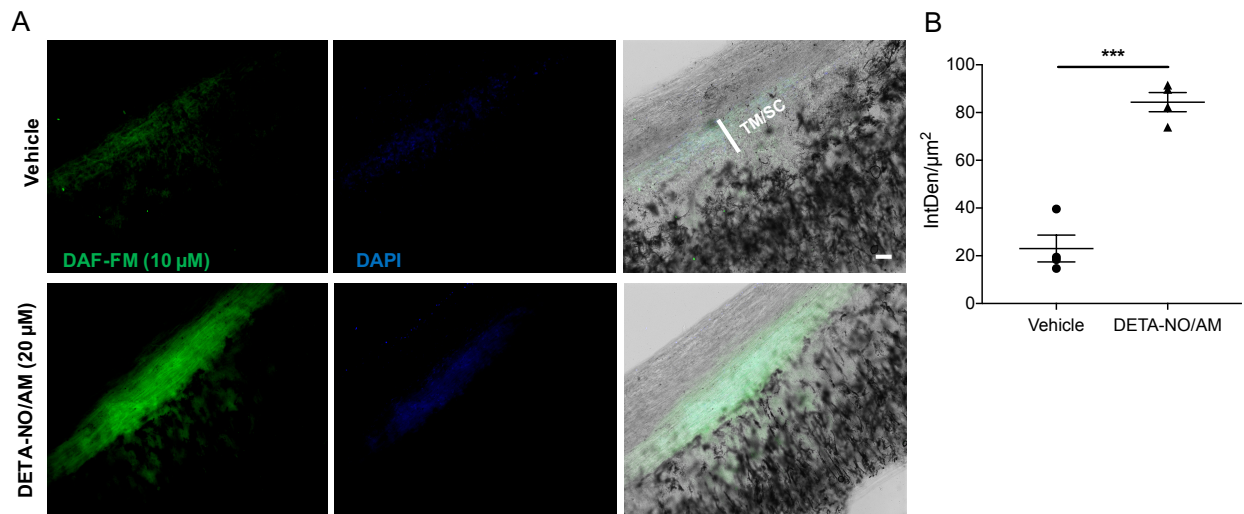


Figure 4. A. Increase in DAF-FM fluorescence intensity in quadrants of human corneoscleral segments after treatment with DETA-NONOate/AM (exogenous NO donor) compared to vehicle treated controls. Quadrants of human donor corneoscleral segments from each eye (n = 4 per group) were pretreated with intracellular NO-indicator dye DAF-FM dye (10 μM) and then treated with DETA-NONOate/AM (20 μM) or vehicle (0.1% DMSO) at 37°C for 30 min. Images were taken using fluorescence microscopy at 100X magnification (Scale bar = 50 μm). B. Quantification of DAF-FM fluorescence intensity per unit area (IntDen/μm²) in DETA-NO/AM and vehicle treated corneoscleral segments using ImageJ analysis. Data are expressed as means ± SEM; n = 4 for each group; *** P < 0.001; Two-tailed unpaired Student's t test.

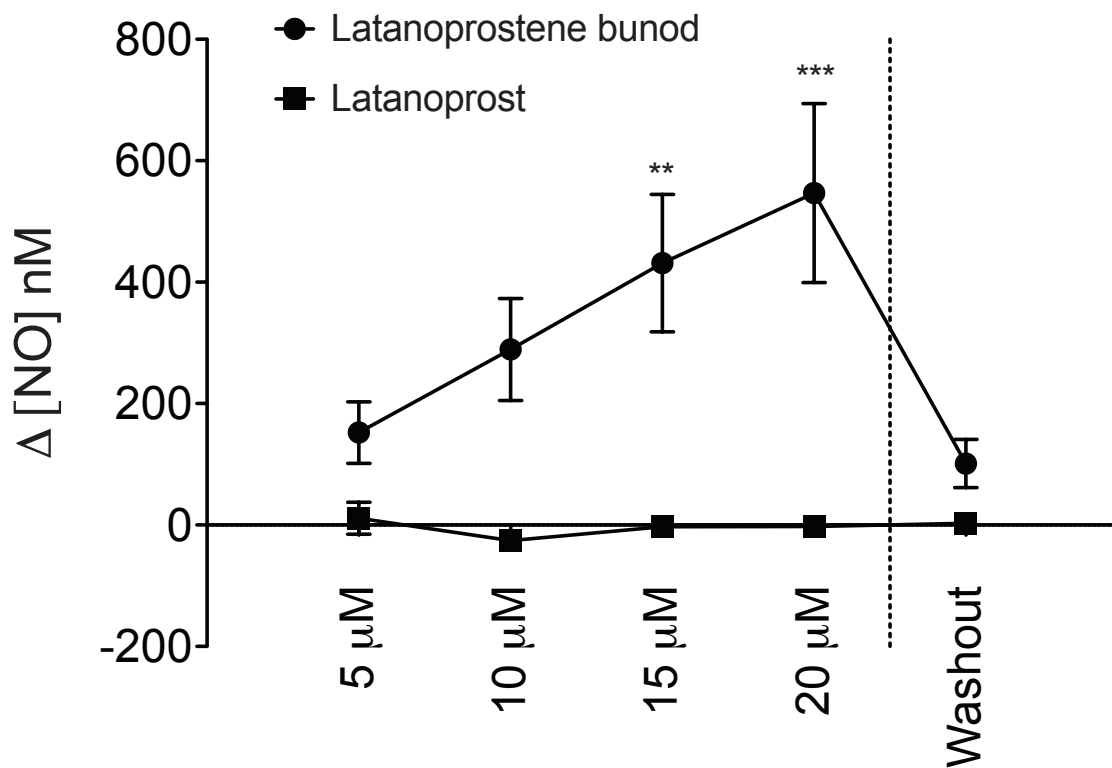


Figure 5. Dose dependent increase in NO levels in human corneoscleral segments after treatment with Latanoprostene bunod compared to Latanoprost vehicle control. Cultured human donor corneoscleral segments were treated with increasing doses of Latanoprostene bunod (5-20 μM) or equivalent volume of Latanoprost (vehicle) and change in levels of NO from baseline were recorded. Each subsequent bolus dose was given after the signal plateaued (~ 10 min). Washout readings were recorded after a 30 min period. Data are expressed as means \pm SEM; $n = 4$ for each group; ** $P < 0.01$, *** $P < 0.001$; Two-way ANOVA.

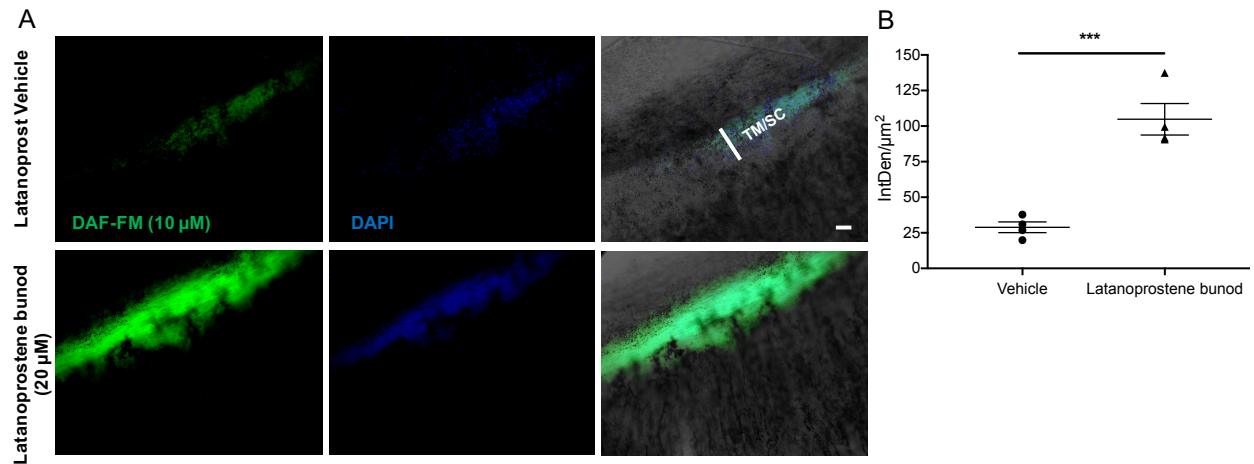


Figure 6. A. Increase in DAF-FM fluorescence intensity in quadrants of human corneoscleral segments after treatment with Latanoprostene bunod compared to controls treated with vehicle Latanoprost. Quadrants of human donor corneoscleral segments from each eye ($n = 4$ per group) were pretreated with intracellular NO-indicator dye DAF-FM dye ($10 \mu\text{M}$) and then treated with Latanoprostene bunod ($20 \mu\text{M}$) or Latanoprost vehicle. Quadrants treated with LBN showed increased DAF-FM fluorescence intensity compared to vehicle treated controls. Images were taken using fluorescence microscopy at 100X magnification (Scale bar = $50 \mu\text{m}$). B. Quantification of DAF-FM fluorescence intensity per unit area ($\text{IntDen}/\mu\text{m}^2$) in Latanoprostene bunod and Latanoprost Vehicle treated corneoscleral segments using ImageJ analysis. Data are expressed as means \pm SEM; $n = 4$ for each group; *** $P < 0.001$; Two-tailed unpaired Student's t test.

Table 1. Troubleshooting solutions for real-time electrochemical measurement of NO in human corneoscleral segments (adapted from Worlds Precision Instruments).

Issue	Possible cause	Solution
Baseline current below specified range	Incorrect setting selected on the TBR1025 analyzer.	Set the poise voltage to 865 mV (NO setting) on TBR1025. Set the range to 100 nA
	Sensor may be nearing the end of its usable life.	Perform calibration using fresh standard solutions. If problem persists, change NO sensor.
Unstable baseline	Interference from chemical contaminants from growth media.	Wash corneoscleral segments with PBS at least 5 times prior to initiating measurement.
	The polarizing solution may be contaminated.	Prepare fresh polarizing solution (0.1M CuCl ₂). After polarization, we recommend using PBS to stabilize the electrode.
	External electrical interferences may be a problem.	Identify and isolate electrical interference.
	Interference from external heat sources.	Identify external heat sources and isolate equipment. We recommend using a laminar airflow hood.
Non-linear calibration	Stock solutions have deteriorated.	Prepare fresh SNAP standard solution and repeat calibration.
	Chemical contaminants in water or on glassware.	Use ultrapure milliQ water in preparing solutions. Wash glassware with milliQ water prior to use.
	Uneven aliquots may have been used.	Check pipette calibration.
Low sensitivity	Probe not in contact with the trabecular meshwork (TM) rim.	Secure the sensor in a manner that it is in constant contact with the TM rim.
	Use of disintegrated TM rim tissue corneoscleral segment tissue.	Use corneoscleral segments with intact TM rim and overall tissue morphology for a robust response.
	Foreign material adsorbed on the sensor surface.	Wash the sensor with detergent if the material is protein from growth media or Ultrapure milliQ water if it is salt from PBS.
	Sensor has reached the end of its usable life.	Replace the sensor.

DISCUSSION

Cornea is the most commonly donated human tissue in the world. In the United States alone, 116,990 corneas were donated in the year 2016, of which only 63,596 corneas were used for transplantation (38). Due to low specular cell counts (<2000 cells), accidental damage, or abnormal medical history of the patient (suspected cases of dementia or risk of prions disease) majority of donated corneas are deemed ineligible for transplant. These ineligible corneoscleral explants having intact conventional outflow pathway tissue are made available for research with lower processing cost compared to intact whole globes. Cost and tissue availability are the two barriers that prevent wider use of human tissue in biomedical research. Vision scientists that collaborate with eye banks are in a unique position to overcome these barriers and study disease pathophysiology in an ex vivo system that closely mimics the in vivo state. We have previously reported the versatility of ex vivo cultured human donor corneoscleral segments in modeling glaucomatous pathology (manuscript in review). We have shown that treatment of human corneoscleral segments with glaucoma-associated factors like dexamethasone and recombinant transforming growth factor (TGF) $\beta 2$ results in glaucoma-related phenotypes which include increased ECM production and ER stress in the AH outflow pathway. In this study, we determine the feasibility of using donated human corneoscleral segments for directly measuring NO production in real-time.

In POAG, dysfunction in the NO signaling pathway and reduced bioavailability of NO has often been associated with the disease pathology (39-41). As a result, enhancement of NO signaling using exogenous NO donor compounds has emerged as a promising new therapeutic avenue. Furthermore, the recent push in the development of IOP lowering NO-donor compounds has

unraveled an unmet need for direct measurement of NO in ocular tissues. However, high reactivity, rapid diffusion, and short half-life makes it challenging to accurately measure the level of NO in biological tissues. Currently, electrochemical measurement is the sole method for directly quantifying physiologically relevant amounts of NO in real-time. A previous study used a derivative of the Clark-type electrode setup for direct, electrochemical measurement of NO in bovine eyes (33). Since then, electrode technology has seen considerable progress with the development of smaller, flexible, and more sensitive electrodes for NO measurement in tissues. We used a commercially available NO-sensing electrode with high selectivity for NO to measure real-time NO production in human tissues. To our knowledge, this is the first study utilizing ex vivo cultured human corneoscleral segments to directly measure NO generated from donor compounds in real-time. We electrochemically measured NO produced in the AH outflow pathway after treatment of human corneoscleral segment tissues with two structurally different exogenous NO-donor compounds, both having esterase-dependent intracellular NO release mechanism. Each pair of human corneoscleral segments were treated with either the NO-donor compounds DETA-NONOate/AM (20 μ M) and Latanoprostene bunod (5-20 μ M) against equivalent vehicle control. The detected NO currents which corresponds to the amount of NO produced were significantly higher in the tissues treated with NO-donors compared to equivalent vehicle treated controls (Figures 3A-B, 5). Furthermore, we used DAF-FM assay as a secondary technique for validation of the electrochemical data. The fluorescence intensity of NO-binding dye DAF-FM was higher in the quadrants of corneoscleral segment tissues treated with the NO-donors compared to controls (Figures 4A-B and 6A-B). These results indicate that the NO-sensing electrode is able to successfully detect the exogenous NO produced by NO-donors in human tissues. We also examined whether there were differences in NO-donor compounds in terms of NO release. We

observed relatively robust NO currents and higher DAF-FM fluorescence intensity in segments treated with Latanoprostene bunod (20 μ M) when compared to DETA-NONOate/AM (20 μ M) treated segments. Latanoprostene bunod appears to be superior in tissue penetration, rate of metabolization, and NO production. This was surprising because the stoichiometric ratio for NO release from Latanoprostene bunod is lower (1 mol of NO/mol) than that of DETA-NONOate/AM (1.83 mol of NO/mol). A possible explanation for this is that Latanoprostene bunod is an aqueous soluble compound compared to DETA-NONOate/AM. Furthermore, Latanoprostene bunod formulation used in this study is clinically approved and refined for superiority compared to the relatively untested DETA-NONOate/AM.

Ocular tissues like the TM, corneal endothelium, and Schlemm's canal endothelium can metabolize the donor compounds and produce NO currents. It is important to note that both the NO-donors used in the study can indiscriminately enter cells of any tissue and produce exogenous NO currents. Although this makes it difficult to determine the exact tissue source for the detected NO currents, we consider that the majority of detected NO is produced at the conventional outflow pathway tissues. Given the short half-life and rapid reactivity of NO, proximity of the electrode to the tissue is important for capturing the NO and generating a robust electrical signal. Similar to the previous study by Millar, we placed the electrode on the TM in order to maximize the capture of local NO released from the TM (33). Therefore, close proximity of the electrode to the TM and SC ensures maximum contribution from the conventional AH outflow pathway tissues.

In this study, we electrochemically measure the levels of exogenous NO released in the outflow pathway tissues. However, we recognize that this setup may also be able to detect endogenous NO levels from ex vivo cultured human corneoscleral segments. This is evident in the fact that we were able to detect baseline NO currents in vehicle treated corneoscleral segments (Figure 3A).

Endogenous NO within cells is produced by the constitutive and induced nitric oxide synthase (NOS) enzymes, as well as via reduction of nitrates/nitrites by cellular reductases (42). Future work will focus on refining this system further to improve detection of endogenous NO in ocular tissues.

Although the electrochemical method for quantifying NO holds much promise and utility in studying the pharmacodynamic properties of glaucoma medications in real-time, it is also important to understand the limitations of this technique. Electrodes used for detecting NO are inherently sensitive to environmental influences. Current iteration of this setup is an open system that is sensitive to temperature and pH changes. Our setup utilizes a laminar airflow hood for electrical and thermal isolation to reduce effect of temperature fluctuations on the system. However, development of a closed system is necessary in order to control for the confounding effects of temperature and pH. Future iterations will need integration of temperature and pH sensors within a closed measurement chamber. This closed measurement chamber can be placed in an incubator for quantifying endogenously produced NO at physiologically relevant temperatures, which will increase tissue viability for longer measurement timepoints.

REFERENCES

1. Quigley HA, Broman AT. The number of people with glaucoma worldwide in 2010 and 2020. *Br J Ophthalmol.* 2006;90(3):262-7. Epub 2006/02/21. doi: 10.1136/bjo.2005.081224. PubMed PMID: 16488940; PMCID: PMC1856963.
2. Tham YC, Li X, Wong TY, Quigley HA, Aung T, Cheng CY. Global prevalence of glaucoma and projections of glaucoma burden through 2040: a systematic review and meta-analysis. *Ophthalmology.* 2014;121(11):2081-90. Epub 2014/07/01. doi: 10.1016/j.ophtha.2014.05.013. PubMed PMID: 24974815.
3. Omoti AE, Edema OT. A review of the risk factors in primary open angle glaucoma. *Niger J Clin Pract.* 2007;10(1):79-82. Epub 2007/08/03. PubMed PMID: 17668721.
4. Rosenthal J, Leske MC. Open-angle glaucoma risk factors applied to clinical area. *J Am Optom Assoc.* 1980;51(11):1017-24. Epub 1980/11/01. PubMed PMID: 7440868.
5. Weinreb RN, Leung CK, Crowston JG, Medeiros FA, Friedman DS, Wiggs JL, Martin KR. Primary open-angle glaucoma. *Nat Rev Dis Primers.* 2016;2:16067. Epub 2016/09/23. doi: 10.1038/nrdp.2016.67. PubMed PMID: 27654570.
6. Rohen JW. Why is intraocular pressure elevated in chronic simple glaucoma? Anatomical considerations. *Ophthalmology.* 1983;90(7):758-65. Epub 1983/07/01. doi: 10.1016/s0161-6420(83)34492-4. PubMed PMID: 6413918.

7. Kwon YH, Fingert JH, Kuehn MH, Alward WL. Primary open-angle glaucoma. *N Engl J Med.* 2009;360(11):1113-24. Epub 2009/03/13. doi: 10.1056/NEJMra0804630. PubMed PMID: 19279343; PMCID: PMC3700399.
8. Raghunathan VK, Morgan JT, Park SA, Weber D, Phinney BS, Murphy CJ, Russell P. Dexamethasone Stiffens Trabecular Meshwork, Trabecular Meshwork Cells, and Matrix. *Invest Ophthalmol Vis Sci.* 2015;56(8):4447-59. Epub 2015/07/22. doi: 10.1167/iovs.15-16739. PubMed PMID: 26193921; PMCID: PMC4509060.
9. Fleenor DL, Shepard AR, Hellberg PE, Jacobson N, Pang IH, Clark AF. TGFbeta2-induced changes in human trabecular meshwork: implications for intraocular pressure. *Invest Ophthalmol Vis Sci.* 2006;47(1):226-34. Epub 2005/12/31. doi: 10.1167/iovs.05-1060. PubMed PMID: 16384967.
10. Keller KE, Aga M, Bradley JM, Kelley MJ, Acott TS. Extracellular matrix turnover and outflow resistance. *Exp Eye Res.* 2009;88(4):676-82. Epub 2008/12/18. doi: 10.1016/j.exer.2008.11.023. PubMed PMID: 19087875; PMCID: PMC2700052.
11. Aliancy J, Stamer WD, Wirostko B. A Review of Nitric Oxide for the Treatment of Glaucomatous Disease. *Ophthalmol Ther.* 2017;6(2):221-32. Epub 2017/06/07. doi: 10.1007/s40123-017-0094-6. PubMed PMID: 28584936; PMCID: PMC5693832.

12. Toda N, Nakanishi-Toda M. Nitric oxide: ocular blood flow, glaucoma, and diabetic retinopathy. *Prog Retin Eye Res.* 2007;26(3):205-38. Epub 2007/03/06. doi: 10.1016/j.preteyeres.2007.01.004. PubMed PMID: 17337232.
13. Wareham LK, Buys ES, Sappington RM. The nitric oxide-guanylate cyclase pathway and glaucoma. *Nitric Oxide.* 2018;77:75-87. Epub 2018/05/04. doi: 10.1016/j.niox.2018.04.010. PubMed PMID: 29723581; PMCID: PMC6424573.
14. Chang JY, Stamer WD, Bertrand J, Read AT, Marando CM, Ethier CR, Overby DR. Role of nitric oxide in murine conventional outflow physiology. *Am J Physiol Cell Physiol.* 2015;309(4):C205-14. Epub 2015/06/05. doi: 10.1152/ajpcell.00347.2014. PubMed PMID: 26040898; PMCID: PMC4537932.
15. Dismuke WM, Liang J, Overby DR, Stamer WD. Concentration-related effects of nitric oxide and endothelin-1 on human trabecular meshwork cell contractility. *Exp Eye Res.* 2014;120:28-35. Epub 2014/01/01. doi: 10.1016/j.exer.2013.12.012. PubMed PMID: 24374036; PMCID: PMC3943640.
16. Dismuke WM, Mbadugha CC, Ellis DZ. NO-induced regulation of human trabecular meshwork cell volume and aqueous humor outflow facility involve the BKCa ion channel. *Am J Physiol Cell Physiol.* 2008;294(6):C1378-86. Epub 2008/04/04. doi: 10.1152/ajpcell.00363.2007. PubMed PMID: 18385281.

17. Dismuke WM, Sharif NA, Ellis DZ. Human trabecular meshwork cell volume decrease by NO-independent soluble guanylate cyclase activators YC-1 and BAY-58-2667 involves the BKCa ion channel. *Invest Ophthalmol Vis Sci.* 2009;50(7):3353-9. Epub 2009/02/24. doi: 10.1167/iovs.08-3127. PubMed PMID: 19234350.
18. Ellis DZ, Sharif NA, Dismuke WM. Endogenous regulation of human Schlemm's canal cell volume by nitric oxide signaling. *Invest Ophthalmol Vis Sci.* 2010;51(11):5817-24. Epub 2010/05/21. doi: 10.1167/iovs.09-5072. PubMed PMID: 20484594.
19. Heyne GW, Kiland JA, Kaufman PL, Gabelt BT. Effect of nitric oxide on anterior segment physiology in monkeys. *Invest Ophthalmol Vis Sci.* 2013;54(7):5103-10. Epub 2013/06/27. doi: 10.1167/iovs.12-11491. PubMed PMID: 23800771; PMCID: PMC3729238.
20. Schneemann A, Dijkstra BG, van den Berg TJ, Kamphuis W, Hoyng PF. Nitric oxide/guanylate cyclase pathways and flow in anterior segment perfusion. *Graefes Arch Clin Exp Ophthalmol.* 2002;240(11):936-41. Epub 2002/12/18. doi: 10.1007/s00417-002-0559-7. PubMed PMID: 12486517.
21. Kotikoski H, Alajuuma P, Moilanen E, Salmenpera P, Oksala O, Laippala P, Vapaatalo H. Comparison of nitric oxide donors in lowering intraocular pressure in rabbits: role of cyclic GMP. *J Ocul Pharmacol Ther.* 2002;18(1):11-23. Epub 2002/02/23. doi: 10.1089/108076802317233171. PubMed PMID: 11858611.

22. Weinreb RN, Liebmann JM, Martin KR, Kaufman PL, Vittitow JL. Latanoprostene Bunod 0.024% in Subjects With Open-angle Glaucoma or Ocular Hypertension: Pooled Phase 3 Study Findings. *J Glaucoma*. 2018;27(1):7-15. Epub 2017/12/02. doi: 10.1097/IJG.0000000000000831. PubMed PMID: 29194198.
23. Weinreb RN, Scassellati Sforzolini B, Vittitow J, Liebmann J. Latanoprostene Bunod 0.024% versus Timolol Maleate 0.5% in Subjects with Open-Angle Glaucoma or Ocular Hypertension: The APOLLO Study. *Ophthalmology*. 2016;123(5):965-73. Epub 2016/02/15. doi: 10.1016/j.ophtha.2016.01.019. PubMed PMID: 26875002.
24. Medeiros FA, Martin KR, Peace J, Scassellati Sforzolini B, Vittitow JL, Weinreb RN. Comparison of Latanoprostene Bunod 0.024% and Timolol Maleate 0.5% in Open-Angle Glaucoma or Ocular Hypertension: The LUNAR Study. *Am J Ophthalmol*. 2016;168:250-9. Epub 2016/05/24. doi: 10.1016/j.ajo.2016.05.012. PubMed PMID: 27210275.
25. Liu JHK, Slight JR, Vittitow JL, Scassellati Sforzolini B, Weinreb RN. Efficacy of Latanoprostene Bunod 0.024% Compared With Timolol 0.5% in Lowering Intraocular Pressure Over 24 Hours. *Am J Ophthalmol*. 2016;169:249-57. Epub 2016/07/28. doi: 10.1016/j.ajo.2016.04.019. PubMed PMID: 27457257.
26. Weinreb RN, Ong T, Scassellati Sforzolini B, Vittitow JL, Singh K, Kaufman PL, Group V. A randomised, controlled comparison of latanoprostene bunod and latanoprost 0.005% in the treatment of ocular hypertension and open angle glaucoma: the VOYAGER study. *Br J*

Ophthalmol. 2015;99(6):738-45. Epub 2014/12/10. doi: 10.1136/bjophthalmol-2014-305908.
PubMed PMID: 25488946; PMCID: PMC4453588.

27. Araie M, Sforzolini BS, Vittitow J, Weinreb RN. Evaluation of the Effect of Latanoprostene Bunod Ophthalmic Solution, 0.024% in Lowering Intraocular Pressure over 24 h in Healthy Japanese Subjects. *Adv Ther.* 2015;32(11):1128-39. Epub 2015/11/14. doi: 10.1007/s12325-015-0260-y. PubMed PMID: 26563323; PMCID: PMC4662725.

28. Canto A, Olivar T, Romero FJ, Miranda M. Nitrosative Stress in Retinal Pathologies: Review. *Antioxidants (Basel).* 2019;8(11):543. Epub 2019/11/14. doi: 10.3390/antiox8110543. PubMed PMID: 31717957; PMCID: PMC6912788.

29. Stamer WD, Lei Y, Boussommier-Calleja A, Overby DR, Ethier CR. eNOS, a pressure-dependent regulator of intraocular pressure. *Invest Ophthalmol Vis Sci.* 2011;52(13):9438-44. doi: 10.1167/iops.11-7839. PubMed PMID: 22039240; PMCID: PMC3293415.

30. Ashpole NE, Overby DR, Ethier CR, Stamer WD. Shear stress-triggered nitric oxide release from Schlemm's canal cells. *Invest Ophthalmol Vis Sci.* 2014;55(12):8067-76. Epub 2014/11/15. doi: 10.1167/iops.14-14722. PubMed PMID: 25395486; PMCID: PMC4266075.

31. Davies IR, Zhang X. Nitric oxide selective electrodes. *Methods Enzymol.* 2008;436:63-95. Epub 2008/02/02. doi: 10.1016/S0076-6879(08)36005-4. PubMed PMID: 18237628.

32. Archer S. Measurement of nitric oxide in biological models. *FASEB J.* 1993;7(2):349-60. Epub 1993/02/01. doi: 10.1096/fasebj.7.2.8440411. PubMed PMID: 8440411.
33. Millar JC. Real-time direct measurement of nitric oxide in bovine perfused eye trabecular meshwork using a clark-type electrode. *J Ocul Pharmacol Ther.* 2003;19(4):299-313. Epub 2003/09/11. doi: 10.1089/108076803322279363. PubMed PMID: 12964955.
34. Saavedra JE, Shami PJ, Wang LY, Davies KM, Booth MN, Citro ML, Keefer LK. Esterase-sensitive nitric oxide donors of the diazeniumdiolate family: in vitro antileukemic activity. *J Med Chem.* 2000;43(2):261-9. Epub 2000/01/29. doi: 10.1021/jm9903850. PubMed PMID: 10649981.
35. Peters JC, Bhattacharya S, Clark AF, Zode GS. Increased Endoplasmic Reticulum Stress in Human Glaucomatous Trabecular Meshwork Cells and Tissues. *Invest Ophthalmol Vis Sci.* 2015;56(6):3860-8. doi: 10.1167/iovs.14-16220. PubMed PMID: 26066753; PMCID: 4468426.
36. Medina-Ortiz WE, Belmares R, Neubauer S, Wordinger RJ, Clark AF. Cellular fibronectin expression in human trabecular meshwork and induction by transforming growth factor-beta2. *Invest Ophthalmol Vis Sci.* 2013;54(10):6779-88. doi: 10.1167/iovs.13-12298. PubMed PMID: 24030464; PMCID: PMC3799562.
37. Kaufman PL. Latanoprostene bunod ophthalmic solution 0.024% for IOP lowering in glaucoma and ocular hypertension. *Expert Opin Pharmacother.* 2017;18(4):433-44. Epub 2017/02/25. doi: 10.1080/14656566.2017.1293654. PubMed PMID: 28234563.

38. Gain P, Jullienne R, He Z, Aldossary M, Acquart S, Cognasse F, Thuret G. Global Survey of Corneal Transplantation and Eye Banking. *JAMA Ophthalmol.* 2016;134(2):167-73. Epub 2015/12/04. doi: 10.1001/jamaophthalmol.2015.4776. PubMed PMID: 26633035.
39. Doganay S, Evereklioglu C, Turkoz Y, Er H. Decreased nitric oxide production in primary open-angle glaucoma. *Eur J Ophthalmol.* 2002;12(1):44-8. Epub 2002/04/09. doi: 10.1177/112067210201200109. PubMed PMID: 11936443.
40. Galassi F, Renieri G, Sodi A, Ucci F, Vannozzi L, Masini E. Nitric oxide proxies and ocular perfusion pressure in primary open angle glaucoma. *Br J Ophthalmol.* 2004;88(6):757-60. Epub 2004/05/19. doi: 10.1136/bjo.2003.028357. PubMed PMID: 15148207; PMCID: PMC1772173.
41. Hannappel E, Pankow G, Grassl F, Brand K, Naumann GO. Amino acid pattern in human aqueous humor of patients with senile cataract and primary open-angle glaucoma. *Ophthalmic Res.* 1985;17(6):341-3. Epub 1985/01/01. doi: 10.1159/000265398. PubMed PMID: 4069571.
42. Lundberg JO, Weitzberg E, Gladwin MT. The nitrate-nitrite-nitric oxide pathway in physiology and therapeutics. *Nat Rev Drug Discov.* 2008;7(2):156-67. Epub 2008/01/03. doi: 10.1038/nrd2466. PubMed PMID: 18167491.